Academic Journal of Health Sciences

Medicina Balear

Volume 40 | Issue 5

SEPTEMBER - OCTOBER 2025

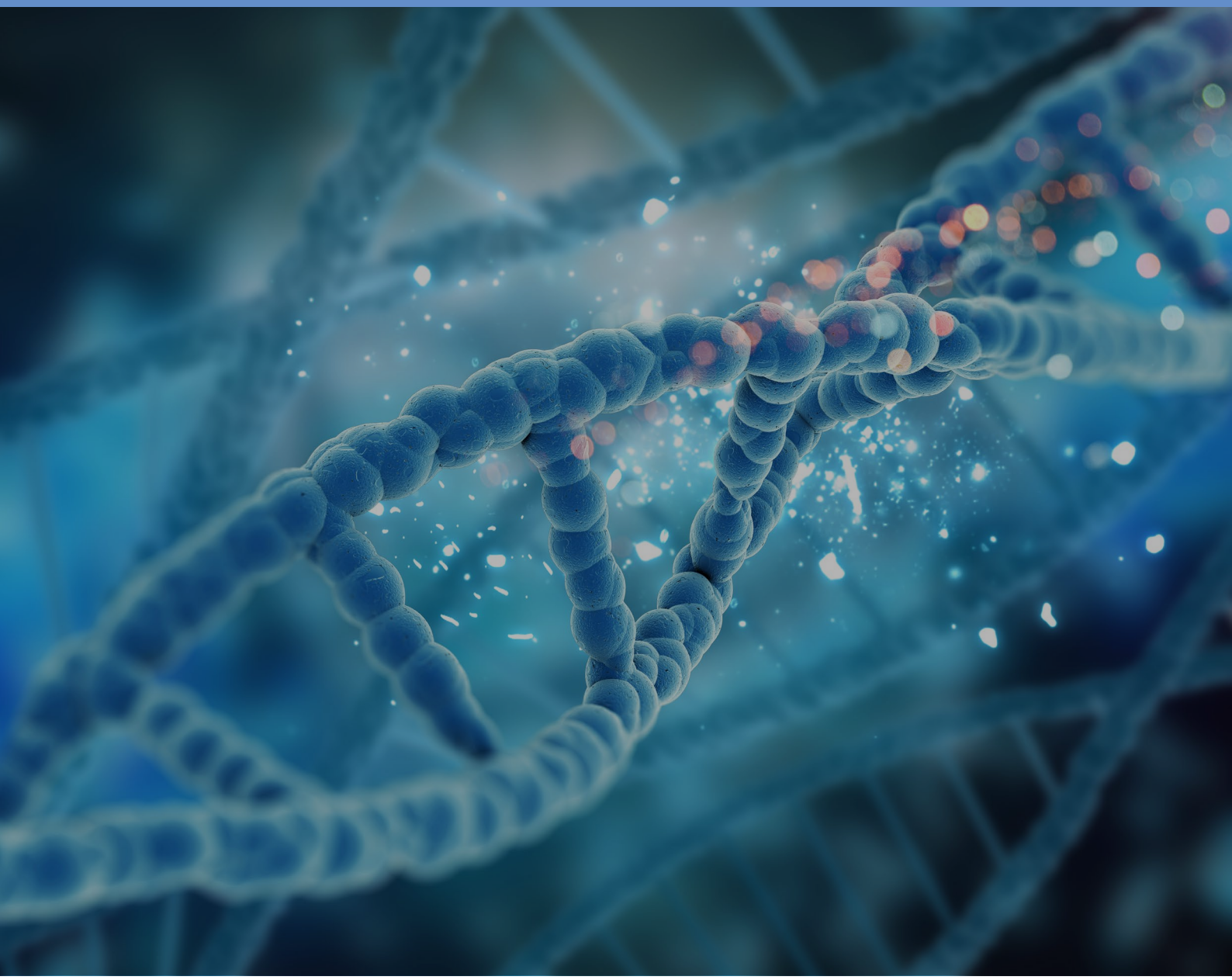

www.ajhealthsciences.com

Published by index

ACADEMIC JOURNAL OF HEALTH SCIENCES
MEDICINA BALEAR

Academic Journal of Health Sciences Medicina Balear is the organ of the **Royal Academy of Medicine of the Balearic Island**, It was created in 1986 with the aim of following up the scientific concerns and promoting the research spirit of health professionals in the Balearic Islands and with the additional objective of projecting health issues of interest to society.

Currently **Academic Journal of Health Sciences Medicina Balear** publishes in English, Spanish or Catalan original papers, review articles, letters to the editor and other writings of interest related to health sciences. The journal submits the originals to the anonymous review of at least two external experts (peer review).

Impact Factor: 0.5
Quartile: Q3
Año: 2024

Medicina Balear is included in the Digital Library of the Balearic Islands, of the University of the Balearic Islands, and is included in the following databases: Emerging Sources Citation Index (ESCI), Sherpa Romeo, Dulcinea, Latindex (catàleg), Dialnet, Índice Médico Español, DOAJ, Imbiomed, REDIB, Google Scholar, Journal Citation Indicator (JCI) and Scielo España.

Impact Factor: 0.5
Cuartile: Q3
Year: 2024

Edit
Royal Academy of Medicine of the Balearic Islands

Campaner, 4, 07003 Palma de Mallorca Tel. 971 72 12 30 Email: info@ramib.org
Pàgina web: http://www.ramib.org

Dipòsit Legal: PM 486 - 95
eISSN: 2255 - 0569

ACADEMIC JOURNAL
OF HEALTH SCIENCES
MEDICINA BALEAR

EDITOR

EDITORIAL COUNCIL

SCIENTIFIC COUNCIL

With the colaboration:

Conselleria de Presidència i Administracions Públiques
Direcció General de Funció Pública

Fundació Patronat Científic
Col·legi de Metges Illes Balears

Fundació
Patronat Científic

Col·legi de Metges
Illes Balears

CONCESIÓN DE BECAS Y PREMIOS 2024

Becas *RELYENS-GRUP MED* de rotación externa para MIR, Beca de rotación externa internacional para MIR, Becas de Innovación, Premios de investigación, Premio Camilo José Cela de Humanidades Médicas, Premio *Fundació Mutual Mèdica* al mejor proyecto de tesis doctoral y Certamen Banco Santander de casos clínicos para MIR.

El jurado calificador de los premios y becas convocados por la *Fundació Patronat Científic* del COMIB, reunido el día 7 de noviembre del presente, acordó la concesión de las siguientes becas y premios:

BECAS *RELYENS-GRUP MED* DE ROTACIÓN EXTERNA PARA MIR

Dos becas para estancias en hospitales nacionales, dotadas cada una de 1.500 euros.

- Joan Siquier Padilla, residente de la especialidad de Cardiología en el Hospital Universitario Son Espases, para una estancia de tres meses en el Servicio de Cardiología y Unidad UCI Coronaria e Insuficiencia Cardíaca del Hospital Universitari de Bellvitge en Barcelona.
- Bernat Mas Matas, residente de la especialidad de Dermatología en el Hospital Universitario Son Llàtzer, para una estancia de dos meses en el Servicio de Dermatología Pediátrica del Hospital Sant Joan de Déu en Barcelona.

BECA DE ROTACIÓN EXTERNA INTERNACIONAL PARA MIR

Una beca para la estancia en un hospital internacional, dotada de 3.000 euros.

- Natasha Woods Kreisler, residente de la especialidad de Pediatría y Áreas Específicas en el Hospital Universitario Son Espases, para una estancia de un mes y medio en el Servicio de Gastroenterología, Hepatología y Nutrición Pediátrica del *Hospital for Sick Children (SickKids)* en Toronto, Canadá

BECAS DE INNOVACIÓN

Dos becas para estancias en centros sanitarios extranjeros, dotadas cada una con 3.000 euros.

- Carla Soldevila Verdeguer, FEA de Cirugía General y del Aparato Digestivo en el Hospital Universitario Son Espases, para una estancia de cuatro semanas en la Unidad de Carcinomatosis Peritoneal del *Mount Sinai Hospital* en Toronto, Canadá.
- Olga Claramonte Bellmunt, FEA de Cirugía General y del Aparato Digestivo en el Hospital Universitario Son Llàtzer, para una estancia de tres meses en el Servicio Cirugía Hepato-Biliar en el *Centre Hépato-Biliaire. Hopital Paul Brousse* en Villejuif, Francia.

Desierta la adjudicación de las dos becas para estancias en centros sanitarios nacionales.

PREMIOS DE INVESTIGACIÓN

Tres premios de 1.500 euros.

"Premio Damià Carbó"
Al trabajo científico titulado *"Effects of six months treatment with liraglutide among patients with psoriasis and obesity, beyond metabolic control?"*,
presentado por Joana Nicolau, Antoni Nadal, Pilar Sanchís, Cristina Nadal y Lluís Masmiquel.

"Premio Mateu Orfila"
Desierta la adjudicación.

"Premio Metge Matas"
Al artículo *"The coexistence of low albumin levels and obesity worsens clinical outcomes among subjects admitted for sars-cov-2 infection"*, cuyos autores son Joana Nicolau, Irene Rodríguez, Andrea Romano, Keyla Dotres, Antelm Pujol y Lluís Masmiquel.

PREMIO CAMILO JOSÉ CELA DE HUMANIDADES MÉDICAS

Un premio dotado de 1.500 euros concedido al trabajo titulado "La compasión me ha hecho ser más persona y mejor médico", firmado por María Belén González Gragera.

PREMIO FUNDACIÓ MUTUAL MÈDICA AL MEJOR PROYECTO DE TESIS DOCTORAL

Un premio dotado de 2.000 euros al proyecto titulado "Deterioro cognitivo en la diabetes mellitus tipo 2: relación con las características clínicoepidemiológicas y papel de la dieta con especial referencia a la ingesta de fitato", presentado por Antelm Pujol Calafat.

CERTAMEN BANCO SANTANDER DE CASOS CLÍNICOS PARA MIR

Tras la exposición de los cinco casos clínicos seleccionados como finalistas, el jurado, reunido el día 14 de noviembre del presente, acordó conceder:

- **El primer premio, dotado de 1.000 euros,** al caso titulado "Cuando la piel revela el diagnóstico: el rol decisivo del dermatólogo en una paciente con insuficiencia respiratoria grave",
  cuya autora es Verónica Fernández Tapia.
- **El segundo premio, dotado de 500 euros,** al caso titulado "Neumonía necrotizante por SAMS ¿productor de PLV? A propósito de un caso", cuya autora es Noelia Plaza Mendoza.

ÍNDICE / CONTENTS

ARTÍCULO ORIGINAL / ORIGINAL ARTICLE

REPORTE DE CASO / CASE REPORT

¿Qué profesional puede tener 45 años de edad y 90 de experiencia?

La respuesta es Banca March

La experiencia de un profesional no está únicamente en su edad, sino también en la edad de la firma para la que trabaja.

Y 90 años de experiencia es lo que ofrecen los profesionales de Banca March.

90 años gestionando patrimonios y demostrando entre otras cosas, que la prudencia no está reñida con la rentabilidad.

BancaMarch

90 ANIVERSARIO

www.bancamarch.es

ACADEMIC JOURNAL OF HEALTH SCIENCES
MEDICINA BALEAR

Original

Modification of hydroablation technique in a third level hospital

Modificación de la técnica de hidroablación en un hospital de tercer nivel

Héctor Ricardo Ayllón-Blanco, Juan Antonio Mainez-Rodríguez, José Ramón Cansino-Alcaide, Carlos Toribio-Vázquez, José Ramón Pérez-Carral, Manuel Girón-De Francisco, Pablo Abad-López, Luis Martínez-Piñeiro

Hospital Universitario La Paz, Madrid, Spain

Received: 21-01-25
Accepted: 23-03-25

***Corresponding author**: Héctor Ricardo Ayllón-Blanco. hector.ayllonb@gmail.com

Abstract

Introduction and objective: This study aims to compare the learning curves of two novice surgeons with no prior experience (Group A) to patients operated on by an experienced surgeon (Group B), who refined the technique after observing Group A.

Materials and methods: The first 15 patients operated by each surgeon with Aquabeam were studied. Patients included for analysis had undergone surgery in our department from April 2021 to December 2022. The following parameters where analysed: surgical time, haemoglobin (Hb) loss, length of stay, variation in Q-max at 1 and 4 months after surgery, PSA, presence of ejaculation and perioperative morbidity. We combined data from the patients who were operated by the two novel surgeons and we compared it with data coming from patients who were operated by the one with practical knowledge of this surgery.

Results: Haemoglobin loss was smaller in patients operated by surgeon 3 (2.57±2.32g/dL vs 0.89±2.38 g/dL, p<0.001). Increase in Qmax 4 months after surgery was bigger in patients operated by surgeon 3 (6.27±2.96 vs 12.93±4,92, p<0.027). PSA descend after hidroablation was bigger in group 2, near statistical significance (0.13±0.76 vs 0.93±0.64, p=0,078). No difference in complications during income were found between groups (6.7% vs 13.3%).

Conclusions: Having previous knowledge about this surgery and a modification on surgical technique, may improve functional results and decrease blood loss. More studies are needed to perfect the technique.

Keywords: Hydroablation. Bening prostatic hyperplasia. Learning curve.

Resumen

Introducción y objetivo: El objetivo de este estudio es comparar las curvas de aprendizaje de hidroablación prostática de dos cirujanos sin experiencia previa, con datos de pacientes operados por un cirujano con conocimiento práctico de la técnica, quien la modificó tras observar al primer grupo.

Materiales y métodos: Se analizaron los primeros 15 pacientes operados por cada cirujano con Aquabeam. Se incluyeron pacientes intervenidos en nuestro servicio entre abril de 2021 y diciembre de 2022. Se evaluaron los siguientes parámetros: tiempo quirúrgico, pérdida de hemoglobina (Hb), estancia hospitalaria, variación del Q-max al mes y a los 4 meses, PSA, presencia de eyaculación y morbilidad perioperatoria. Se combinaron los datos de los pacientes operados por los dos cirujanos noveles y se compararon con los de los pacientes operados por el cirujano con experiencia práctica.

Cite as: Ayllón-Blanco HR, Mainez-Rodríguez JA, Cansino-Alcaide JR, Toribio-Vázquez C, Pérez-Carral JR, Girón-De Francisco M, et al. Modification of hydroablation technique in a third level hospital. Acad J Health Sci 2025; 40(5): 7-13. Available from: https://doi.org/10.3306/AJHS.2025.40.05.1

Acad J Health Sci 2025; 40(5): 7-13
https://doi.org/10.3306/AJHS.2025.40.05.1
www.ajhealthsciences.com

Resultados: La pérdida de hemoglobina fue menor en los pacientes operados por el cirujano 3 (2,57±2,32 g/dL vs 0,89±2,38 g/dL, p<0,001). El aumento del Q-max a los 4 meses fue mayor en los pacientes operados por el cirujano 3 (6,27±2,96 vs 12,93±4,92, p<0,027). La reducción del PSA tras la hidroablación fue mayor en el grupo 2, con tendencia a la significación estadística (0,13±0,76 vs 0,93±0,64, p=0,078). No hubo diferencias en complicaciones entre grupos (6,7% vs 13,3%).

Conclusiones: Tener experiencia previa en hidroablación junto a una modificación de la técnica quirúrgica, mejora los resultados funcionales y reduce la pérdida sanguínea. Se requieren más estudios para optimizar la técnica.

Palabras clave: Hidroablación. Hiperplasia benigna de próstata. Curva de aprendizaje.

Introduction

Hyperplasia of the epithelium and fibromuscular tissue, primarily affecting the transitional and periurethral zones of the prostate, is referred to as benign prostatic hyperplasia (BPH)[1]. The degree of bladder outlet obstruction (BOO) influences the patient's symptoms[2]. Men with BPH may experience voiding symptoms (such as poor flow, post-void dribbling) and storage symptoms (such as urgency, frequency, nocturia, and occasional incontinence), as well as detrusor overactivity[3]. Some individuals may remain asymptomatic until they experience acute urinary retention[4].

According to the study by Chicharro et al.[5], the prevalence of clinical BPH in men over the age of 40 in the Spanish population is approximately 11.8%. In men over 70 years old, this proportion can exceed 30%. Clinical BPH can be defined as a prostate adenoma causing a varying degree of BOO, which may eventually lead to harm in patients. Clinical BPH can be diagnosed with ultrasound, grading it according to the shape (intravesical prostatic protrusion) and size of the prostate, as well as uroflowmetry[4].

Surgical treatment of lower urinary tract symptoms (LUTS) related to BPH is one of the available options for managing this condition. TURP, also known as transurethral resection of the prostate, is regarded as the gold standard according to the EAU guidelines[6]. However, there have been many surgical advancements in the last decade. Recently, prostatic hydroablation using Aquabeam® technology, which is based on a high-pressure water jet, has provided patients with a new minimally invasive option. The procedure is regulated by transrectal ultrasound and is carried out robotically, with the surgeon designating the treatment zone. Since the introduction of Aquablation in 2015, numerous clinical trials have shown Aquablation to be an effective and safe treatment for men with LUTS[7]. However, the method to achieve an adecuate hemostasis is still unclear. Hydroablation is a technique which that does not cauterize prostatic tissue and may require coagulation of the bladder neck with bipolar energy, once the treatment is finished. Other strategies to ensure a good haemostasis could be administration of tranexamic acid before induction or mechanical traction on the urinary catheter[8].

Although this is a robotic-guided procedure; we believe that the surgeon plays a major role during the operation. Aquablation is divided into three steps[9]: 1) Planning, 2) Treatment and 3) Coagulation, with only the second being entirely dependent on the robot. This provides a conformal, quantifiable, and standardised treatment for BPH and could minimise human error, but there is a learning curve for the surgeon, especially for steps one and three. A recent study showed that after only five cases, the trifecta achievement rate surpassed 50%. The trifecta concept was defined as an operative time of less than 60 minutes, a hemoglobin drop of ≤ 2 g/dL, and absence of immediate postoperative complications[10]. Based on these results and following Procept BioRobotics® recommendations for the development of the surgical technique, we propose to establish the learning curve with 15 patients.

This study aims to compare the learning curves of two novice surgeons with no prior experience (Group A) to patients operated on by an experienced surgeon (Group B), who refined the technique after observing Group A.

Methods

Given the limited published data on the learning curve for a robotic procedure such as hydroablation, and following the recommendation of Procept BioRobotics®, we established the learning curve at 15 patients. The first 15 patients operated on by each surgeon using this new technology were studied. All the surgeons were trained by an expert representative from the company. Patients included in the analysis underwent surgery in our department between February 2021 and December 2022.

A prospective analysis of demographical, clinical, and surgical data was performed. Patients were evaluated at urology consultations, where they received different treatment options for BPH, including hydroablation, if they met at least one of the

following criteria: medical treatment failure, haematuria of prostatic origin, renal failure due to bladder outlet obstruction or impossibility to remove urinary catheter. There was no limit to prostate volume and patients could have received previous surgical treatment for BPH. Patients with bladder stones or anticoagulant treatment were excluded. All patients gave written and oral consent.

The following parameters were analysed: surgical time (planification, hydroablation and haemostasis time), haemoglobin (Hb) loss, length of stay, variation in Q-max preoperative and 4 months after surgery, PSA and perioperative morbidity.

The following demographical and perioperative items where collected; PSA level, prostatic volume, surgical time (planification, hydroablation and haemostasis), haemoglobin (hb) loss, hospital stay and perioperative complications using Clavien-Dindo scale were recorded.

Statistical analysis

The values of discrete qualitative or quantitative variables are presented as absolute values or percentages, and continuous variables as mean ± standard deviation. Statistical analysis was performed using the SPSS21.0 software package for Windows (IBM Corp. Released 2012. IBM SPSS Statistics for Windows, Version 21.0. Armonk, NY: IBM Corp.). For each variable, its normal range was established according to the reference values of the hospital laboratory or the best available evidence in the medical literature. Student's t-test for independent samples was used for univariate comparison of means between groups, and Fisher's exact test was used to compare percentages, considering a p-value of less than 0.05 as significant.

Surgical technique

Hydroablation was performed using the Aquabeam® system (PROCEPT BioRobotics) by three different surgeons. Two had no prior experience with this procedure, while one had practical knowledge gained by observing the other surgeons and identifying key postoperative issues. The surgical technique used in group A followed the manufacturer's recommendations. A complete description of the technique was published by Barber et al. in 2019[9]. Aquabeam® technology treats an ultrasound-delimited zone and ablates prostatic tissue with a high-pressure water jet. Subsequently, selective haemostasis is performed using bipolar energy with a Karl-Storz 26Ch resectoscope. Finally, a 22Ch bladder catheter with continuous irrigation is placed.

In our case, patients from both groups received a preoperative second-generation cephalosporin before surgery. The patient is placed in lithotomy position, and spinal anaesthesia is administered in all cases. A transrectal ultrasound probe is then inserted and adjusted to obtain a complete and centred image of the prostate in both sagittal and transverse views. The handpiece probe is inserted under direct visualisation. After planning, the surgeon sets the treatment limits, and the robot guides the ablation from the bladder neck to the verumontanum protection zone. The number of treatment passes depends on the ultrasound appearance of the prostate after tissue removal. Once the patient is deobstructed, the handpiece and ultrasound probe are removed, and a 26Ch resectoscope is inserted to cauterise selective bleeding sources. After bleeding control is achieved, a 22Ch bladder catheter with continuous irrigation is placed. This catheter is removed once haematuria is resolved.

Modification in surgical technique and postoperative care

Group B underwent some modifications in surgical technique and postoperative care. The main changes consisted of adjusting the treatment zone. During hydroablation planning, we positioned the treatment area between the verumontanum and the prostate, just below the bladder neck, excluding it from ablation. This area of the prostate is treated with a 26Ch resector using bipolar energy in order to achieve a better haemostasis. During the hospital stay, this group of patients received continuous irrigation for at least 48 hours, regardless of the degree of haematuria. After 48 hours, if the urine is clear, the catheter is removed.

Results

The mean age of patients in Group A was 68.67±8.49 years, and 70.73±6.19 in Group B. The mean prostatic volume was 88.43±32.97 cubic centimetres(cc) in Group A, compared to 74.40±25,72cc in Group B. No statistical difference was found between groups (p=0.083). An indwelling urinary catheter as present in 16.7% of patients in Group A and 6.7% in Group B, with no difference between groups (p=0,352) (**Table 1**).

Mean Hb loss was 2.57±1.16g/dL in the group operated by surgeons with no previous experience, and 0.89±1.19g/dL in the group operated on by the surgeon with practical knowledge of this new technique. A statistical difference was found for this outcome (p=0,03) (**Figure 1**).

Table 1. Demographical, clinical and surgical data.

	Group A	Group B	p value
Mean age	68.67 ± 8.49	70.73 ± 6.19	p = 0.469
Mean prostatic volume (cc)	88.43 ± 32.97	74.40 ± 25.72	p = 0.083
Indwelling urinary catheter	16.7%	6.7%	p = 0.352
Preoperative Qmax (ml/s)	8.37 ± 3.94	8.53 ± 2.01	p = 0.958
Preoperative PSA (ng/ml)	3.10 ± 2.03	3.44 ± 2.54	p = 0.847
Surgical time (minutes)	52.23 ± 11.52	46.07 ± 15.34	p = 0.153
N° passes	2.17 ± 0.38	1.93 ± 0.26	p = 0.075

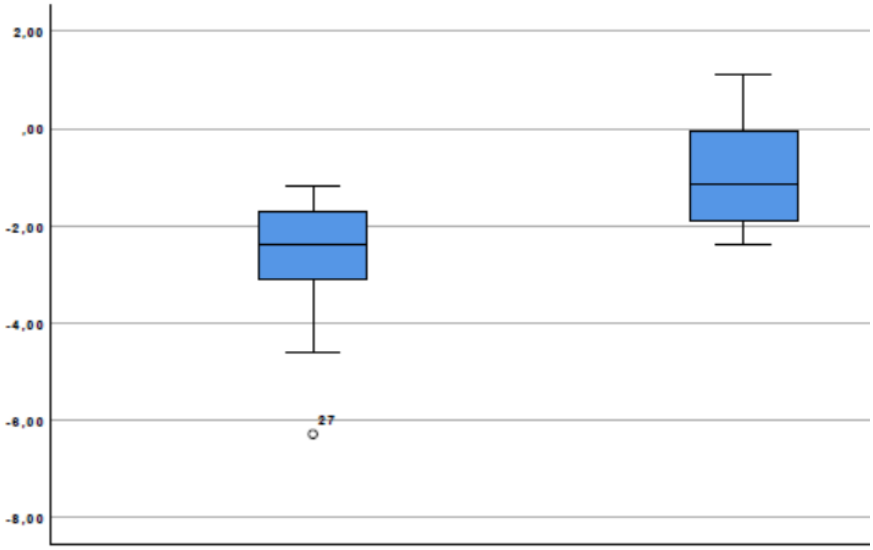

Figure 1. Mean Hb loss between group A (left box) and group B (right Box).

Mean hospital stay was 2.37±1.52 days in the first group and 2.13±0.35 days in the other group. Mean preoperative Q-max was similar between groups: 8.37±3.94 ml/s in Group A and 8.53±2.01 ml/s in Group B. The increase in Qmax four months after surgery was greater in Group B (12.93±8.70ml/s) compared with Group A (6.27±6.93ml/s) (p=0,034) (**Figure 2**).

Mean preoperative PSA was similar as well between groups: 3.10±2.03 ng/ml in the first group and 3.44±2.54 ng/ml in group B. Mean PSA reduction after 4 months was 0.13±1.86 ng/ml in group A, and 0.93±1.21 ng/ml in group B (p=0.078) (**Figure 3**).

Regarding postoperative complications in the first month after surgery, one patient required a blood transfusion (Clavien-Dindo II), and one patient developed a urinary tract infection (Clavien-Dindo II) in group A. In group B, two patients presented with acute urinary retention (Clavien-Dindo I).

Discussion

This analysis reports on our experience with the first 15 cases of hydroablation by three different surgeons treating BPH in a public hospital. To our knowledge, this is the first series published in a public setting in Spain. The presented results confirm that having prior practical knowledge of the procedure may lead to modifications in the technique that improve functional outcomes four months after surgery and decreases Hb loss during hospital stay.

Surgical technique changes

Previous studies have described hydroablation as a procedure with minimal or no learning curve[11].

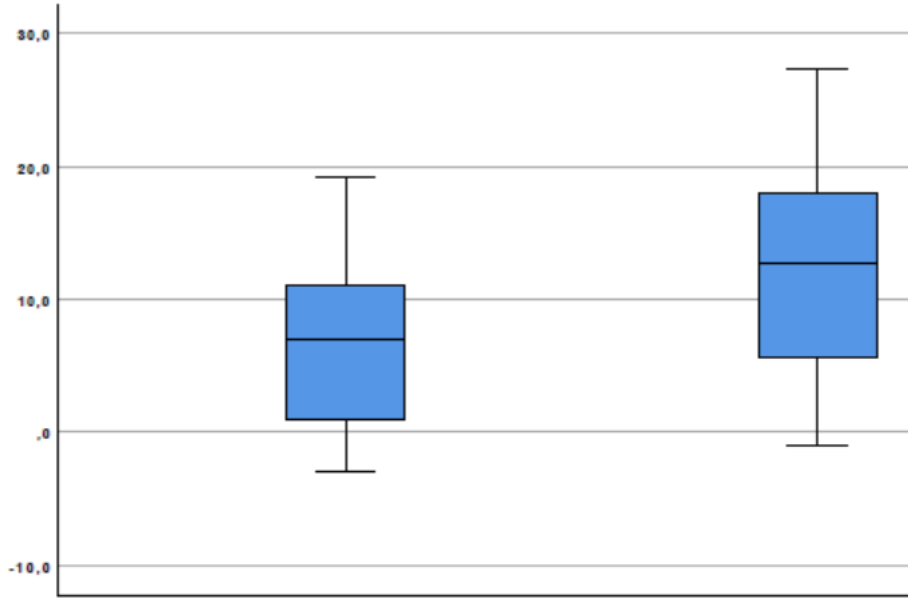

Figure 2. Mean Qmax increase 4 months after surgery between group A (left box) and group B (right Box).

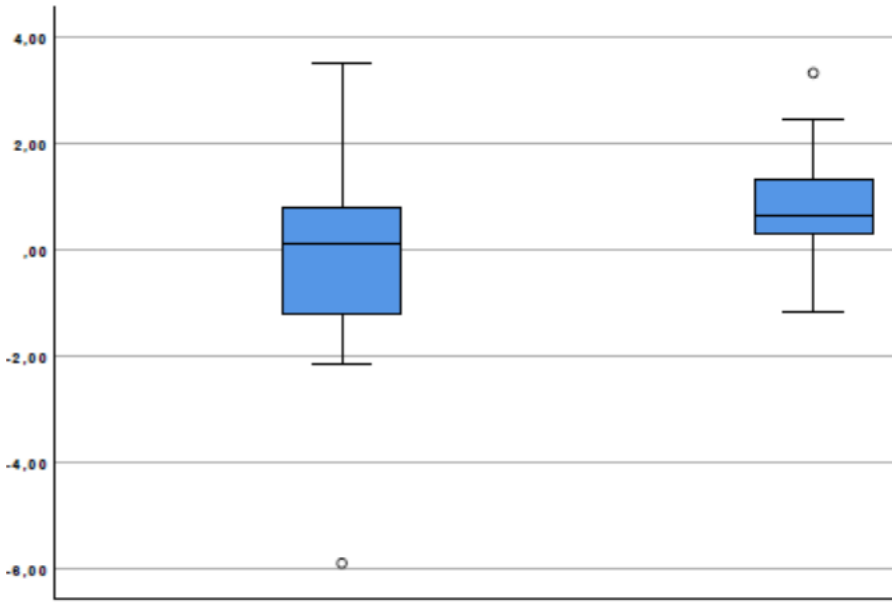

Figure 3. Mean PSA reduction 4 months after surgery between group A (left box) and group B (right Box).

However, our results suggest that this robotic technique still requires a learning curve. As shown, one of the main challenges of this procedure is bleeding due to of the energy mechanism based on a high-pressure saline jet. The surgeon in Group B implemented a modification in the definition of the treatment zone during surgical planning. Arterial bleeding from the bladder neck is difficult to control and can cause significant blood loss[12]. With this modification of the technique, we avoid treating the bladder neck with a high-pressure saline jet, which changes the limits of hydroablation. This area is treated during haemostasis by resection of the bladder neck using the Nesbit procedure[13], ensuring better haemostasis control, as in conventional TURP, using a 26Ch resectoscope with a bipolar loop. This modification provides an additional advantage over the classic hydroablation technique: it provides tissue for analysis.

In addition, the management of postoperative haematuria differed between Group A and Group B. In Group A, patients received continuous bladder irrigation with saline until haematuria resolved. In Group B, all patients underwent at least 48 hours of saline irrigation, regardless of urine appearance, before

catheter removal. Although this approach could increase the length of hospital stay, no significant differences were observed between the groups.

Functional results

Functional outcomes were better in Group B compared to Group A, taking improvement in Q-max at four months as an outcome. This may be explained by the fact that in Group B, the surgeon resects the bladder neck and creates a regular and open bladder neck. In Group A, it was observed that prostate tissue treated with a high-pressure saline jet tends to be floppy and prone to bleeding. Because of this, resection is less effective in terms of haemostasis, so surgeons only apply cautery to the bladder neck without any resection. The jet creates a tunnel through the transitional zone of the prostate, which may be sufficient to relieve LUTS in most patients, but with our modification, functional outcomes are improved and safety is enhanced.

PSA changes

The reduction in PSA was close to statistical significance between groups, perhaps with a larger sample size we could reach it. Although there were no statistically significant difference in the number of passes, there was greater prostate tissue removal in Group B, considering the additional resection of the bladder neck using bipolar energy. This may explain the greater PSA reduction observed four months after surgery.

Complications

One of the challenges observed in our initial hydroablation series was the need for blood transfusion, affecting 5% of patients treated with this new technique. In this study, there is one patient who required blood transfusion during hospital stay in Group A, and no patients in group B. This percentage is higher compared with WATER II study[14], where the percentage is about 1%. We hope that adopting modifications to the surgical technique, as shown in this article, may help achieve similar outcomes.

In Group B we observed two patients who presented with acute urinary retention requiring emergency department consultation during the first week after surgery. Removing more tissue increases the risk of this complication. One strategy that could be used is to treat all patients with NSAIDs for one week to reduce inflammation of prostatic cell and bladder neck.

Limitations

This study presents some limitations. First of all, it is an observational study with a limited number of patients. We established sample size in 15 patients given the recommendation of Procepts. Despite it we found some differences between groups. We have no questionnaires as International Consultation on Incontinence Questionnaire Short-Form (ICIQ-SF) or IPSS after surgery in all patients, to know if the increase in Q-max has clinical impact.

Conclusion

Hydroablation has been presented as a new convenient, standardized and reproducible technique in the treatment of benign prostatic hyperplasia. Few studies talk about the learning curve as it is a robotic procedure. With the results presented in this article, we argue that there is a learning curve in this procedure and that a modification in the surgical technique could improve the functional and perioperative results.

Acknowledgements

The authors of the manuscript have no financial support for this study.

References

1. Devlin CM, Simms MS, Maitland NJ. Benign prostatic hyperplasia – what do we know? BJU Int. 2021;127(4):389–99. Available from: http://dx.doi.org/10.1111/bju.15229.
2. Abrams P, Cardozo L, Fall M, Griffiths D, Rosier P, Ulmsten U, et al. The standardisation of terminology in lower urinary tract function: report from the standardisation sub-committee of the International Continence Society. Urology. 2003;61(1):37–49. Available from: http://dx.doi.org/10.1016/s0090-4295(02)02243-4.
3. Speakman M, Kirby R, Doyle S, Ioannou C. Burden of male lower urinary tract symptoms (LUTS) suggestive of benign prostatic hyperplasia (BPH) – focus on the UK. BJU Int. 2015;115(4):508–19. Available from: http://dx.doi.org/10.1111/bju.12745.
4. Foo KT. What is a disease? What is the disease clinical benign prostatic hyperplasia (BPH)? World J Urol. 2019;37(7):1293–6. Available from: http://dx.doi.org/10.1007/s00345-019-02691-0.
5. Chicharro-Molero JA, Burgos-Rodriguez R, Sanchez-Cruz JJ, del Rosal-Samaniego JM, Rodero-Carcia P, Rodriguez-Vallejo JM. Prevalence of benign prostatic hyperplasia in Spanish men 40 years old or older. J Urol. 1998;159(3):878–82.
6. EAU Guidelines. Edn. presented at the EAU Annual Congress Milan March 2023. ISBN 978-94-92671-19-6.
7. Ng KL, Giona S, Barber N. Feasibility of Aquablation prostate surgery performed as day cases. BJU Int.

2024 Aug;134(2):185-186. Available from: http://dx.doi.org/10.1111/bju.16272.

8. Bach T, Giannakis I, Bachmann A, Fiori C, Gomez-Sancha F, Herrmann TRW, et al. Aquablation of the prostate: single-center results of a non-selected, consecutive patient cohort. World J Urol. 2019;37(7):1369–75.
9. Lim Ng K, Barber N. Prostatic hydroablation (Aquablation): A new effective ultrasound guided robotic waterjet ablative surgery for treatment of benign prostatic hyperplasia. Arch Esp Urol. 2019;72(8).
10. Abboudi H, Khan MS, Guru KA, Froghi S, de Win G, Van Poppel H, et al. Learning curves for urological procedures: a systematic review. BJU Int. 2014 Oct;114(4):617-29. Available from: http://dx.doi.org/10.1111/bju.12315.
11. Zorn KC, Elterman D, Gonzalez R, Bach T, Kriteman L, Pickens R, et al. Aquablation treatment for benign prostate hyperplasia: Current standardized procedure. J Endourol. 2022;36(S2):S-1-S-5. Available from: http://dx.doi.org/10.1089/end.2022.0439.
12. Rassweiler J, Teber D, Kuntz R, Hofmann R. Complications of transurethral resection of the prostate (TURP)—incidence, management, and prevention. Eur Urol. 2006;50(5):969–80.
13. Nesbit R. Transurethral prostatectomy. Springfield: CC Thomas; 1943.
14. Nguyen D-D, Barber N, Bidair M, Gilling P, Anderson P, Zorn KC, et al. Waterjet Ablation Therapy for Endoscopic Resection of prostate tissue trial (WATER) vs WATER II: comparing Aquablation therapy for benign prostatic hyperplasia in 30–80 and 80–150 mL prostates. BJU Int. 2020;125(1):112–22. Available from: http://dx.doi.org/10.1111/bju.14917.

Haz algo grande por tu salud

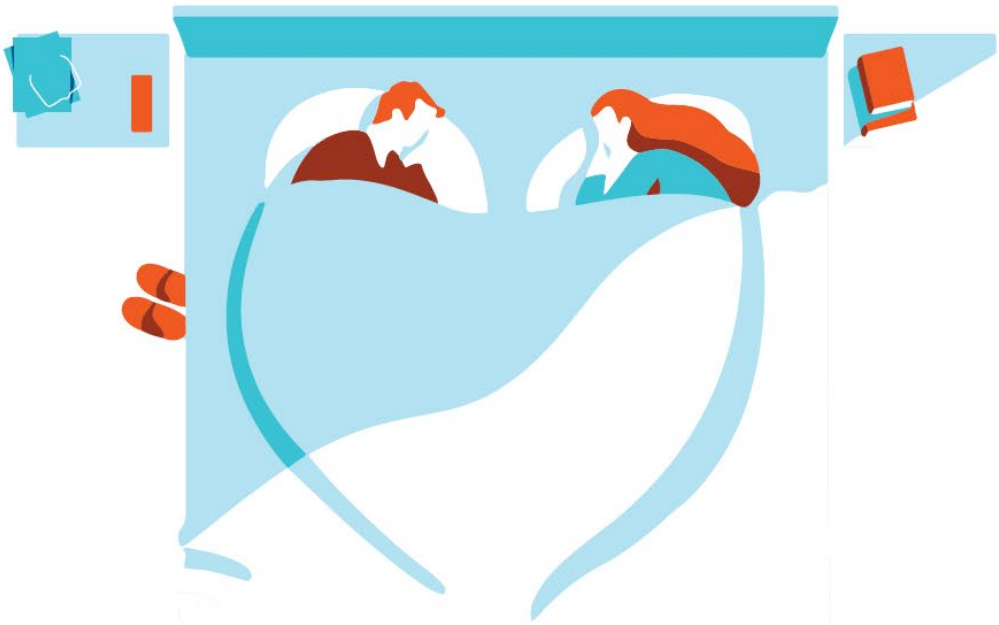

#Duerme1HoraMás

En Asisa somos expertos en salud y sabemos que el sueño es vital para el buen funcionamiento de tu corazón, tu cerebro y todo tu organismo.
Los especialistas determinan que **una persona adulta necesita entre 7 y 9 horas diarias de sueño** para estar bien.
Sin embargo, se estima que el 80% de los españoles duermen menos de este tiempo, exponiéndose a **sufrir hipertensión, taquicardia, depresión, pérdida de memoria, sobrepeso y diabetes**, entre otros problemas. Y como sabes, **en Asisa solo nos preocupa tu salud. Por eso invertimos todos nuestros recursos en cuidarte**, incluido este anuncio en el que te aconsejamos que duermas una hora más todos los días.

Empresa Colaboradora:

R 200 AÑOS

Asisa Palma de Mallorca.
C/ Pere Dezcallar i Net, 10
asisa.es 901 10 10 10

Nada más que tu salud
Nada menos que tu salud

asisa

ACADEMIC JOURNAL OF HEALTH SCIENCES
MEDICINA BALEAR

Original

Comparative study of treatment planning outcomes in bladder cancer: 3D conformal radiation therapy vs volumetric modulated arc therapy

Estudio comparativo de los resultados de la planificación del tratamiento en el cáncer de vejiga: radioterapia conformacional tridimensional frente a radioterapia de arco modulado volumétrico

Ruaa Emad Al-Khalidi[1]*, Nashwan Karkhi Abdulkareem[1], Cheman Baker Ismael[2], Ibrahim Jalal Mustafa[3], Arthur Saniotis[4,5], Rojgar Najat Yousif[5], Ahmed Sami Kamal[6]

[1]Department of Pharmacology and Medical Physics and Clinical Biochemistry, College of Medicine, Hawler Medical University, Kurdistan Region, Iraq

[2]Department of Radiology, Erbil Polytechnic University, Kurdistan Region, Iraq

[3]Awat Radiation Oncology Center, Department of Plan and Dosimetry, Erbil, Kurdistan Region, Iraq

[4]Department of Medical Microbiology, College of Applied Sciences, Cihan University-Erbil, Kurdistan Region, Iraq

[5]School of Biomedicine, Faculty of Health and Medical Sciences, University of Adelaide, Adelaide, Australia

[6]Awat Radiation Oncology Center, Department of Plan and Dosimetry, Erbil, Kurdistan Region, Iraq

Received: 11-03-2025
Accepted: 20-04-2025

***Corresponding author**: Ruaa Emad Al-Khalidi. ruaa.hussien@hmu.edu.krd

Abstract

Objective: this study aimed to compare the dosimetric outcomes of two radiotherapy plan techniques, three-dimensional conformal radiotherapy (3D-CRT) and volumetric modulated arc therapy (VMAT), in patients with bladder cancer (BC).

Materials and methods: seventeen patients with BC were first treated with VMAT and then replanning using 3D the CRT technique. Dosimetric parameters, including the homogeneity index (HI), conformity index (CI), mean dose, maximum dose, minimum dose, monitor unit MUs, and organ at risk (OAR) doses, were assessed and compared for both methods.

Results: the mean of D95 (cGy) of the PTV was not significantly different between 3D-CRT 5389.05 cGy and VMAT 5219.6926 cGy, p = 0.07, indicating better target coverage in both techniques. Both 3D-CRT and VMAT methods showed similar HI for dose distribution within target volume, while the mean PTV CI for 3D-CRT was (0.97), for VMAT was (0.99). In terms of dose-volume coverage across the organs small bowel (SB), rectum, and femoral heads, the results of spiring the organ at risk demonstrate that VMAT usually outperforms 3D-CRT, especially at high doses. Comparison of MUs in both techniques, VMAT demonstrated a notably higher MUs with mean (975.04±267.12) compared to 3D-CRT (368.04±37.29), with a p-value of <0.001.

Conclusions: VMAT provides superior conformity and spares OARs at high dose levels, potentially reducing toxicity and improving patient tolerance despite higher MUs. These findings highlight VMAT's clinical relevance of VMAT for optimizing bladder cancer radiotherapy, balancing precision, and OAR protection.

Keywords: Bladder cancer. 3D-CRT. VMAT. OAR.

Cite as: Al-Khalidi RE, Abdulkareem NK, Baker Ismael C, Jalal Mustafa I, Saniotis A, Najat Yousif R, et al. Comparative study of treatment planning outcomes in bladder cancer: 3D conformal radiation therapy vs volumetric modulated arc therapy. Acad J Health Sci 2025; 40(5): 15-21. Available from: https://doi.org/10.3306/AJHS.2025.40.05.2

Acad J Health Sci 2025; 40(5): 15-21
https://doi.org/10.3306/AJHS.2025.40.05.2
www.ajhealthsciences.com

Resumen

Objetivo: este estudio tuvo como objetivo comparar los resultados dosimétricos de dos técnicas de planificación en radioterapia, la radioterapia conformacional tridimensional (3D-CRT) y la radioterapia de arco modulado volumétrico (VMAT), en pacientes con cáncer de vejiga (CV).

Materiales y métodos: se incluyeron diecisiete pacientes con CV, quienes fueron inicialmente tratados mediante VMAT y posteriormente se realizó una nueva planificación utilizando la técnica 3D-CRT. Se evaluaron y compararon para ambas técnicas los parámetros dosimétricos, incluidos el índice de homogeneidad (HI), el índice de conformidad (CI), la dosis media, la dosis máxima, la dosis mínima, las unidades monitoras (MUs) y las dosis a órganos de riesgo (OAR).

Resultados: La media de D95 (cGy) del volumen objetivo planificado (PTV) no mostró diferencias significativas entre 3D-CRT (5389,05 cGy) y VMAT (5219,69 cGy), con un valor de p = 0,07, lo que indica una adecuada cobertura del objetivo en ambas técnicas. Tanto 3D-CRT como VMAT presentaron índices de homogeneidad similares en la distribución de dosis dentro del volumen objetivo, mientras que el CI medio del PTV fue de 0,97 para 3D-CRT y de 0,99 para VMAT. En cuanto a la cobertura dosis-volumen en órganos como el intestino delgado (SB), el recto y las cabezas femorales, los resultados demostraron que VMAT generalmente supera a 3D-CRT, especialmente en niveles de dosis elevados. En la comparación de las unidades monitoras entre ambas técnicas, VMAT presentó un número significativamente mayor de MUs (975,04 ± 267,12) en comparación con 3D-CRT (368,04 ± 37,29), con un valor de p < 0,001.

Conclusiones: VMAT proporciona una conformidad superior y una mayor protección de los órganos de riesgo a niveles de dosis elevados, lo que potencialmente reduce la toxicidad y mejora la tolerancia del paciente, a pesar de requerir un mayor número de unidades monitoras. Estos hallazgos destacan la relevancia clínica de VMAT para optimizar la radioterapia en el cáncer de vejiga, equilibrando precisión y protección de órganos de riesgo.

Palabras clave: Cáncer de vejiga. 3D-CRT. VMAT. Órganos de riesgo (OAR).

Introduction

Bladder cancer continues to be a major health issue that requires efficient treatment strategies to improve patient outcomes[1]. Advanced radiation therapy methods, including three-dimensional conformal radiotherapy (3DCRT) and volumetric modulated arc therapy (VMAT), are being utilized more frequently to improve dose administration while reducing exposure of nearby healthy tissues[2,3]. Nonetheless, the comparative effectiveness of these modalities in treatment planning for bladder cancer has not been sufficiently examined, thereby prompting this study to investigate their relative efficacy.

Earlier research aimed to overcome the drawbacks of traditional radiation therapy methods by investigating different advanced approaches. For example, Krug et al. showed that IMRT effectively lowers toxicity while preserving tumor control[4]. Similarly, Tonetto et al. evaluated 3DCRT and VMAT in prostate cancer, highlighting VMAT's capability of VMAT to improve dose distribution[5].

Table 1 presents an overview of additional pertinent studies that emphasize the advancement of treatment planning approaches in the management of bladder cancer. Taken together, these studies highlight the necessity for additional research regarding the comparative results of 3DCRT and VMAT, specifically in bladder cancer cases.

Despite these advancements, previous studies on bladder cancer have notable limitations. Many investigations, such as those by Palma et al.[6] and Foroudi et al.[2], have relied on small cohorts or short follow-up periods, limiting their ability to assess long-term toxicity or survival outcomes. Additionally, existing comparisons often prioritize generic dosimetric metrics without addressing bladder-specific

Table 1. Previous approaches to summarizing studies comparing 3D-CRT and VMAT specifically for bladder cancer.

Ref	First author surname	Description
1	Palma et al. (2008)	Compared to 3D-CRT, VMAT was found to lower bladder dose (e.g., lower V20 and Dmean); however, additional research on long-term damage is required[6].
2	Regnier et al. (2017)	Compared to 3D-CRT, VMAT was found to have no significant changes in patient-reported outcomes, except for hair loss and weight issues. However, more studies are needed[7].
3	Foroudi et al. (2012)	This study advocates for future studies that focus on the bladder and emphasizes how VMAT exposes the bladder to less radiation than 3D-CRT[2].

challenges, such as organ motion due to variable filling states or proximity to critical structures, such as the small intestine and femoral heads. Regnier et al. further highlighted the lack of standardized protocols for bladder cancer, which complicates cross-study comparisons[7]. These gaps are critical because bladder tumors require precise dose escalation to account for intrafractional movement while minimizing exposure to radiosensitive organs. VMAT's dynamic arc delivery and superior dose modulation may better address these anatomical complexities than static 3DCRT beams. However, no conclusive evidence exists on whether these dosimetric advantages translate to reduced toxicity or improved local control in patients with bladder cancer. This underscores the need for rigorous, bladder-focused evaluation of 3DCRT and VMAT to guide clinical decision-making and optimize therapeutic outcomes. Therefore, the present study aimed to compare the dosimetric outcomes of two radiotherapy plan techniques, three-dimensional conformal radiotherapy (3D-CRT) and volumetric modulated arc therapy (VMAT), in patients with BC.

Materials and methods

Patients were consecutively enrolled from June to August 2024 based on the following predefined eligibility criteria: histologically confirmed T2-stage bladder cancer, absence of distant metastases, and no prior pelvic radiation. All patients referred for curative radiotherapy during this period were included to minimize selection bias.

In this study, 17 patients with BC were treated with VMAT at the Awat Radiation Oncology Center, Iraq, Erbil. Fourteen patients (82.53%) were male, and three patients (17.65%) were female, with a mean age of 68.18 years (**Table 2**). This study was approved by the Ethical Committee of Hawler Medical University/ College of Medicine (KR, meeting code: 2, paper code: 7, date: 14/6/2024).

Every patient underwent a simulation optima (CT 580 RT General Electric Health care USA) 80 cm wide bore CT- Scanner special foy RT with a flat Rt couch. All patients were scanned in the head-first orientation in the supine position with (A) a head rest with a lung board. Patients breathed normally during the scan without contrast. Some patients were scanned with only an empty bladder, while others were scanned with both a full bladder in the first scan and an empty bladder in the second scan. The isocenter location was in the mid-pelvis, and the slice thickness was 2–5 mm depending on the size, shape, and type of cancer. The scan was performed from the upper abdomen to mid-thigh. The image sets were transferred to the Monaco treatment planning system version 6,1,4,0 for countering and planning.

Table 2. Patient and tumor characteristics.

Characteristics	
Mean age (range) (y)	68.18 (50-86)
Gender	
Male	14 (82.53%)
Female	3 (17.65%)

The dose prescription and delineation processes were conducted by the same radiation oncologist. The prescription dose for all cases and for both techniques was 55 Gy in 20 fractions, which was prescribed in accordance with the International Commission on Radiation Measurements (ICRU) 83 recommendations. The clinical target volumes, planning target volumes (PTVs), and OARs volumes were contoured according to the RTOG guidelines. The PTV volume was obtained from a uniform 1.5 to 2 cm expansion of the whole bladder clinical target volume; the small bowel, rectum, and femoral heads were contoured as organs at risk.

Both techniques were planned to use Elekta's Monaco treatment planning system (TPS), which can accurately calculate 3D, IMRT, VMAT, SRS, and Brachytherapy plans using the Monte Carlo algorithm (the most accurate dose calculation available). The first treatment plane was created using VMAT, and the 3D-CRT approach was used to re-plane the initial plans. VMAT plans were delivered at a daily dose of 300 cGy. Each plan used two full arcs with clockwise and counterclockwise rotations ranging from 181° to 179°. The collimator angles were set to 355° and 5°, with gantry spacings of 2° and 180 control points per arc. This standardized approach ensured consistency across the VMAT plans, minimizing the variability in beam parameters for a more reliable comparison with 3DCRT. The 3D-CRT plans employed an isocentric technique and contained four photon beams: posteroanterior, anteroposterior, and two opposing lateral fields with varying gantry angles (0°, 90°, 180°, and 270°), utilizing 10 MV of energy, provided by an Elekta infinity linear accelerator machine. The optimization was performed using Monaco version 6,1,4,0 which works on a network of three main high-performance computers (Intel (R) Xeon (R) Gold 6132 CPU @ 2.60 GHz, 2.59 GHz (2 processors), 128 GB, 64-bit operating system, x64-based processors) and is connected to the center's main network.

Evaluation and statistical analysis

A dose-volume histogram was used to evaluate and compare the two techniques. The dosimetrist

required that at least 95% of the volume of each PTV received 95% of the prescribed dose, whereas the OARs received the lowest feasible dose. The PTV was evaluated using the following data: Dmin, Dmax, Dmean, D95cGy, D50cGy, and HI, which is a fast and easy-to-use scoring tool used to assess and quantify dose homogeneity in a target volume. This index can be used to evaluate and compare dose distributions in treatment plans[8]. The formula used in this study to calculate the HI was:

$$HI = \frac{D_{2\%} - D_{98\%}}{D_p}$$

Where Dp denotes the prescribed dose for the PTV, D2% dose to 2% of volume, D98% dose to 98% of volume, and the (CI) which is the ratio of dosage volumes covered to PTV volume, and the following equation is used to calculate CI:

$$CI = \frac{volume\ covered\ by\ 95\%\ of\ prescribed\ dose}{volume\ of\ PTV}$$

The dose limitation for the OARs in the case of BC was defined as the volume of SB that received 45 Gy less than 195cc (V45 < 195 cc). The reference volume percentages (Ref. %) of rectum that received 40 Gy should be less than 80%, (V40 < 80%). The reference volume percentages (Ref. %) of L, R femoral heads that received 40Gy should be less than 10% (V40 < 10%). At dosage levels of 10, 20, 30, 40, and 50 Gy, the irradiated rectum, SB, and femoral heads were calculated and compared between the two distinct treatment planning modalities.

Statistical Package for Social Sciences (SPSS) version 26 was used for data entry and analysis. Two approaches were used. In the first approach, descriptive statistics were used to calculate frequencies and percentages. In the second approach, the normality of data distribution was assessed using the Shapiro-Wilk test. Parametric paired t-tests were used for normally distributed parameters (e.g., Dmean, HI), whereas non-normally distributed metrics (e.g., D50, CI) were analysed using the Wilcoxon Signed Rank test. These paired tests accounted for within-patient correlations, as both techniques were applied to the same cohort, reducing inter-patient variability and increasing statistical power. The significance threshold ($p \leq 0.05$) was chosen a priori to balance Type I error control and sensitivity to clinically meaningful differences.

Results

The study revealed significant variations in dosimetric parameters between the two techniques in patients with BC (**Table 3**). 3D-CRT demonstrated a high mean minimum dose to the PTV (4984.457±327.87 cGy) compared to VMAT (4695.91±215.19cGy), with a p-value=0.01, indicating superior coverage. However, the Dmax, Dmean, and D50 cGy for the PTV was statistically non-significant between 3D-CRT (5997.41±429.53, 5559.92±61.78, 5508.39±188.73) cGy and VMAT (5950.36±56.33, 5551.51±60.90, 5558.14±80.77) cGy, p=(0.64, 0.75, 0.55) respectively. Also, the D95% (cGy) of the PTV was not significantly different between 3D-CRT (5389.05±78.54cGy) and VMAT (5219.6926±328.39cGy, p=0.07), indicating better target coverage in both techniques. As for the HI, which measures the uniformity of dose distribution within the target volume, both 3D-CRT and VMAT had similar homogeneity indices (0.08±0.02 and 0.09±0.02, respectively), with no significant difference (p=0.22). A statistically significant difference was observed when the CI for BC was compared between the 3D-CRT and VMAT methods (p=0.02). The mean CI and SD for VMAT were 0.99±0.02, while for

Table 3. Dosimetric comparison between 3D-CRT and VMAT.

Petameter	3D-CRT	VMAT	p-value
Dmin (cGy)	4984.457±327.87	4695.91±215.19	0.01
Dmax (cGy)	5997.41±429.53	5950.36±56.33	0.64
Dmean (cGy)	5559.92±61.78	5551.51±60.90	0.75
D50 (cGy)	5508.39±188.73	5558.14±80.77	0.55*
D95 (cGy)	5389.05±78.54	5219.6926±328.39	0.07
HI	0.08±0.02	0.09±0.02	0.22
CI	0.97±0.02	0.99±0.02	0.02*
Mus	368.04±37.29	975.04±267.12	<0.001

Notes: Dmin = minimum dose; Dmax = maximum dose; Dmean = mean dose; HI = homogeneity index; D*x* = dose to *x*% of volume; 3D-CRT = three-dimensional conformal radiation therapy; VMAT = volumetric modulated arc therapy; CI = conformity index; PTV = planning target volume; *= Wilcoxon singed rank test.

Table 4. Comparison of (OARs) dosimetric volume in 3D-CRT plan and VMAT plan.

OARs	Dose volume (Gy)	3D-CRT (%)	VMAT (%)	p-value
SB	V10	15.58±6.63	57.70±27.98	<0.001
	V20	12.84±5.73	43.93±22.22	<0.001
	V30	9.21±4.08	27.27±15.04	<0.001
	V40	7.18±2.55	15.70±8.98	<0.001
	V45	6.94±2.91	6.50±3.11	0.43
	V50	5.94±2.69	3±1.19	<0.001
Rectum	V10	89.39±7.78	88.17±9.05	0.46
	V20	84.86±9.94	70.52±15.31	<0.001
	V30	58.66±27.18	37.04±18.72	0.001
	V40	15.97±12.57	17.29±14.49	0.39
	V50	9.95±9.19	4.49±5.41	<0.001
RFH	V10	77.81±16.64	80.59±12.69	0.41
	V20	67.81±18.75	40.48±13.57	<0.001
	V30	56.91±25	6.81±4.06	<0.001
LFH	V10	75.90±16.73	84.68±13.09	0.01
	V20	68.87±17.83	37.34±4.41	<0.001
	V30	57.42±23.29	7.39±5.15	<0.001

Notes: D*x* = dose to *x*% of volume; 3D-CRT = three-dimensional conformal radiation therapy; Gy= grey; VMAT = volumetric modulated arc therapy; RFH= right femoral heads; OAR = organs at risk; V*x* = volume receiving *x* Gy; LFH = left femoral head; SB= small bowel.

3D-CRT they were 0.97±0.02. This suggests that the VMAT conformance is better than that of 3D-CRT.

The comparison of the MUs for the both techniques, VMAT demonstrated a notably higher MU with mean (975.04 ± 267.12) compared to 3D-CRT (368.04 ± 37.29), with a p-value of <0.001, indicating that VMAT uses dynamic modulation of radiation dose, requiring more MUs for precise dose conformity, especially in complex target shapes like bladders. Higher MUs may be necessary for a highly conformal dose distribution, ensuring that tumours receive the full prescribed dose while minimizing exposure to organs at risk (OARs). VMAT's ability of VMAT to modulate the dose intensity within each arc allows for the superior protection of healthy tissues. Increased MUs may also reflect efforts to achieve consistent and comprehensive dose coverage in BC cases.

Significant discrepancies were found between the 3D-CRT and VMAT dosimetric comparisons at different dose-volume levels for the OAR, as shown in **Table 4**. For the SB, at V10, V20, V30, and V40, 3D-CRT exhibited a significantly lower than the VMAT (p-value < 0.001), with the VMAT continuously offering greater dosage coverage. At higher doses, such as V45 and V50, the result for VMAT was very high, significantly lower than that for 3D-CRT with a p-value < 0.001. For the rectum, the 3D-CRT technique had significantly higher values, especially at V20 and V50, with a p-value<0.001, which suggested a broader dosage distribution across volume levels. At V40, the results showed that the statistical difference between the two techniques was not significant. Again, in the RFH and LFH, the 3D-CRT technique demonstrated a significantly higher statistical significance than VMAT throughout V20 and V30 (p < 0.001).

Discussion

In the current study, 3D-CRT and VMAT plan comparisons were conducted to determine the most effective treatment planning method for patients with BC.

Regarding PTV parameters, it has been noted that the PTV parameters such as: Dmax, Dmean, D50 cGy, and D95 cGy of the two modalities were not statistically significant. This indicated that both VMAT and

3D-CRT can ensure adequate target coverage. These outcomes are consistent with earlier studies that showed the dosimetric benefits of VMAT over 3D-CRT methods. In 2022, Agrawal et al. compared the dosimetric outcomes of 3D-CRT and VMAT in locally advanced cervical cancer, offering important information on their relative efficacy. Improved D95% and D50% values from VMAT demonstrated a more consistent dose distribution and higher coverage of the planning target volume PTV[9]. Pasciuti et al.[10] found that a better minimum target coverage was observed in VMAT plans than in 3D-CRT plans, and this result aligns with the outcome of this study. In terms of HI, the results were not statistically significant for both techniques, demonstrating improved dose homogeneity for both techniques. VMAT provides patients with BC with a more accurate treatment plan and an improved conformity index compared to 3D-CRT. These results confirmed its use as a suggested treatment method for bladder cancer by improving tumor control and reducing side effects. These outcomes are consistent with earlier research that showed the dosimetric benefits of VMAT over 3D-CRT methods. According to Matsumoto et al., the CIs of the VMAT and IMRT plans were superior to those of the 3D-CRT plan (p=0.047 and p=0.047, respectively). Concerning the OARs, Comparative dosimetric benefits are identified when small-bowel radiation therapy with VMAT is used instead of 3D-CRT in BC reirradiation, especially at high doses. VMAT is more effective in reducing radiation to the OARs, specifically the small intestine, and provides adequate coverage of the tumor[11].

While Alnagmy et al. reported that VMAT benefits OARs and treatment efficiency, other studies suggest that, in some cases, 3D-CRT can be clinically effective, especially in instances where the complexity of treatment is a concern[12]. Based on Rooijen et al.[13] study, VMAT markedly reduces the volume receiving a high dose to the small bowel when compared to 3D-CRT. The VMAT methods recorded a reduction in V (40 Gy) from 114 cc to 66 cc through IMRT. In relation to other OARs, including the rectum, RFH, and LFH, our results demonstrated that VMAT has a superior dose distribution, which may increase patient tolerance to therapy and better spare OARs. This result is aligned with that of Sherry et al. in 2019[3], who showed that, as compared to 3D-CRT, VMAT dramatically reduces the radiation exposure to vital organs such as the small intestine and rectum, with reductions of >50% in some dose volumes. Finally, in terms of LFH, the two techniques performed similarly at lower dosage levels, but at greater dose volumes, the VMAT technique had better coverage, indicating its possible benefit in more precisely sparing or targeting tissue.

The comparison of MUs, VMAT, and 3D-CRT revealed significant implications for treatment planning outcomes in patients with BC. VMAT generally requires more MUs than 3D-CRT, which can lead to a longer treatment planning. This is due to the fact that the VMAT employs radiation with a continuous gantry motion, precisely targeting tumours while preserving healthy tissues by varying beam intensity, speed, and MLC locations. 3D-CRT is simple and employs static beams without intensity modulation. To attain the superior dosage conformance that VMAT seeks, additional MUs are needed. In contrast to the more straightforward uniform beams of 3D-CRT, the sophisticated modulation results in a higher MU count. Furthermore, our results concur with those of earlier studies, such as Foroudi et al. (2012), who reported that VMAT has a mean of 403 MUs compared to 267 MUs for 3D-CRT, indicating a more efficient delivery system[2].

Although the findings of this study provide valuable insights into the dosimetric advantages of VMAT over 3D-CRT in bladder cancer treatment, it is important to acknowledge several limitations. First, the small sample size may limit the generalizability of the results, particularly given the heterogeneity of bladder cancer cases and anatomical variations. Additionally, the study focused solely on dosimetric outcomes without correlating them with clinical endpoints, such as tumor control rates, survival, or toxicity profiles, which are critical for assessing real-world therapeutic efficacy. The short enrollment period and single-institution design may also introduce selection or institutional bias despite efforts to standardize protocols. Future research should prioritize larger multicenter trials with extended follow-up to evaluate long-term clinical outcomes, including patient-reported toxicity and quality of life. Furthermore, integrating advanced imaging techniques (e.g., MRI-guided planning) or exploring hybrid approaches that combine VMAT with immunotherapy or chemotherapy could enhance treatment precision and outcomes. Finally, comparative studies with other modalities, such as proton therapy or stereotactic body radiation therapy (SBRT), may further refine bladder cancer radiotherapy strategies.

Conclusions

The study demonstrated that both VMAT and 3D-CRT achieved comparable target coverage for bladder cancer radiotherapy, with no significant differences in PTV dose metrics, such as Dmax, Dmean, or D95. However, VMAT exhibits superior conformity (higher CI) and statistically significant advantages in sparing organs at risk (OARs), particularly at higher dose levels (e.g., reduced small bowel V45, rectum V50, and femoral head doses). These dosimetric benefits suggest that VMAT may lower the risk of late toxicities such as gastrointestinal complications or bone

marrow suppression, potentially improving patient quality of life during and after treatment.

Fundings

This article has not received any specific grant from funding agencies in the public, commercial, or for-profit sectors.

Conflict of interest

The authors declare no conflicts of interest.

Author contributions

All authors contributed to the study conception and design. All authors read and approved the final manuscript.

Ruaa Emad Al-Khalidi, Nashwan Karkhi Abdulkareem, Cheman Baker Ismael, Ibrahim Jalal Mustafa, Arthur Saniotis, Rojgar Najat Yousif, Ahmed Sami Kamal: material preparation, data collection and analysis were performed.

Arthur Saniotis, Ruaa Emad Al-Khalidi, Nashwan Karkhi Abdulkareem, Cheman Baker Ismael, Ibrahim Jalal Mustafa, Arthur Saniotis, Rojgar Najat Yousif, Ahmed Sami Kamal: the first draft of the manuscript was written, and all authors commented on previous versions of the manuscript.

Ethics approval

Ethical approval was waived by the local Ethics Committee of Hawler Medical University in view of the retrospective nature of the study and all the procedures being performed were part of the routine care. In this study, anonymized treatment planning data was employed in a retrospective analysis. No identifying patient information was obtained, and no direct patient interaction took place.

References

1. Dobruch J,Oszczudłowski M, Bladder Cancer: current challenges and future directions. Medicina (Kaunas) 2021;57(8):749. Available from: https://doi.org/10.3390/medicina57080749.
2. Foroudi F, Wilson L, Bressel M, Haworth A, Hornby C, Pham D, et al., A dosimetric comparison of 3D conformal vs intensity modulated vs volumetric arc radiation therapy for muscle invasive bladder cancer. Radiat Oncol 2012;7:111. Available from: https://doi.org/10.1186/1748-717x-7-111.
3. Sherry AD, Stewart A, Luo G,Kirschner AN. Intensity-modulated radiotherapy is superior to three-dimensional conformal radiotherapy in the trimodality management of muscle-invasive bladder cancer with daily cone beam computed tomography optimization. J Radiat Oncol 2019;8(4):395-403. Available from: https://doi.org/10.1007/s13566-019-00411-0.
4. Krug D, Köder C, Häfner MF, Arians N, Harrabi SB, Koerber SA, et al. Acute toxicity of normofractionated intensity modulated radiotherapy with simultaneous integrated boost compared to three-dimensional conformal radiotherapy with sequential boost in the adjuvant treatment of breast cancer. Radiat Oncol 2020;15(1):235. Available from: https://doi.org/10.1186/s13014-020-01652-x.
5. Tonetto F, Magli A, Moretti E, Guerini AE, Tullio A, Reverberi C, et al., Prostate cancer treatment-related toxicity: comparison between 3D-conformal radiation therapy (3D-CRT) and volumetric modulated arc therapy (VMAT) techniques. J Clin Med 2022;11(23):6913. Available from: https://doi.org/10.3390/jcm11236913.
6. Palma D, Vollans E, James K, Nakano S, Moiseenko V, Shaffer R, et al. Volumetric modulated arc therapy for delivery of prostate radiotherapy: comparison with intensity-modulated radiotherapy and three-dimensional conformal radiotherapy. Int J Radiat Oncol Biol Phys 2008;72(4):996-1001. Available from: https://doi.org/10.1016/j.ijrobp.2008.02.047.
7. Regnier A, Ulbrich J, Münch S, Oechsner M, Wilhelm D, Combs SE, et al., Comparative analysis of efficacy, toxicity, and patient-reported outcomes in rectal cancer patients undergoing preoperative 3D conformal radiotherapy or VMAT. Front Oncol 2017;7:225. Available from: https://doi.org/10.3389/fonc.2017.00225.
8. Desai DD, Johnson EL,Cordrey IL, The surface area effect: how the intermediate dose spill depends on the PTV surface area in SRS. J Appl Clin Med Phys 2021;22(3):186-195. Available from: https://doi.org/10.1002/acm2.13203.
9. Agrawal A, Hadi R, Rath S, Bharati A, Rastogi M, Khurana R, et al. Dosimetric comparison of 3-dimensional conformal radiotherapy (3D-CRT) and volumetric-modulated arc therapy (VMAT) in locally advanced cancer cervix. Journal of Radiotherapy in Practice 2022;21(1):60-67. Available from: https://doi.org/10.1017/S1460396920000849.
10. Pasciuti K, Kuthpady S, Anderson A, Best B, Waqar S, Chowdhury S. Bladder radiotherapy treatment: a retrospective comparison of 3-dimensional conformal radiotherapy, intensity-modulated radiation therapy, and volumetric-modulated arc therapy plans. Med Dosim 2017;42(1):1-6. Available from: https://doi.org/10.1016/j.meddos.2016.09.003.
11. Matsumoto T, Toya R, Shimohigashi Y, Watakabe T, Matsuyama T, Saito T, et al. Plan quality comparisons between 3D-CRT, IMRT, and VMAT based on 4D-CT for gastric MALT lymphoma. Anticancer Res 2021;41(8):3941-3947. Available from: https://doi.org/10.21873/anticanres.15190.
12. Alnagmy A, Zaghloul MS, Mahmoud M, Aboelkasem H, Mokhtar MH, Awad A. Dosimetric comparison between intensity modulated radiotherapy and three-dimensional conformal radiotherapy in adjuvant setting after radical cystectomy in high-risk urothelial bladder cancer. International Journal of Health Sciences 2022;6(S6):7366-7375. Available from: https://doi.org/10.53730/ijhs.v6nS6.11819.
13. Van Rooijen DC, Van de Kamer JB, Hulshof MC, Koning CC, Bel A. Improving bladder cancer treatment with radiotherapy using separate intensity modulated radiotherapy plans for boost and elective fields. J Med Imaging Radiat Oncol 2010;54(3):256-63. Available from: https://doi.org/10.1111/j.1754-9485.2010.02169.x.

ACADEMIC JOURNAL OF HEALTH SCIENCES
MEDICINA BALEAR

Original

The effect of a removable partial denture on the periodontal health of abutments in patients wearing dental prostheses

Efecto de una prótesis parcial removible sobre la salud periodontal de los pilares en pacientes portadores de prótesis dentales

Tabarek A. Fakhri[1], Vian Mohammed Hussein[2]*

[1]Dental Surgery, Hawler Center, Erbil, Kurdistan Region, Iraq
[2]Dental Public Health Department, Kurdistan Higher Council of Medical Specialties, Kurdistan Region, Iraq

Received:12-03-2025
Accepted: 30-04-2025

***Corresponding author**: Vian Mohammed Hussein. vian_jaf@yahoo.com.

Abstract

Introduction: removable partial dentures (RPDs) are widely used to restore oral function in partially edentulous patients. However, their long-term success depends on preserving the periodontal health of abutment teeth. This study aimed to evaluate periodontal health in primary and secondary abutment teeth supporting RPDs in Erbil, Iraq.

Materials and method: a cross-sectional study of 130 RPD wearers at Khanzad Teaching Center assessed periodontal parameters (plaque index (PI), calculus index (CI), bleeding on probing (BOP), probing depth (PD), tooth mobility (TM), and gingival recession) in abutment versus adjacent non-abutment teeth. Data were analyzed using Mann-Whitney U tests and paired-sample t-tests.

Results: abutment teeth exhibited significantly higher mean scores than adjacent teeth for PI (1.90 ± 0.59 vs. 1.23 ± 0.42), gingival index (1.95 ± 0.66 vs. 1.15 ± 0.32), TM (1.25 ± 0.43 vs. 1.02 ± 0.12), and recession (1.51 ± 2.02 vs. 0.82 ± 1.41) ($p < 0.001$ for all except recession $p = 0.010$). Poor oral hygiene, inadequate denture design, and delayed periodontal care exacerbated these outcomes.

Conclusions: RPD abutment teeth face heightened periodontal risks due to mechanical stress, plaque retention, and hygiene challenges. Emphasis on precise RPD design, patient education, and regular periodontal monitoring is critical to mitigate tooth loss and prosthetic failure.

Keywords: Periodontal diseases. Oral hygiene. Tooth mobility.

Resumen

Introducción: las prótesis parciales removibles (PPR) se utilizan ampliamente para restaurar la función oral en pacientes parcialmente edéntulos. Sin embargo, su éxito a largo plazo depende de la preservación de la salud periodontal de los dientes pilares. Este estudio tuvo como objetivo evaluar la salud periodontal de los dientes pilares primarios y secundarios que soportan PPR en Erbil, Irak.

Materiales y método: se realizó un estudio transversal en 130 usuarios de PPR en el Centro Docente Khanzad, evaluando parámetros periodontales (índice de placa [IP], índice de cálculo [IC], sangrado al sondaje [SS], profundidad de sondaje [PS], movilidad dentaria [MD] y recesión gingival) en dientes pilares en comparación con dientes adyacentes no pilares. Los datos se analizaron mediante pruebas U de Mann-Whitney y pruebas t para muestras emparejadas.

Cite as: Fakhri TA, Hussein VM. The effect of a removable partial denture on the periodontal health of abutments in patients wearing dental prostheses. Acad J Health Sci 2025; 40(5): 22-29. Available from: https://doi.org/10.3306/AJHS.2025.40.05.3

Acad J Health Sci 2025; 40(5): 22-29
https://doi.org/10.3306/AJHS.2025.40.05.3
www.ajhealthsciences.com

Resultados: los dientes pilares presentaron puntuaciones medias significativamente más altas que los dientes adyacentes para el IP (1,90 ± 0,59 vs 1,23 ± 0,42), el índice gingival (1,95 ± 0,66 vs 1,15 ± 0,32), la MD (1,25 ± 0,43 vs 1,02 ± 0,12) y la recesión (1,51 ± 2,02 vs 0,82 ± 1,41) (p<0,001 para todos, excepto recesión p=0,010). La mala higiene oral, un diseño protésico inadecuado y el retraso en la atención periodontal agravaron estos resultados.

Conclusiones: los dientes pilares de PPR enfrentan mayores riesgos periodontales debido al estrés mecánico, la retención de placa y los desafíos de higiene. Es fundamental enfatizar un diseño preciso de la PPR, la educación del paciente y un monitoreo periodontal regular para reducir la pérdida dentaria y el fracaso protésico.

Palabras clave: Enfermedades periodontales. Higiene oral. Movilidad dentaria.

Introduction

Removable partial dentures (RPDs) remain a cornerstone in prosthetic dentistry for rehabilitating partially edentulous patients, offering functional and aesthetic restoration while preserving remaining dental structures[1]. As a cost-effective and non-invasive solution, RPDs are particularly vital for individuals with financial constraints or anatomical limitations precluding implant-supported alternatives[2].

The periodontium is the supporting structure of teeth, and its health is crucial for maintaining the stability and function of teeth[3]. Therefore, the RPDs' long-term success is intrinsically linked to the preservation of periodontal health in teeth serving as abutments. These teeth, which anchor the prosthesis, are subjected to altered biomechanical forces, microbial challenges, and hygiene accessibility issues, all of which may compromise periodontal stability[4].

Clinical studies consistently report higher plaque index (PI), gingival index (GI), and probing depth (PD) in abutments compared to non-abutment teeth, suggesting a heightened risk of gingivitis and periodontitis[4,5]. For instance, a longitudinal study involving 205 RPD wearers revealed significant differences in periodontal parameters, with abutments exhibiting greater plaque retention, gingival recession, and mobility over 1–10 years of use[4]. This is attributed to factors such as plaque accumulation beneath denture bases, altered salivary flow, and stress concentration on supporting teeth during mastication[6]. Similarly, a 3-month follow-up demonstrated progressive deterioration in bleeding on probing (BOP) and PD among abutments, emphasizing the dynamic nature of periodontal compromise[7].

Conversely, some studies argue that meticulously fabricated RPDs with precise fit and occlusal harmony do not inherently jeopardize periodontal health, provided preprosthetic periodontal therapy is completed and oral hygiene is maintained[8]. Such discrepancies underscore the role of confounding variables, including patient-specific factors and denture-related characteristics, in modulating outcomes[4,7].

Despite advances in understanding RPD-periodontium interactions, significant gaps persist in the literature. The novelty of the present study lies in its comprehensive evaluation of periodontal health in both primary and secondary abutment teeth, addressing a critical oversight in prior research. The present study aimed to assess the periodontal health of the primary and secondary abutment teeth supporting partial denture prostheses. Since very few studies have examined the periodontal health of primary and secondary abutments supporting partial dentures simultaneously, the current study aimed to assess the periodontal health of the primary and secondary abutment teeth supporting partial denture prostheses in Erbil, Kurdistan region, Iraq.

Materials and method

Study design and setting

This cross-sectional analytical study was conducted at Khanzad Teaching Center in Erbil, Kurdistan Region, Iraq, between January 2022 and June 2023. The study aimed to evaluate the periodontal health of primary and secondary abutment teeth supporting RPDs.

Participants

Participants were recruited from patients attending the Prosthodontics Department of Khanzad Teaching Center. Patients aged 18 years and older who were partial wearers of RPDs and willing to participate in the study were included. Participants were chosen using convenience sampling, contingent upon their availability and willingness to engage at their regular dentist appointments. A total of 130 participants entered the study.

Inclusion criteria were as follows: patients aged 18 years and older, partial wearers of RPDs, both male and female, and those willing to participate in the study. Exclusion criteria included patients wearing overdentures, removable prostheses for maxillofacial defects, or those using denture adhesives.

Additionally, patients with systemic conditions that could affect periodontal health, such as uncontrolled diabetes or immunocompromising diseases, were excluded to minimize confounding factors.

Data collection

Data collection involved clinical examinations and patient questionnaires. Patient questionnaires collected demographic information (age, gender, education level), smoking status, denture type (acrylic or chrome cobalt), occlusion status, denture fit, frequency of denture cleaning, and history of periodontal treatment.

Clinical examinations were conducted by calibrated dentists using standardized periodontal probes (Williams Probe, Hu-Friedy) and oral mirrors. Measurements were taken on the mesial, distal, buccal, and lingual surfaces of each tooth. The following periodontal parameters were assessed for abutment and non-abutment teeth:

Plaque index (PI)

The PI according to Silness and Löe (1964) was used to assess the amount of dental plaque on the teeth. The index ranges from 0 to 3. 0: no plaque present; 1: a film of plaque adhering to the gingival area; 2: moderate accumulation of soft deposits; 3: abundance of soft matter within the gingival pockets. The normal range for PI is 0-1, indicating good oral hygiene. A score of 2-3 is considered abnormal and suggests poor plaque control[9].

Calculus index (CI)

The CI according to Green and Vermillion (1964) was used to evaluate the presence of dental calculus. The index ranges from 0 to 3. 0: no calculus present; 1: supragingival calculus covering up to 1/3 of the tooth surface; 2: supragingival calculus covering between 1/3 and 2/3 of the tooth surface; 3: supragingival calculus covering more than 2/3 of the tooth surface or presence of subgingival calculus. A CI score of 0-1 is considered normal, while a score of 2-3 indicates significant calculus accumulation[10].

Bleeding on probing (BOP)

The BOP metric, as defined by Ainamo and Bay (1975), was evaluated by delicately probing the gingival sulcus and monitoring for blood within a 10-second interval. The normal range is 0 or - (no bleeding), and a score of 1 or + (bleeding) is considered abnormal and indicative of gingival inflammation[11].

Probing pocket depth (PD)

The PD was assessed from the gingival edge to the base of the periodontal pocket using a Williams Probe (Hu-Friedy). The normal range for PD is 0-3 mm. A PD of 4 mm or more was considered abnormal and suggests periodontal disease[12].

Tooth mobility (TM)

TM was recorded according to Miller (1985) on a scale from 0 to 3. 0: no mobility; 1: mobility less than 1 mm in the horizontal direction; 2: mobility greater than 1 mm in the horizontal direction; 3: mobility in the apical-vertical direction. A TM score of 0-1 was considered normal, while a score of 2-3 indicates abnormal TM and may suggest periodontal support loss[7].

Gingival recession

Gingival recession was assessed as the distance from the cementoenamel junction to the gingival margin. A recession of 0-1 mm is considered normal, while a recession of 2 mm or more is abnormal and may be associated with gingival tissue loss.

Statistical analysis

Data were analyzed using IBM SPSS Statistics software (version 26.0). Descriptive statistics, including mean, standard deviation, median, and interquartile range, were calculated for PI, gingival index, TM, and gingival recession. The Kolmogorov-Smirnov and Shapiro-Wilk tests were used to assess data normality. Differences in PI between clasped and adjacent non-clasped teeth were analyzed using the Mann-Whitney U test. The Mann-Whitney U test was also applied to compare TM scores between groups. The paired samples t-test (or Wilcoxon signed- rank test for non-normally distributed data) was used to evaluate differences in gingival recession within the primary abutment group. Multivariate analyses were conducted to adjust for potential confounding variables. A significant level of $p \leq 0.05$ was set for all statistical tests.

Results

Table 1 presents the demographic and sample characteristics of participants in the study evaluating the effect of RPDs on the periodontal health of abutments. The sample comprised 130 patients, with a higher proportion of females 74 (56.9%) than males 56 (43.1%). Most participants, 60 (46.2%), were aged 50–59 years. Education levels were predominantly primary/secondary 70 (53.8%). Most participants were non-smokers 83 (63.8%), and over half reported no systematic diseases 73 (56.2%).

Table 1. Demographic and sample characteristics.

Variable		Frequency	Percentage
Sex	Male	56	43.1%
	Female	74	56.9%
Age	40–49	21	16.2%
	50–59	60	46.2%
	≥60	49	37.7%
Education	Illiterate	4	3.1%
	Read/Write	30	23.1%
	Primary/Secondary	70	53.8%
	Diploma/Higher	26	20.0%
Smoking	Yes	47	36.2%
	No	83	63.8%
Systematic disease	Yes	57	43.8%
	No	73	56.2%

Table 2. Denture characteristics and clinical status.

Variable		Frequency	Percentage
Denture type	Acrylic	124	95.4%
	Chrome Cobalt	4	3.1%
	3.00	2	1.5%
Abutment tooth status	Sound	45	34.6%
	Carious	71	54.6%
	Filled	14	10.8%
Occlusion status	Class 1	36	27.7%
	Class 2	90	69.2%
	Class 3	4	3.1%
Denture location	Maxilla	57	43.8%
	Mandible	73	56.2%
	New wearing	4	3.1%
Duration of use	One year or less	4	3.1%
	1-5 years	97	74.6%
	More than 5 years	25	19.2%
Kennedy classification	Class 1	20	15.4%
	Class 2	54	41.5%
	Class 3	54	41.5%
	Class 4	2	1.5%

Acrylic dentures predominated (124, 95.4%), with carious abutment teeth being the most common status (71, 54.6%). Class 2 occlusion was the most frequent occlusal relationship (90, 69.2%), and dentures were more often placed in the mandible (73, 56.2%). Most participants had used their dentures for 1–5 years (97, 74.6%), while Kennedy Class 2 and Class 3 were equally prevalent (54, 41.5% each) (**Table 2**).

Table 3 presents the maintenance and oral hygiene practices of patients wearing dental prostheses. The majority of patients (92, 70.8%) reported cleaning their dentures regularly. Most patients (97, 74.6%) brushed their teeth once a day and a significant number of patients (108, 83.1%) experienced gingival bleeding during brushing. Regarding periodontal treatment, an equal number of patients (65, 50.0%) had received treatment and had not. The majority of patients (118, 90.8%) removed their dentures overnight.

The descriptive statistics of periodontal indices comparing abutment teeth to adjacent teeth are shown in **Table 4**. Abutment teeth exhibited higher mean PI (1.90 ± 0.59 vs. 1.23 ± 0.42), gingival index (1.95 ± 0.66 vs. 1.15 ± 0.32), mobility index (1.25 ± 0.43 vs. 1.02 ± 0.12), and recession index (1.51 ± 2.02 vs. 0.82 ± 1.41) compared to adjacent teeth.

The results of the normality tests and comparisons between clasped and adjacent teeth for periodontal health indices are presented in **Table 5**. The Kolmogorov-Smirnov and Shapiro- Wilk tests confirmed non-normal distributions for all indices (p=0.000). Mann-Whitney U tests revealed statistically significant differences between clasped and adjacent

Table 3. Maintenance and oral hygiene practices.

Variable		Frequency	Percentage
Cleaning denture	Yes	92	70.8%
	No	38	29.2%
Brushing frequency	Once a day	97	74.6%
	Twice a day	29	22.3%
	Three times daily	4	3.1%
Gingival bleeding on brushing	Yes	108	83.1%
	No	22	16.9%
Periodontal treatment	Yes	65	50.0%
	No	65	50.0%
Denture removal overnight	Yes	118	90.8%
	No	12	9.2%

Table 4. Descriptive statistics of periodontal indices (abutment vs adjacent teeth).

Index		Statistic	
		Mean ± SD	Median (IQR)
Plaque index	Abutment tooth	1.90 ± 0.59	1.75 (0.5)
	Adjacent tooth	1.23 ± 0.42	1.00 (0.25)
Gingival index	Abutment tooth	1.95 ± 0.66	2.00 (0.5)
	Adjacent tooth	1.15 ± 0.32	1.00 (0.25)
Mobility index	Abutment tooth	1.25 ± 0.43	1.00 (0.25)
	Adjacent tooth	1.02 ± 0.12	1.00 (0.0)
Recession index	Abutment tooth	1.51 ± 2.02	0.00 (4.0)
	Adjacent tooth	0.82 ± 1.41	0.00 (2.0)

Table 5. Normality tests and clasped vs adjacent teeth comparisons.

Index	Kolmogorov- Smirnov	Shapiro- Wilk	Mann-Whitney U	Mean Rank (Clasped)	Mean Rank (Adjacent)	p-value
Plaque	0.232 (p=0.000)	0.872 (p=0.000)	2772.50	174.17	86.83	0.000
Gingival	0.240 (p=0.000)	0.856 (p=0.000)	2127.00	179.14	81.86	0.000
Mobility	0.469 (p=0.000)	0.535 (p=0.000)	6500.00	145.50	115.50	0.000
Recession	0.395 (p=0.000)	0.687 (p=0.000)	7153.50	140.47	120.53	0.010

teeth for PI (U=2772.50, mean rank: 174.17 vs. 86.83, p=0.000), gingival index (U=2127.00, mean rank: 179.14 vs. 81.86, p=0.000), mobility (U=6500.00, mean rank: 145.50 vs. 115.50, p=0.000), and recession (U=7153.50, mean rank: 140.47 vs. 120.53, p=0.010).

Discussion

The results of the current study indicate that abutment teeth supporting RPDs in patients at Khanzad Teaching Center exhibit significantly poorer periodontal health compared to adjacent non-abutment teeth. Specifically, abutment teeth demonstrated higher plaque accumulation, gingival inflammation, mobility, and gingival recession, suggesting that the presence and use of RPDs may contribute to localized periodontal deterioration.

The oral health status of geriatric patients is influenced by their educational attainment and socioeconomic status. Previous research has shown a positive correlation between higher levels of education and socioeconomic stability with greater interest in maintaining oral health[13]. The relationship between smoking and oral hygiene has been extensively examined in the literature. Previous studies have consistently reported that smoking negatively impacts oral hygiene. The findings of this study, which indicate a higher prevalence of good oral and denture hygiene among non-smokers compared to smokers, align with the results of several prior investigations[14,15].

Research by Geiballa et al. highlights a notable gap in clinical practice, as most dental professionals demonstrated insufficient adherence to providing comprehensive post-treatment instructions for maintaining fixed prosthetic restorations[16]. This lack of emphasis on long- term care protocols may contribute to compromised outcomes in patients with fixed prostheses.

Similarly, findings from the current study reveal a heightened prevalence of gingival inflammation and bleeding among individuals utilizing removable RPDs. Furthermore, clinical observations identified increased TM and localized gingival recession, particularly in abutment teeth, when compared to adjacent non-abutment teeth, suggesting a disproportionate susceptibility to periodontal compromise in these critical supporting structures.

These observations align with prior evidence from Dubravka's study, which systematically evaluated the periodontal health of abutment and non-abutment teeth in RPD wearers. The study reported statistically significant differences in key clinical parameters, including higher plaque accumulation, gingival inflammation, PDs, gingival recession, and TM in abutment teeth relative to their non-abutment counterparts. Such disparities underscore the mechanical and microbial challenges inherent in prosthetic support systems, which may exacerbate periodontal deterioration specifically at abutment sites[4].

Further longitudinal insights were provided by Linda Dula et al., who assessed the temporal impact of RPD placement on periodontal health through serial measurements of PI, CI, BOP, PD, and TM at baseline, one month, and three months post-insertion. Their results demonstrated a progressive decline in periodontal stability, with abutment teeth exhibiting significantly greater increases in BOP scores (1.53 ± 0.50 vs. 1.76 ± 0.43), PD changes (0.28± 0.45 mm vs. 0.12 ± 0.33 mm), and plaque accumulation (PLI: 1.20 ± 0.46 vs. 0.75 ± 0.64) compared to non-abutment teeth by the three-month follow-up. These findings emphasize the dynamic interplay between prosthetic

design, oral hygiene maintenance, and periodontal health, particularly in teeth subjected to the biomechanical stresses of RPD support[7].

The construction of a RPD should ensure adequate support from abutment teeth, maintain periodontal health, and achieve proper occlusion. The number of abutment teeth incorporated in the RPD is a critical factor influencing periodontal status[17]. Additionally, occlusal rests in partial dentures play a vital role in transmitting masticatory forces along the vertical axis of the teeth. These rests are designed to fit into a spoon-shaped preparation on the abutment teeth, with the floor inclined such that its deepest point aligns with the vertical axis of the teeth, thereby optimizing force distribution[18].

The primary factor contributing to the failure of RPDs is the loss of abutment teeth, primarily due to periodontal deterioration and dental caries. Failure to replace temporary partial dentures with cast partial dentures results in excessive occlusal stress on the primary abutment teeth. This stress is subsequently transmitted to the supporting periodontal structures, leading to progressive deterioration characterized by gingival recession, loss of attachment, and eventual alveolar bone resorption[19].

To mitigate these risks, meticulous treatment planning is essential, including the appropriate design of RPDs, patient education on oral hygiene practices, regular prosthesis maintenance, and routine dental evaluations to ensure long-term periodontal and prosthetic stability.

Conclusions

The findings of this study demonstrate that abutment teeth supporting RPDs exhibit significantly compromised periodontal health compared to adjacent non-abutment teeth, with higher plaque accumulation, gingival inflammation, tooth mobility, and gingival recession observed in abutment sites. These results underscore the mechanical and microbial challenges associated with RPDs, including altered force distribution, plaque retention beneath denture bases, and hygiene accessibility issues, which collectively exacerbate periodontal deterioration. Factors such as inadequate denture design, insufficient oral hygiene practices, and delayed periodontal care further contribute to the vulnerability of abutment teeth. The study highlights the critical need for meticulous RPD fabrication with optimal occlusal harmony, comprehensive patient education on oral and prosthetic hygiene, and regular clinical follow-ups to mitigate periodontal risks.

Acknowledgments

We extend our heartfelt appreciation to everybody who dedicated their time, effort, and skill to ensure the success of this research.

Funding

This article has not received any specific grant from funding agencies in the public, commercial, or for-profit sectors.

Conflict of interest

The authors declare no conflicts of interest.

Data availability

Upon reasonable request, the data from the research may be obtained from the corresponding author.

Authors contribution

Each author made an equal contribution to this research work.

Ethical considerations

The study protocol was approved by the Ethics Committee of Khanzad Teaching Center (approval number: 2374). Written informed consent was obtained from all participants prior to data collection. Participants were informed about the study objectives, procedures, potential risks, and benefits. Confidentiality of participant data was ensured by assigning unique identification numbers to all records.

References

1. Awawdeh M, Alotaibi MB, Alharbi AH, Alnafisah SA, Alasiri TS, Alrashidi NI. A systematic review of patient satisfaction with removable partial dentures (RPDs). Cureus 2024;16(1):e51793. Available from: https://doi.org/10.7759/cureus.51793.
2. Gotfredsen K, Rimborg S, Stavropoulos A. Efficacy and risks of removable partial prosthesis in periodontitis patients: A systematic review. J Clin Periodontol 2022;49(24):167-81. Available from: https://doi.org/10.1111/jcpe.13519.
3. Torabi S, Soni A. Histology, periodontium. In: StatPearls. Treasure Island (FL): StatPearls Publishing. 2025. PMID: 34033366. Bookshelf ID: NBK570604.
4. Knezovic D, Celebić A, Valentic M. The effect of removable partial dentures on periodontal health of abutment and non-abutment teeth. J Periodontol 2002;73(2):137-44. Available from: http://dx.doi.org/10.1902/jop.2002.73.2.137.
5. Almeida ML, De Oliveira ÉPS, Tôrres CdP, Calderon PDS, Carreiro A, Gurgel BdV. Evaluation of periodontal parameters on removable partial denture abutment teeth with direct and indirect retainers: a 48-month follow-up. J Int Acad Periodontol 2020;22(2):10-7.

6. Boumediene S, Houari H, Cheham A, Rahal S, Mhabli D. Effect of removable partial denture on periodontal health. International Dental Journal 2024;74:S368. Available from: https://doi.org/10.1016/j.identj.2024.07.490.
7. Dula LJ, Shala KS, Pustina-Krasniqi T, Bicaj T, Ahmedi EF. The influence of removable partial dentures on the periodontal health of abutment and non-abutment teeth. Eur J Dent 2015;9(3):382-6. Available from: https://doi.org/10.4103/1305-7456.163234.
8. Petridis H, Hempton T. Periodontal considerations in removable partial denture treatment: a review of the literature. Int J Prosthodont 2001;14(2):164-72.
9. AYAN GaD, Burak. Evaluation of plaque index, gingival index and oral health-related quality of life in obese patients. Odovtos 2023;25(1):166-78. Available from: http://dx.doi.org/10.15517/ijds.2022.52533.
10. Garg S, Nasir S. Comparative evaluation of oral hygiene status by using oral hygiene index, simplified oral hygiene index, and modified oral hygiene index: revalidation of modified oral hygiene index. Journal of Indian Society of Periodontology 2024;28(4):461-7. Available from: https://doi.org/10.4103/jisp.jisp_399_23.
11. Trombelli L, Farina R, Silva CO, Tatakis DN. Plaque-induced gingivitis: case definition and diagnostic considerations. J Periodontol 2018;89(S1):S46-S73. Available from: https://doi.org/10.1002/JPER.17-0576.
12. Al Shayeb K, Turner W, Gillam D. Periodontal probing: a review. Primary Dental Journal 2014;3(3):1-11. Available from: http://dx.doi.org/10.1308/205016814812736619.
13. Almajed OS, Aljouie AA, Alharbi MS, Alsulaimi LM. The impact of socioeconomic factors on pediatric oral health: a review. Cureus 2024;16(2):e53567. Available from: https://doi.org/10.7759/cureus.53567.
14. Zimmermann H, Hagenfeld D, Diercke K, El-Sayed N, Fricke J, Greiser KH, et al. Pocket depth and bleeding on probing and their associations with dental, lifestyle, socioeconomic and blood variables: a cross-sectional, multicenter feasibility study of the German National Cohort. BMC oral health 2015;15:7. Available from: https://doi.org/10.1186/1472-6831-15-7.
15. Beklen A, Yildirim BG, Mimaroglu M, Yavuz MB. The impact of smoking on oral health and patient assessment of tobacco cessation support from Turkish dentists. Tobacco Induced Diseases 2021;19:49. Available from: https://doi.org/10.18332/tid/136418.
16. Geiballa GH, Abubakr NH, Ibrahim YE. Patients' satisfaction and maintenance of fixed partial denture. Eur J Dent 2016;10(2):250-3. Available from: https://doi.org/10.4103/1305-7456.178313.
17. Rissin L, Feldman RS, Kapur KK, Chauncey HH. Six-year report of the periodontal health of fixed and removable partial denture abutment teeth. The Journal of Prosthetic Dentistry 1985;54(4):461-7. Available from: https://doi.org/10.1016/0022-3913(85)90413-5.
18. Ellakwa A. Damage caused by removable partial dentures: reality. Dentistry 2012;2(4):2161- 1122.000. Available from: https://doi.org/10.4172/2161-1122.1000e107.
19. Lavanya E, Ganapathy D, Sheeba S. Effect of removable partial denture on periodontal health of abutments. Research Journal of Pharmacy and Technology 2018; 11(6):2587-90. Available from: https://doi.org/10.5958/0974-360X.2018.00478.X.

ACADEMIC JOURNAL OF HEALTH SCIENCES
MEDICINA BALEAR

Original

Evaluation of antifungal effect of bismuth oxide nanoparticle incorporated with heat-cured acrylic

Evaluación del efecto antifúngico de nanopartículas de óxido de bismuto incorporadas en acrílico termoactivado

Mohammed Bawer Dhahir Hanari[1]*, Dara Hamarashid Saeed[2], Saud Jasim Othman[3], Veen Sagvan Jamil[4]

[1]Department of Restorative Dentistry, Khanzad Teaching Center, Erbil, Iraq
[2]Faculty of Dentistry, Hawler Medical University, Erbil, Iraq
[3]Conservative Dentistry, Faculty of Dentistry, Kurdistan Higher Council of Medical Specialties, Erbil, Iraq
[4]Conservative Dentistry, Kurdistan Higher Council of Medical Specialties, Erbil, Iraq

Received: 15-03-2025
Accepted: 02-04-2025

***Corresponding author**: Mohammed Bawer Dhahir Hanari. mohammed.hanari@gmail.com

Abstract

Objectives: The potential action of metal nanoparticles against fungal species of relevance in the pharmaceutical, medical, and agricultural fields has drawn a lot of attention. Metal oxide nanoparticles have distinctive features like a high surface-to-volume ratio that give these particles antifungal capabilities. The objective of this study is to determine the antifungal activity of acrylic resin modified by bismuth oxide nanoparticles.

Materials and methods: This experimental *in-vitro* study conducted in Erbil-Kurdistan region of Iraq from (25 March 2025- 10 April 2025). To evaluate the antifungal properties of heat-cured acrylic resin modified by varying concentrations of bismuth oxide nanoparticles against *Candida albicans*. The evaluation focused on the following details: Colony-Forming Unit, Biofilm Assay, Zone of Inhibition Test.

Result: Five groups were compared to show the antifungal effect. Modified heat-cure acrylic resin by (High concentration: acrylic with 2% (w/w) Bi_2O_3) was gave a good response in 70% of the samples (p-value of ≤ 0.05) and a moderate response in 30% of the samples, while the responses to heat-cure acrylic resin without additives, (Low concentration: acrylic with 0.5% (w/w) Bi_2O_3), and (Medium concentration: acrylic with 1% (w/w) Bi_2O_3) were either poor or moderate (p<0.001).

Conclusions: The antimicrobial test results confirmed that 2% (w/w) Bi_2O_3 Minimal Inhibitory Concentration is crucial for optimizing potential antimicrobial properties of the modified acrylic resin denture base material against *C. albicans*.

Keywords: Antifungal. Bismuth oxide. *Candida albicans*. Metal nanoparticles. Polymethyl methacrylate.

Resumen

Objetivos: la acción potencial de las nanopartículas metálicas contra especies fúngicas de relevancia en los ámbitos farmacéutico, médico y agrícola ha captado una atención considerable. Las nanopartículas de óxidos metálicos presentan características distintivas, como una elevada relación superficie-volumen, que les confieren propiedades antifúngicas. El objetivo de este estudio fue determinar la actividad antifúngica de una resina acrílica modificada mediante la incorporación de nanopartículas de óxido de bismuto.

Cite as: Hanari MBD, Saeed DH, Othman SJ, Jamil VS. Evaluation of antifungal effect of bismuth oxide nanoparticle incorporated with heat-cured acrylic. Acad J Health Sci 2025; 40(5): 30-37. Available from: https://doi.org/10.3306/AJHS.2025.40.05.4

Acad J Health Sci 2025; 40(5): 30-37
https://doi.org/10.3306/AJHS.2025.40.05.4
www.ajhealthsciences.com

Materiales y métodos: este estudio experimental *in vitro* se llevó a cabo en Erbil, región del Kurdistán (Irak), entre el 25 de marzo y el 10 de abril de 2025. Se evaluaron las propiedades antifúngicas de una resina acrílica termoactivada modificada con diferentes concentraciones de nanopartículas de óxido de bismuto frente a *Candida albicans*. La evaluación se centró en los siguientes aspectos: unidades formadoras de colonias (UFC), ensayo de biopelículas y prueba de zona de inhibición.

Resultados: se compararon cinco grupos para evaluar el efecto antifúngico. La resina acrílica termoactivada modificada con una alta concentración (2 % p/p de Bi_2O_3) mostró una buena respuesta en el 70 % de las muestras (valor p≤0,05) y una respuesta moderada en el 30 % restante. En contraste, las respuestas observadas en la resina acrílica sin aditivos, así como en las concentraciones baja (0,5 % p/p de Bi_2O_3) y media (1 % p/p de Bi_2O_3), fueron pobres o moderadas (p<0,001).

Conclusiones: los resultados del ensayo antimicrobiano confirmaron que una concentración mínima inhibitoria del 2 % p/p de Bi_2O_3es determinante para optimizar las propiedades antimicrobianas potenciales de la resina acrílica modificada empleada como base protésica frente a *C. albicans*.

Palabras clave: Antifúngico. Óxido de bismuto. *Candida albicans*. Nanopartículas metálicas. Polimetilmetacrilato.

Introduction

Polymethyl methacrylate (PMMA) is the most often used acrylic resin in the manufacturing of complete and partial removable dentures. Considering its advantages, PMMA denture base resin has several disadvantages that persist in posing challenges in prosthodontic clinical operations, such as perceived porosity and surface roughness, which can serve as bacterial sources[1,2]. In recent decades, the prevalence and incidence of oral candidiasis have increased. Oral candidiasis affects about 54% of patients who wear removable dentures[3]. Denture-induced stomatitis, even if asymptomatic, should be addressed since it might cause infection and promote alveolar bone resorption. This condition can be addressed by improving denture and oral hygiene, correcting the adaptation of the old denture using a tissue conditioner, and using a systemic antifungal and/or topical antifungal treatment when yeast is found[4]. The species of invading *Candida*, dental hygiene habits, and denture properties can all have an impact on *Candida* colonization and biofilm growth on dentures[1].

Oral candidiasis treatment involves the use of standard antifungal medications; however, the rise of drug-resistant *Candida* species compromises this strategy's effectiveness. Therefore, it is necessary to design new therapeutic strategies[5]. Research interest in innovative therapeutic alternatives has grown. The strategies under investigation include the use of natural antifungal essential oils and extracts, antimicrobial nanoparticles (NPs), and intrinsic anti-Candidal materials; substituting biomaterials that can prevent biofilm formation for traditional prosthesis materials and denture adhesives; integrating traditional antifungal medications into delivery systems with controlled and targeted release; and combining strategies to provide the best possible treatment[6-8]. Research has focused on metal oxide nanoparticles for pharmaceutical and medical and agricultural applications because their malfunction of microbial biofilms and pathogen-mediated oxidative stress creates significant antifungal properties[9,10]. The antifungal effectiveness of metal oxide nanoparticles improves due to their exclusive physicochemical properties that create an elevated surface-to-volume ratio thus facilitating membrane contact toward microbes[11]. Reports have indicated that Bismuth Oxide (Bi_2O_3) NPs have antifungal, antibacterial, and anticancer effects[12,13].

The objective was to examine bismuth oxide nanoparticle (Bi_2O_3 NP)-modified acrylic resin antifungal performance while determining the best nanoparticle quantity needed to block *Candida albicans* growth and biofilm formation at its peak, and to assess the potential of the modified acrylic for use in dental or medical applications to prevent fungal growth.

Materials and methods

The *in vitro* assessment of bismuth oxide nanoparticle (Bi_2O_3 NPs) antifungal impact on heat-cured acrylic resin against *Candida albicans* was performed with different nanoparticle concentrations. The investigations took place during a period of seventeen days from 25 March 2025 to 10 April 2025 within Khanzad Teaching Center and Medya Diagnostic Center (Erbil, Kurdistan Region, Iraq).

Experimental groups and sample size

Ten samples comprised each experimental group among the established five groups. The unmodified heat-cured acrylic resin serves as Group A (negative control). Group B (low concentration): acrylic resin with 0.5% (w/w) Bi_2O_3 NPs. Group C (medium concentration): Acrylic resin with 1% (w/w) Bi_2O_3 NPs. Group D (high concentration): acrylic resin with 2% (w/w) Bi_2O_3 NPs. Group E received acrylic resin with nystatin (100,000 IU) to serve as the reference substance providing an antifungal effect.

Sample preparation

High-speed mixing with a mechanical stirrer (3000 rpm for 10 minutes) was used to achieve homogeneous blend consistency of PMMA powder with predetermined concentrations of Bi_2O_3 NPs. The mixture received methyl methacrylate monomer until it adopted dough-like texture. The mixture received stainless steel molding prior to polymerization through two-stage water bath processing at 74°C for 2 hours before reaching 100°C for 30 minutes.

Before testing began the researchers finished the specimens using silicon carbide paper and autoclaved them (121°C, 15 psi, 15 minutes) for sterilization.

Microbiological assays

Scientific personnel standardized *C. albicans* suspension from ATCC 10231 using sterile saline to create a concentration of 10^6 CFU/mL. Each test sample received 1 mL of prepared suspension before the plates entered an incubator at 37 degrees celsius for 24-hour aerobic incubation. Three antifungal assessments were performed:

- After incubation the serial dilutions of suspensions went onto sabouraud dextrose agar (SDA) for colony-forming unit counting. Investigators counted colonies from each plate after the cultivation period of 48 hours at 37°C.
- The biofilm assay process involved twice washing biofilm specimens with PBS before methanol fixation and subsequent crystal violet staining at 0.1% concentration. Germs retained from the biofilm were washed twice after staining then biofilm density was determined through visual scoring.
- Discs were placed onto SDA petri dishes containing *C. albicans* strains for the zone of inhibition testing. Researchers measured inhibition zones in millimeters by using digital calipers after keeping the samples at 37°C for 24-48 hours.

Statistical analysis

Data analysis occurred through IBM SPSS Statistics version (v26). We used Fisher's exact test to evaluate categorical data such as the response categories poor, moderate, good, and excellent because expected cell frequencies were less than five in more than twenty percent of the contingency table cells as per recommendations for small samples. The research adopted $p \leq 0.05$ as the standard for statistical significance.

Results

Five groups were compared to show the antifungal effect. It is evident in **table 1** that Group E (positive control, acrylic with standard antifungal agent, nystatin 100,000IU) was the best to clear the fungal colonies as it gave either a good response (80% of the samples) or an excellent response (20% of the samples). Group D (high concentration: acrylic with 2% (w/w) Bi_2O_3) also gave a good response in 70% of the samples and a moderate response in 30% of the samples, while the responses to Group A (heat-cure acrylic resin without additives), B (low concentration: acrylic with 0.5% (w/w) Bi_2O_3), and C (medium concentration: acrylic with 1% (w/w) Bi_2O_3) were either poor or moderate ($p < 0.001$) (**Table 1.**)

Table 1. Distribution of antifungal responses based on colony-forming unit counts.

	Colony-forming unit counting					
Groups*	**Poor response**	**Moderate response**	**Good response**	**Excellent response**	**Total**	**p-value****
	No. (%)	**No. (%)**	**No. (%)**	**No. (%)**	**No. (%)**	
A	10 (100.0)	0 (0.0)	0 (0.0)	0 (0.0)	10 (100.0)	
B	8 (80.0)	2 (20.0)	0 (0.0)	0 (0.0)	10 (100.0)	
C	4 (40.0)	6 (60.0)	0 (0.0)	0 (0.0)	10 (100.0)	
D	0 (0.0)	3 (30.0)	7 (70.0)	0 (0.0)	10 (100.0)	
E	0 (0.0)	0 (0.0)	8 (80.0)	2 (20.0)	10 (100.0)	<0.001
Total	22 (44.0)	11 (22.0)	15 (30.0)	2 (4.0)	50 (100.0)	

*A: heat-cure acrylic resin without additives (control group). B: low concentration: acrylic with 0.5% (w/w) Bi_2O_3. C: medium concentration: acrylic with 1% (w/w) Bi_2O_3. D: high concentration: acrylic with 2% (w/w) Bi_2O_3. E: positive control acrylic with standard antifungal agent 100,000IU. **Calculated by Fisher's exact test.

Suspension group E demonstrated another outcome success rate as it achieved 70% good results combined with 30% excellent results. The bacteria in Group D (2% Bi_2O_3) experienced 50% "moderate" and 50% "good" reactions yet Groups A–C demonstrated exclusively "poor" or "moderate" results (p<0.001). The results indicated that Group E showed wider antimicrobial inhibition areas compared to Group D (p<0.001) (**Table 2**.)

Regarding the biofilm, group E gave a good response in 80% of the samples and an excellent response in 20% of the samples. Group D gave moderate, good, and excellent responses in 20%, 70%, and 10% of the samples respectively (p<0.001) (**Table 3.**)

No significant difference was found between Group D and E regarding colony-forming unit count (p=0.102) (**Figure 1**).

Regarding zone inhibition, the effect of the antifungal agent (Group E) was significantly better than that of the high-concentration acrylic with 2% (w/w) Bi_2O_3 (Group D) where 70% and 30% of Group E samples gave good and excellent responses respectively, compared with 50% and 0% of Group D respectively (p=0.016) (**Figure 2**).

Table 2. Antifungal activity based on zone of inhibition measurements.

	Zone of inhibition					
Groups*	**Poor response**	**Moderate response**	**Good response**	**Excellent response**	**Total**	**p-value****
	No. (%)	**No. (%)**	**No. (%)**	**No. (%)**	**No. (%)**	
A	10 (100.0)	0 (0.0)	0 (0.0)	0 (0.0)	10 (100.0)	
B	7 (70.0)	3 (30.0)	0 (0.0)	0 (0.0)	10 (100.0)	
C	6 (60.0)	4 (40.0)	0 (0.0)	0 (0.0)	10 (100.0)	
D	0 (0.0)	5 (50.0)	5 (50.0)	0 (0.0)	10 (100.0)	
E	0 (0.0)	0 (0.0)	7 (70.0)	3 (30.0)	10 (100.0)	<0.001
Total	23 (46.0)	12 (24.0)	12 (24.0)	3 (6.0)	50 (100.0)	

*A: heat-cure acrylic resin without additives (control group). B: low concentration: acrylic with 0.5% (w/w) Bi_2O_3. C: medium concentration: acrylic with 1% (w/w) Bi_2O_3. D: high concentration: acrylic with 2% (w/w) Bi_2O_3. E: positive control acrylic with standard antifungal agent 100,000IU. **Calculated by Fisher's exact test.

Table 3. Biofilm inhibition by modified acrylic resin.

	Biofilm assay					
Groups*	**Poor response**	**Moderate response**	**Good response**	**Excellent response**	**Total**	**p-value****
	No. (%)	**No. (%)**	**No. (%)**	**No. (%)**	**No. (%)**	
A	10 (100.0)	0 (0.0)	0 (0.0)	0 (0.0)	10 (100.0)	
B	8 (80.0)	2 (20.0)	0 (0.0)	0 (0.0)	10 (100.0)	
C	5 (50.0)	5 (50.0)	0 (0.0)	0 (0.0)	10 (100.0)	
D	0 (0.0)	2 (20.0)	7 (70.0)	1 (10.0)	10 (100.0)	
E	0 (0.0)	0 (0.0)	8 (80.0)	2 (20.0)	10 (100.0)	<0.001
Total	23 (46.0)	9 (18.0)	15 (30.0)	3 (6.0)	50 (100.0)	

*A: heat-cure acrylic resin without additives (control group). B: low concentration: acrylic with 0.5% (w/w) Bi_2O_3. C: medium concentration: acrylic with 1% (w/w) Bi_2O_3. D: high concentration: acrylic with 2% (w/w) Bi_2O_3. E: positive control acrylic with standard antifungal agent 100,000IU. **Calculated by Fisher's exact test.

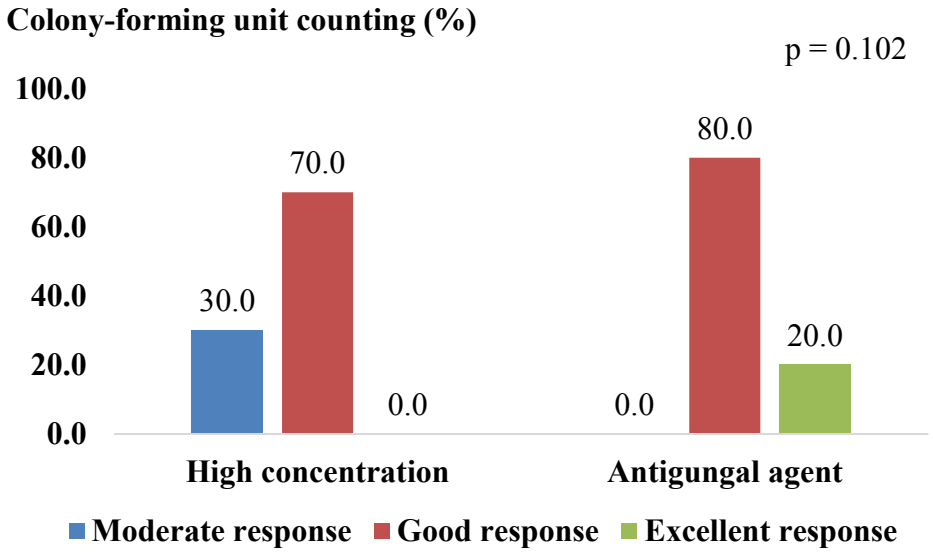

Figure 1. Comparing effects of Group D (high concentration) and Group E (antifungal agent) regarding colony-forming unit counting.

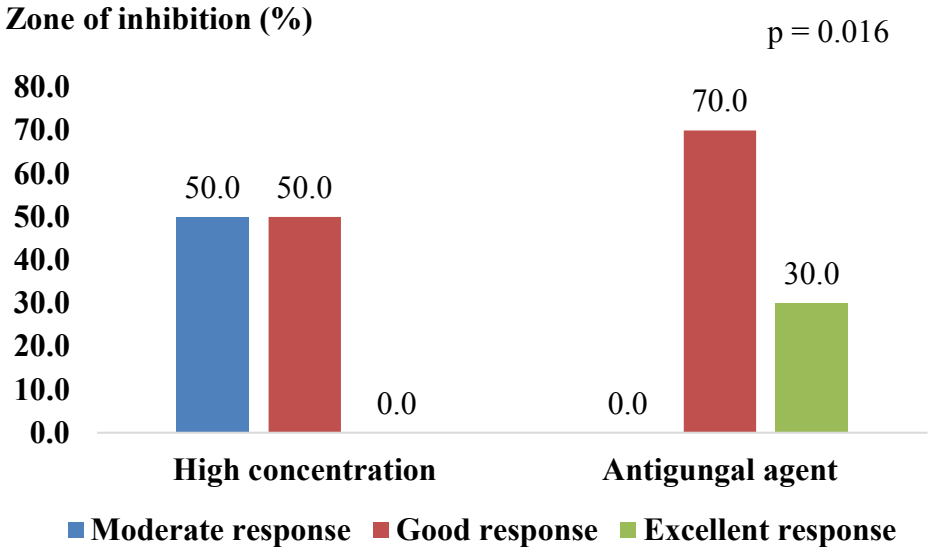

Figure 2. Comparing effects of Group D (high concentration) and Group E (antifungal agent) regarding zone inhibition.

Regarding the biofilm assay, no significant difference was found between the effect of Group D and E (p=0.582). The response to group E was either good or excellent in 80% and 20% of the samples respectively, compared with 70% and 10% of Group D samples respectively (**Figure 3**).

Discussion

This experimental research conducted to evaluate the antifungal properties of heat-cured acrylic resin modified with varying concentrations of Bi_2O_3 NPs against *C. albicans*. To characterize the antifungal activity of Bi_2O_3 NPs, the minimal inhibitory concentration (MIC) was calculated, yielding a value of 2% (w/w). This finding is significant as it represents the lowest concentration at which Bi_2O_3 NPs effectively inhibit biofilm colony of *C. albicans*. Establishing the MIC is crucial for optimizing the antifungal efficacy of Bi_2O_3 while minimizing potential cytotoxic effects. **Table 1** showing that the number of colonies of viable yeast in the acrylic resin plates modified with high concentration of Bi_2O_3 NPs, was significantly less than those with low and moderate concentration of Bi_2O_3 NPs. The research indicates that Bi_2O_3 NPs function as an antifungal compound with equivalent performance to documented metal oxide nanoparticles including zinc

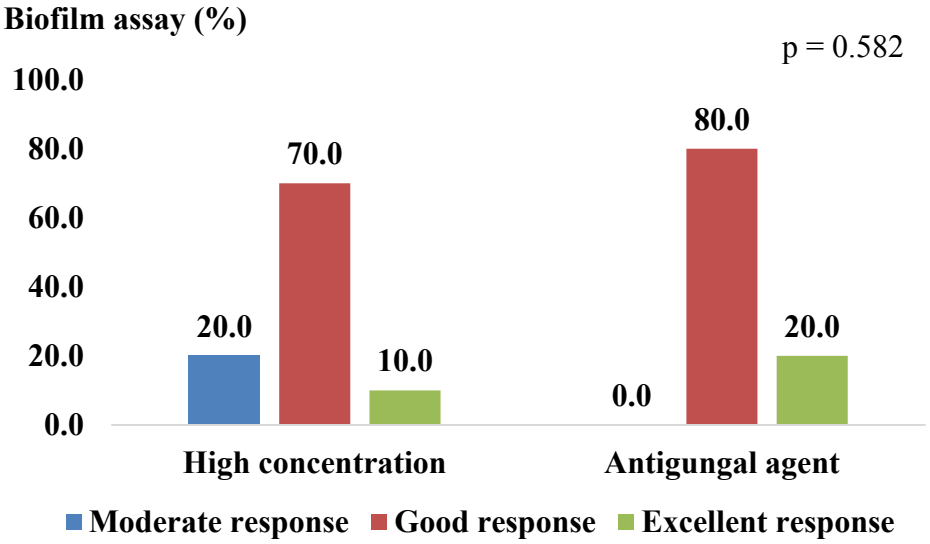

Figure 3. Comparing effects of Group D (high concentration) and Group E (antifungal agent) regarding biofilm assay.

oxide (ZnO), titanium dioxide (TiO_2), and silver (Ag NPs) as previous studies have indicated.[14-16], In parallel to their antifungal activity, the Bi_2O_3 NPs had the potential to interfere with biofilm formation of *C. Albicans*[17]. NPs may interact with cell membranes, enter pathogen cells with ease, and induce microbial death due to their huge surface area, small size, high surface energy, and charge density.

For these reasons, NPS is regarded as a breakthrough in dental and prosthetic treatment[18]. The antifungal function of Bi_2O_3 NPs derives from their electrostatic membrane destabilizing effect on bacterial cells due to their negatively charged surface together with their hydroxyl-rich functional groups that damage positively charged microbial membranes. However, the antibacterial activity of Bi NPs may be mediated by various processes[19]. In this work, we demonstrated that Bi_2O_3 NPs have antimycotic properties. They were substantially just as potent as Nystatin in inhibiting the growth of *C. albicans*.

To be assured that the antifungal effect was due to the nanostructured Bi_2O_3, we compared between control group and with different concentration of Bi_2O_3 NPs, groups and nystatin. Results were significant only to the nystatin 100,000IU and the 2% (w/w) Bi_2O_3 NPs respectively while the ability of inhibiting the fungal growth of the other groups were poor. As is evident in **Table 2**. Bi_2O_3 NPs displayed two-fold effects against *C. albicans* microorganisms as they reduced colony survival by 85% yet inhibited biofilm formation. The evidence for 'total inhibition' needs clarification since the tested conditions allow biofilm formation in 10–20% of samples and laboratory experiments confirmed that surfaces containing *Myrtus communis* extract strongly delayed biofilm formation which suggests its use as an antimicrobial treatment. It is essential to transfer laboratory results to physiological models to evaluate their clinical usefulness.[20], The reported results exhibit strong concordance with those obtained in our analysis (**Table 3)**, the potential antimicrobial properties of the modified acrylic resin for dental or medical applications regarding the biofilm assay result was about 70% for 2% (w/w) Bi_2O_3 NPs. In consideration of these findings, patients who are resistant or at risk of most antifungal medications may benefit from using Bi_2O_3 NPs as antifungal agents.

This research has several limitations that must be acknowledged. The testing of communis extract only covered specific concentrations within the experiment which might have failed to show its complete antimicrobial effectiveness and toxicity tolerance. To establish maximum clinical value researchers, need to investigate a wider range of extract concentrations to discover the most beneficial dose and lowest possible adverse effects.

The experimental data we obtained solely stemmed from laboratory dish tests. The simulation methods provide useful results, but they lack the ability to duplicate the active oral conditions which occur in human mouths. The current model lacks the inclusion of specific variables including enzymatic activity alongside immune responses together with natural biofilm structural characteristics. Additional

research involving clinical trials alongside animal studies must follow the initial study results to achieve official validation. The research did not examine the mechanical properties along with optical color and prolonged stability of the modified restorative material.

The current material demands essential features which make it suitable for clinical use especially during aesthetic and weight-bearing situations. Studies need to determine the impact that *Myrtus communis* extract brings to the compressive strength and wear resistance and color stability of the composite. The study currently lacks data regarding how the extract interacts with the resin matrix as time progresses. Active compound leaching along with any kinetic changes in polymerization may affect both the durability and biocompatibility of the finished product.

Conclusions

In conclusion, adding Bi_2O_3 NPs to the heat-cured acrylic resin can inhibit *C. albicans* growth, and biofilm colonization. The antimicrobial test results confirmed that 2% (w/w) Bi_2O_3 NPs MIC is crucial for optimizing potential antimicrobial properties of the modified acrylic resin denture base material against *C. albicans*. Using these types of modified acrylic resin can be a promising approach in dentistry.

Acknowledgment

We would like to thank the Medya Diagnostic Center for their kind hospitality by performing our antimicrobial laboratory investigations.

Conflict of interest

The authors declare no conflicts of interest.

Fundings

This article has not received any specific grant from funding agencies in the public, commercial, or for-profit sectors.

Ethical considerations

All trials received approval from the Kurdistan Higher Council of Medical Specialties as a condition for beginning research activities.

References

1. Kilic K, Koc AN, Tekinsen FF, Yildiz P, Kilic D, Zararsiz G, et al. Assessment of *Candida* species colonization and denture-related stomatitis in bar- and locator-retained overdentures. J Oral Implantol 2014;40(5):549-56. Available from: 10.1563/AAID-JOI-D-12-00048.
2. Hannah VE, O'Donnell L, Robertson D, Ramage G. Denture stomatitis: causes, cures and prevention. Prim Dent J 2017;6(4):46-51. Available from: 10.1308/205016817822230175.
3. Lyu X, Zhao C, Yan ZM, Hua H. Efficacy of nystatin for the treatment of oral candidiasis: a systematic review and meta-analysis. Drug Des Devel Ther 2016;10:1161-71. Available from: 10.2147/DDDT.S100795.
4. Webb BC, Thomas CJ, Harty DW, Willcox MD. Effectiveness of two methods of denture sterilization. J Oral Rehabil 1998;25(6):416-23. Available from: 10.1046/j.1365-2842.1998.00266.x.
5. Muñoz JE, Rossi DCP, Jabes DL, Barbosa DA, Cunha FFM, Nunes LR, et al. *In vitro* and in vivo inhibitory activity of *Limonene* against different isolates of *Candida* spp. J Fungi (Basel) 2020;6(3):183. Available from: 10.3390/jof6030183.
6. Ahmad N, Jafri Z, Khan ZH. Evaluation of nanomaterials to prevent oral candidiasis in PMMA based denture wearing patients. A systematic analysis. J Oral Biol Craniofac Res 2020;10(2):189-193. Available from: 10.1016/j.jobcr.2020.04.012.
7. Vila T, Sultan AS, Montelongo-Jauregui D, Jabra-Rizk MA. Oral candidiasis: a disease of ppportunity. J Fungi (Basel) 2020;6(1):15. Available from: 10.3390/jof6010015.
8. Cheraghipour K, Ezatpour B, Masoori L, Marzban A, Sepahvand A, Rouzbahani AK, et al. Anti-*Candida* activity of curcumin: a systematic review. Curr Drug Discov Technol 2021;18(3):379-390. Available from: 10.2174/1570163817666200518074629.
9. Kareem HA, Samaka HM, Abdulridha WM. Evaluation of the effect of the gold nanoparticles prepared by green chemistry on the treatment of cutaneous candidiasis. Curr Med Mycol 2021;7(1):1-5. Available from: 10.18502/cmm.7.1.6176.
10. Balabathula P, Whaley SG, Janagam DR, Mittal NK, Mandal B, Thoma LA, et al. Lyophilized iron oxide nanoparticles encapsulated in amphotericin B: a Novel targeted nano drug delivery system for the treatment of systemic fungal infections. Pharmaceutics 2020;12(3):247. Available from: 10.3390/pharmaceutics12030247.
11. Azmy E, Alkholy MR, Helal MA. Microbiological evaluation for antifungal activity of some metal oxides nanofillers incorporated into cold cured soft lining materials: clinical based study. Brazilian Dental Science 2022; 25(1): e2921.
12. Aggrawal S, Chauhan I, Mohanty P. Immobilization of Bi2O3 nanoparticles on the cellulose fibers of paper matrices and investigation of its antibacterial activity against *E. coli* in visible light. Materials Express 2015; 5(5):429-436.
13. Anusha S, Cp B, Mohan CD, Mathai J, Rangappa S, et al. A nano-MgO and ionic liquid-catalyzed 'green' synthesis protocol for the development of adamantyl-imidazolo-thiadiazoles as anti-tuberculosis agents targeting sterol 14α-demethylase (CYP51). PLoS One 2015;10(10):e0139798. Available from: 10.1371/journal.pone.0139798.
14. Lipovsky A, Nitzan Y, Gedanken A, Lubart R. Antifungal activity of ZnO nanoparticles-the role of ROS mediated cell injury. Nanotechnology 2011;22(10):105101. Available from: 10.1088/0957-4484/22/10/105101.
15. Tatlıdil İ, Sökmen M, Breen C. Degradation of C*andida albicans* on TiO_2 and Ag-TiO_2 thin films prepared by sol–gel and nanosuspensions. J Sol-Gel Sci Technol 2011; 60:

23–32. Available from: https://doi.org/10.1007/s10971-011-2546-0.

16. Hwang IS, Lee J, Hwang JH, Kim KJ, Lee DG. Silver nanoparticles induce apoptotic cell death in *Candida albicans* through the increase of hydroxyl radicals. FEBS J 2012;279(7):1327-38. Available from: 10.1111/j.1742-4658.2012.08527.x.
17. Kishen AS. Nanotechnology in endodontics. Current and potential clinical applications; Springer Science &Business Media: Cham, Switzerland, 2015.
18. Guerreiro-Tanomaru JM, Cornélio AL, Andolfatto C, Salles LP. pH and antimicrobial activity of Portland cement associated with different radiopacifying agents. ISRN Dent 2012;2012:469019.
19. Nazari P, Dowlatabadi-Bazaz R, Mofid MR, Pourmand MR, Daryani NE, Faramarzi MA, et al. The antimicrobial effects and metabolomic footprinting of carboxyl-capped bismuth nanoparticles against Helicobacter pylori. Appl Biochem Biotechnol 2014;172(2):570-9. Available from: 10.1007/s12010-013-0571-x.
20. Hernandez-Delgadillo R, Velasco-Arias D, Martinez-Sanmiguel JJ, Diaz D, Zumeta-Dube I, Arevalo-Niño K, et al. Bismuth oxide aqueous colloidal nanoparticles inhibit *Candida albicans* growth and biofilm formation. Int J Nanomedicine 2013;8:1645-52. Available from: 10.2147/IJN.S38708.

ACADEMIC JOURNAL OF HEALTH SCIENCES
MEDICINA BALEAR

Original

The evaluation of anxiety levels and methods of coping with stress in mothers of children with asthma

La evaluación de los niveles de ansiedad y los métodos para afrontar el estrés en madres de niños con asma

Seyfettin Tay, Müsemma Alagöz Karabel*, Velat Şen, Veysiye Hülya Uzel, Rojan İpek, Asuman Akar

Pediatrics Department of Pediatric Health and Illnesses, Dicle University, Diyarbakır, Turkey

Received: 13-03-2025
Accepted: 18-04-2025

***Corresponding author**: Müsemma Alagöz Karabel. musemma.alagoz@gmail.com

Abstract

Introduction: asthma is the most common chronic disease among children. The cases of asthma are increasing dramatically. Families play an important role in childhood asthma management. Children with chronic diseases and their mothers show stress and anxiety incidences, which are supported by publications. The main purpose of this study was to understand parental stress and associated coping behaviors of mothers of children with asthma. To the best of our knowledge, this is the first study conducted in this field.

Materials and method: our study was conducted prospectively, and we included 75 asthmatic children and their mothers as study group. In the control group, 60 healthy children and their mothers were included. Data was collected by the researchers using the Clinical Interview form, the Beck Anxiety Scale and Coping with Stress Scale of Style.

Results: a total of 135 patients (75 patients, 60 control groups) were included in the study. There was no significant difference between the groups in terms of the age of the participants and the age of the mothers. When compared in terms of asthma diagnosis during pregnancy, the mothers in the study group had a statistically significant higher history of asthma during pregnancy ($p<0.05$), but the mothers were similar in terms of smoking. When the mean anxiety scores of the mothers were compared with the duration of asthma of the child in the study group, it was observed that the mean anxiety scores of the mothers increased as the duration of asthma increased, but there was no statistically significant difference, whereas when the anxiety scores of the mothers were compared between the groups, it was observed that the level of severe anxiety was statistically significantly higher in the study group.In the mothers of children with asthma, optimistic attitudes and self-confident approach, compared to healthy children of mothers who had low scores and were found to be statistically significantly different.

Conclusions: this study revealed that asthmatic children's mothers' stress and anxiety levels increased. It has been determined that during the follow-ups and treatments of children with asthma, giving support to families will help and improve both the patients' treatment process and the dialog between doctors and patients' relatives.

Keywords: Chronic. Asthma. Stress. Scale. Anxiety.

Cite as: Tay S, Alagöz Karabel M, Şen V, Uzel VH, İpek R, Akara A. The evaluation of anxiety levels and methods of coping with stress in mothers of children with asthma. Acad J Health Sci 2025; 40(5): 38-43. Available from: https://doi.org/10.3306/AJHS.2025.40.05.5

Acad J Health Sci 2025; 40(5): 38-43
https://doi.org/10.3306/AJHS.2025.40.05.5
www.ajhealthsciences.com

Resumen

Introducción: el asma es la enfermedad crónica más común entre los niños. Los casos de asma están aumentando de forma dramática. Las familias desempeñan un papel importante en el manejo del asma infantil. Los niños con enfermedades crónicas y sus madres presentan niveles de estrés y ansiedad, tal como lo respaldan diversas publicaciones. El objetivo principal de este estudio fue comprender el estrés parental y los comportamientos de afrontamiento asociados en madres de niños con asma. Hasta donde sabemos, este es el primer estudio realizado en este campo.

Materiales y método: nuestro estudio se realizó de forma prospectiva e incluyó a 75 niños asmáticos y sus madres como grupo de estudio. En el grupo control se incluyeron 60 niños sanos y sus madres. Los datos fueron recolectados por los investigadores mediante el Formulario de Entrevista Clínica, la Escala de Ansiedad de Beck y la Escala de Estilos de Afrontamiento del Estrés.

Resultados: se incluyó un total de 135 participantes (75 en el grupo de estudio y 60 en el grupo control). No se encontró una diferencia significativa entre los grupos en cuanto a la edad de los participantes ni a la edad de las madres. Al comparar los antecedentes de diagnóstico de asma durante el embarazo, se observó que las madres del grupo de estudio tenían un historial de asma durante el embarazo significativamente mayor ($p<0,05$), aunque eran similares en cuanto al hábito de fumar. Cuando se compararon las puntuaciones medias de ansiedad de las madres con la duración del asma en el niño dentro del grupo de estudio, se observó que las puntuaciones medias de ansiedad aumentaban conforme aumentaba la duración del asma, aunque esta diferencia no fue estadísticamente significativa. Sin embargo, al comparar las puntuaciones de ansiedad de las madres entre los grupos, se encontró que el nivel de ansiedad severa fue significativamente mayor en el grupo de estudio. En las madres de niños con asma, se observaron actitudes optimistas y enfoques autoconfiados más bajos en comparación con las madres de niños sanos, siendo esta diferencia estadísticamente significativa.

Conclusiones: este estudio reveló que los niveles de estrés y ansiedad en las madres de niños asmáticos estaban aumentados. Se determinó que brindar apoyo a las familias durante el seguimiento y tratamiento de los niños con asma contribuirá a mejorar tanto el proceso terapéutico de los pacientes como el diálogo entre los médicos y los familiares de los pacientes.

Palabras clave: Crónico. Asma. Estrés. Escala. Ansiedad.

Introduction

Asthma is a highly prevalent chronic disease. In 2019, it was estimated that 262 million people worldwide were living with asthma[1]. According to the most recently available statistics for asthma prevalence in Canada, in 2018, an estimated 3.8 million Canadians had asthma, and of these, 850,000 were less than 14 years of age[2].

In asthma, chronic inflammation causes airway hypersensitivity and this chronic picture, which is characterized by recurrent wheezing, dyspnea, chest tightness and cough attacks especially at night or early morning hours, imposes many burdens on the family due to its symptoms, treatment method, prognosis, daily activity restriction, and long-term effects that continue at home as well as in the hospital[3].

The intensive and prolonged care process of chronic diseases leads to feelings such as helplessness, guilt, anger, fear and social isolation in caregivers, dependence on the patient and ultimately a decrease in the time allocated to oneself and other family members[4-7]. Studies on the burden of care have generally been conducted in caregivers of adult patients[8-12] and studies on the burden of care of children with chronic diseases are limited studies on the difficulties experienced by families[13-16]. This study was conducted to determine anxiety levels and stress coping skills in mothers of patients followed up with a diagnosis of asthma. To the best of our knowledge, this is the first study conducted in this field.

Materials and method

The study was conducted prospectively between June 2013 and 2014. Asthmatic patients aged between 5 and 15 years, and their mothers were included in the study group. Also, the study included children without chronic disease who were followed up in a pediatric outpatient clinic with similar age and gender characteristics to the study group, and their mothers, as the control group.

Both groups were administrated the Beck Anxiety Scale[17], which was developed by Beck in 1988 and adapted into Turkish by Ulusoy. They were also administrated the Stress Coping Styles Scale (SCS), which was developed by Folkman in 1980 under the name of Ways of Coping Inventory and adapted into Turkish by Şahin, in order to determine the ways individuals use to cope with general or specific stress situations. In the evaluation of the scale, the higher the scores obtained from the factors of Self-Confident, Optimistic and Referring to Social Support, the more effective coping with stress is; the higher the scores obtained from the factors of Helpless Approach and Submissive Approach, the more ineffective methods are used in coping with stress[18].

Patients with a chronic disease other than asthma, those with a history of prematurity, those who did not respond completely to asthma treatment, and those who did not attend regular follow-up visits were excluded from the study.

After the study, patients who needed psychiatric treatment and patients in the control group were referred to adolescent mental health specialists.

Statistical analysis

SPSS 18.0 package programme was used for statistical analyses. In addition to descriptive statistical methods (mean, standard deviation, frequency), Student-t test was used for comparisons of parameters with normal distribution between two groups and Mann-Whitney-U test was used for comparisons of parameters without normal distribution between two groups. Chi-square test was used for comparison of non-numerical data. The results were evaluated at 95% confidence interval and significance was evaluated at p<0.005 level.

Results

A total of 135 patients (75 patients, 60 control group) were included in the study. 61.3% (n=46) of the study group and 55% (n=33) of the control group were male (p>0.05). There were no significant differences between the groups in terms of the age of the participants and the age of the mothers. In the study group, 85% (n=64) were using inhaled corticosteroids, 78% (n=59) were using B2 agonists and 37% (n=28) were using montelukast sodium.

When the mothers of the subjects in the study and control groups were compared in terms of the presence and treatment of chronic diseases, there was no significant difference. When compared in terms of asthma diagnosis during pregnancy, the mothers in the study group had a statistically significant higher history of asthma during pregnancy (p<0.05), but the mothers were similar in terms of smoking. The sociodemographic characteristics of the groups are shown in **Table 1**.

When the mean anxiety scores of the mothers were compared with the duration of asthma of the child in the study group, it was observed that the mean anxiety scores of the mothers increased as the duration of asthma increased, but there was no statistically significant difference. Whereas when the anxiety scores of mothers were compared between the groups, it was observed that the level of severe anxiety was statistically significantly higher in the study group (**Table 2**).

When the mean anxiety scores were compared with the duration of asthma in the study group, the mean anxiety scores of the mothers increased as the duration of asthma increased, but no statistically significant difference was observed (p>0.005).

When the stress coping scales were evaluated between the groups, the self-confident and optimistic approach score was lower and the helpless and submissive approach score was statistically significantly higher in the mothers of asthmatic children (p<0.01). Social support seeking score was also higher in the study group (p<0.01).

Discussion

Asthma is the most common cause of hospitalisation in children and the chronic disease leading to the most school loss[19]. In children younger than 14 years of age, the incidence of asthma is higher in boys than in girls. In our study, although it was higher in boys, it was not statistically significant. Although the reason for this higher incidence is not known exactly, the role of lower expiratory flow rates and more frequent upper and lower respiratory tract infections in boys is emphasized[20].

Asthma is a chronic disease; nocturnal symptoms, prolonged medication use, hospitalizations due to attacks,

Table 1. Sociodemographic characteristics of the groups.

		Study Group n=75	Control Group n=60	p
Gender	Female	29 (38.6%)	27 (35%)	0.486
	Male	46 (61.3%)	33(55%)	
Age	Year	9.5±2.8	8.7±2.7	0.102
Age of mothers	Year	35.6±6.3	34.3±6.2	0.22
Passive smoker	Yes	40 (46%)	44 (26%)	0.021
Chronic maternal illness	Yes	23 (30.6%)	12 (20%)	0.173
Mother's chronic drug use	Yes	18 (78.2)	8 (66.6%)	0.131
History of asthma in pregnancy	Yes	12 (16%)	2 (3%)	0.021
Mother's smoking	Yes	15 (20%)	11 (18.3%)	0.83
	No	60	49	

Table 2. Anxiety levels of mothers.

	Anxiety Questionnaire Score			
Groups	**8-15 points (light)**	**16-25 points (medium)**	**26-63 points (serious)**	**p**
Study group	29.3%(n=22)	30.6% (n=23)	40% (n=30)	
Control group	50% (n=30)	48.3% (n=29)	1.6% (n=1)	<0.005

Table 3. Mothers' ability to cope with stress.

Stress coping scales	Groups	Average score	Standard deviation	p
Self-confident approach	**Study group**	13.1	3.5	
	Control group	15.5	2.3	<0.001
Desperate approach	**Study group**	15.5	3.2	
	Control group	10.8	2.5	<0.001
Submissive approach	**Study group**	11.0	2.1	
	Control group	7.3	2.0	<0.001
Optimistic approach	**Study group**	8.1	2.2	
	Control group	10.1	1.8	<0.001
Social support search	**Study group**	8.8	2.0	
	Control group	6.8	1.2	<0.001

school and workforce losses may adversely affect the life of the family and the child physically and psychosocially. Children cannot perform their own self-care. Parents, especially the mother, are responsible for their care[21]. It has been shown that having an asthmatic child is a source of stress in mothers and the stress level is higher in parents with a child with chronic disease[22,23]. In our study, the anxiety levels of the mothers in the study group were higher in accordance with the literature.

According to Tseng and Chou, the factors affecting stress are the age of the mother and the severity of the child's disease[24]. In the literature, although there are studies reporting an increase in anxiety level with increasing parental age, there are also studies reporting no change[25]. In our study, there was no difference between the groups in terms of maternal age, and we think that this lack of difference is important in terms of the reliability of the results. An increase in anxiety level may be expected because taking responsibility and caring for the child becomes more difficult with age. In our study, it was found that anxiety levels of mothers were higher as the duration of asthma increased. However, no statistically significant difference was found. This finding suggested that the stress of a family who is constantly admitted to the hospital due to chronic disease is increased one-fold more when their child does not attend school.

The child is evaluated especially as the mother's personal success or failure. Since a child who is not healthy can be considered a failure, the mother may be blamed and even humiliated by her environment. This situation affects the mother's emotions and may cause her to experience guilt, unhappiness and stress more than other family members[26].

The presence of an atopic constitution in the mother is an important risk factor for asthma in the child. The risk of asthma is high in children whose families have asthma and allergies, and it has been observed that asthma starts earlier and has a more severe course in these children[27,28]. In our study, the presence of a diagnosis of asthma during pregnancy in the patient group mothers was statistically significantly higher in accordance with the literature.

In the development of asthma, environmental factors are added to the underlying genetic factors and lead to the emergence of the clinical picture or aggravation of the existing condition. The best known of these and the one with the best-established cause-effect relationship is smoking at home. In our country, 53% of the families of asthmatic children smoke[29]. It has been shown that the risk of asthma is 2.1 times higher in children whose mothers smoke at least half a packet of cigarettes and this risk is 2.6 times higher in the first year of life[30]. In our study, when the

smoking status of the fathers of asthmatic children and other individuals living at home was questioned, the exposure of asthmatic children to passive smoking was higher.

Chronic disease is the most frightening diagnosis that a parent may receive for their child, and the stress experienced is great. Studies showing that the number of parents who perceive this stress as an extremely distressing, humiliating and unsolvable problem and who think that they have no other choice but to take refuge in God and submit to the situation is high[31].

One of the ways for mothers to cope with stress is to seek social support[32]. In our study, the mean scores of optimistic approach and self-confident approach were lower in mothers with asthmatic children, but the mean scores of helpless approach, submissive approach and seeking social support were significantly higher than those in the control group. To the best of our knowledge, this is the first study conducted in this field.

It is stated that when families have a professional who listens and understands them, their worries and anxieties decrease and their feelings of self-confidence increase[33]. Coping with stress is more successful as the social support network expands[34]. An education and behaviour-based programme was applied to families whose children were hospitalized in the intensive care unit, and improvement was observed in depression, anxiety and quality of life[35]. Receiving professional support with educational programmes that support mothers' feelings of self-confidence will be effective in reducing their anxiety.

In the light of these results, it is clear that educational and psychological support programmes to be provided to families with asthmatic children will result in significant improvement in anxiety and quality of life for both families and children. The support to be provided in this direction is the most important step in the treatment of asthmatic children and will contribute both to the continuation of the treatment of the asthmatic child in the best way and to the most appropriate conduct of the physician-patient relatives' dialogue.

Funding

This article has not received any specific grant from funding agencies in the public, commercial, or for-profit sectors.

Conflict of interest

The authors declare no conflicts of interest.

Authors contribution

Seyfettin Tay: conceptualization, project administration, formal analysis, investigation, writing, original draft.

Müsemma Alagöz Karabel: methodology, investigation, writing, original draft.

Velat Şen: validation, resources, formal analysis.

Veysiye Hülya Uzel: formal analysis, resources, investigation.

Rojan İpek: investigation, writing, original draft.

Asuman Akar: investigation, writing, original draft.

References

1. Vos T, Lim SS, Abbafati C, Abbas KM, Abbasi M, Abbasifard M, et al. Global burden of 369 diseases and injuries in 204 countries and territories, 1990–2019: a systematic analysis for the Global Burden of Disease Study 2019. Lancet 2020; 396(10258):1204-1222.
2. Mansouri R, Lavigne E, Talarico R, Smargiassi A, Rodriguez-Villamizar LA, Villeneuve PJ. Residential surrounding greenness and the incidence of childhood asthma: findings from a population-based cohort in Ontario, Canada. Environ Res 2024; 249:118316.
3. Er M. Children, illness, parents and siblings. J Child Health Dis 2006; 49: 155-68.
4. Schene AH. Objective and subjective dimensions of family burden. Soc Psychiatry Psychiatr Epidemiol 1990; 25:289-97.
5. Sales E. Family burden and quality of life. Qual Life Res 2003;12:33-41.
6. Ikeda T, Nagai T, Nishimura KK, Mohri I, Taniike M. Sleep problems in physically disabled children and burden on caregivers. Brain Dev 2012; 34:223-9.
7. Gowen, JW, Johnson-Martin N, Goldman BD, Appelbaum M. Feelings of depression and parenting competence of mothers of handicapped and nonhandicapped infants: a longitudinal study. Am J Ment Retard 1989; 94:259-1.
8. Shyu YL. Patterns of caregiving when family caregivers face competing needs. J Adv Nurs 2000; 31:35-43.
9. Sayer LC, England P, Bittman M, Bianchi SM. How long is the second (plus first) shift? Gender differences in paid, unpaid, and total work time in Australia and The United States. J Comp Fam Stud 2009; 40:523-45.
10. Yach D, Hawkes C, Gould CL, Hofman KJ. The global burden of chronic diseases overcoming impediments to prevention and control. JAMA 2004; 291:2616-22.
11. Atagün MI, Balaban OD, Atagün Z, Elagöz M, Yılmaz-OA. Caregiver burden in chronic diseases. Curr Approaches Psychiatry 2011; 3:513-52.
12. Heller T, Hsieh L, Rowitz L. Maternal and paternal caregiving of persons with mental retardation across the lifespan. Family Relations 1997; 46:407-15.
13. Boyer F, Drame M, Morron I, Novella JL. Factors relating to carer burden for families of persons with muscular dystrophy. J Rehabil Med 2006; 38:309-15.
14. Davidoff AJ. Insurance for children with special health care needs: patterns of coverage and burden on families to provide adequate insurance. Pediatrics 2004; 114:394-403.
15. Moskowitz JT, Butensky E, Harmatz P, et al. Caregiving time in sickle cell disease: psychological effects in maternal caregivers. Pediatr Blood Cancer 2007; 48: 64-71.
16. Snead K, Ackerson J, Bailey K, et al. Taking charge of epilepsy: the development of a structured psychoeducational group intervention for adolescents with epilepsy and their parents. Epilepsy Behav 2004; 5:547-556.

17. Köroğlu E. American Psychiatric Association, Diagnostic and Statistical Manual of Mental Disorders DSM-IV-TR revised full text. 2004.
18. Aydemir Ö, Ve Köroglu E. Clinical scales used in psychiatry, Hekimler Yayın Birligi, Ankara 2000.
19. Gibson PG, Wlodarczyk JW, Hensley MJ, et al. Epidemiological association of airway inflammation with asthma symptoms and airway hyperresponsiveness in childhood. Am J Respir Crit Care Med 1998; 158:36-41.
20. Çevik Ü, Taş F. Investigation of sociodemographic characteristics of asthmatic children and factors that stimulate asthma. 4th National Child Nursing Congress. 2004.
21. Marinner A. Nursing theorists and their work. St. Louis. The Mosby Company, 1986.
22. Wright AL. The epidemiology of the atopic child: who is at risk factor what? J Allergy Clin Immunol 2004; 113:52-7.
23. Glidden LM. Depression: its trajectory and correlates in mothers rearing children with intellectüal disability. J Intellect Disabil Res 2003; 47:250-63.
24. Tseng TJ, Chou CC, Hu Li, Za Hi 2006 Aug;53: 31-4.
25. Güneş P. The effect of informing patients with open heart surgery before discharge on the level of anxiety, Cumhuriyet University Institute of Health Sciences, Nursing Programme Master's Thesis. 2001.
26. Dereli F, Okur S. Determination of the depression status of families with disabled children, New Med J 2008; 25:164–8.
27. London SJ, James Gaunderman W, Avol E, Rappaport EB, Peter JM. Family history and the risk of early-onset persistent, early-onset transient and late-onset asthma. Epidemiology 2001; 12:577-83.
28. Tariq SM, Hakim EA, Matthew SM, Arshad SH. The prevalence of and risk factors for atopy in early childhood. J Allergj Clin Immunol 1998; 101:587-93.
29. Bavbek S, Astım Epidemiyolojisi Ve Risk Faktorleri AYF, Kalaycı O. Immunopathological mechanisms in asthma. T Klin Allerji -Astım 2000; 2:57–72.
30. Damrosch SP, Perry LA. Self-reported adjusment, chronic sorrow, and coping of parents of children with down syndrome, Acta Psychiatr, Scand 1989; 38:25-29.
31. Murin S, Bilello KS, Matthay R. Other smoking-affected pulmonary diseases. Clin Chest Med 2000; 21:121-37.
32. Wiedebusch S, Conrad C. Chronic renal failure. Pediatr Nephrol. 2010;25:1477–85.
33. Kirkham MA. Two-year follow-up of skills training with mothers of children with disabilities. Am J Ment Retard 1993; 97:509-20.
34. Coşkun Y, Akkaş G. The relationship between trait anxiety levels and social support perceptions of mothers with disabled children. J Ahi Evran Univ Kirsehir Fac Educ 2009; 10(1):213–27.
35. Melnyk BM, Feinstein NF, Moldenhouer Z, Small L. Coping in parents of children who are chronically Ill: strategies for assessment and intervention. Pediatr Nurs 2001; 27:548-58.

ACADEMIC JOURNAL OF HEALTH SCIENCES
MEDICINA BALEAR

Original

Can laugh therapy be an intervention for students with psychological problems? A case study

¿Puede la risoterapia ser una intervención para estudiantes con problemas psicológicos? Un estudio de caso

Susanti Niman[1]*, Timothy Rothhaar[2], Ignasia Kewa Pati[3]

[1]Faculty of Nursing Sciences, Institute Kesehatan Immanuel, Bandung, Indonesia
[2]Independent Scholar, Cork, Ireland
[3]Faculty of Vocation, Universitas Santo Borromeus, Padalarang, Indonesia

Received: 21-03-25
Accepted: 25-04-25

***Corresponding author:** Susanti Niman. susantiniman@gmail.com

Abstract

Psychological problems can adversely affect students' academic performance. Nursing care interventions should be given to cope with psychological problems. The purpose of this study was to report the effect of laugh therapy in reducing stress, anxiety, and depression in college students.

A case study was conducted in West Java, Indonesia. The implementation uses the nursing process, the Stuart stress adaptation model, and the Depression Anxiety Stress Scale 21 (DASS 21) instruments to measure stress, anxiety, and depression. Participants were selected by purposive sampling. Three participants were selected for nursing care with an intervention focusing on laugh therapy.

Subjective evaluation of participants stated a decrease in stress, anxiety, and depression. Pre- and post-therapy results, using the DASS 21, showed a significant decrease in stress, anxiety, and depression. Depression and anxiety decreased by 4-10 points, and stress decreased by 5-15 points after therapy.

Laugh therapy is successful in reducing the stress, anxiety, and depression experienced by students. It can be performed alone by students and can be a skill taught to them in order to reduce their psychological problems without recourse to institutional intervention.

Keywords: Anxiety. Case study. College student. Depression. Laugh therapy. Stress.

Resumen

Los problemas psicológicos pueden afectar negativamente el rendimiento académico de los estudiantes. Se deben implementar intervenciones de enfermería para abordar estos problemas. El propósito de este estudio fue reportar el efecto de la risoterapia en la reducción del estrés, la ansiedad y la depresión en estudiantes universitarios.

Se realizó un estudio de caso en Java Occidental, Indonesia. La implementación utiliza el proceso de enfermería, el modelo de adaptación al estrés de Stuart y la Escala de Depresión, Ansiedad y Estrés 21 (DASS 21) para medir el estrés, la ansiedad y la depresión. Los participantes fueron seleccionados mediante muestreo intencional. Tres participantes fueron seleccionados para recibir atención de enfermería con una intervención centrada en la risoterapia.

Cite as: Niman S, Rothhaar T, Kewa Pati I. Can laugh therapy be an intervention for students with psychological problems? A case study. Acad J Health Sci 2025; 40(5): 44-52. Available from: https://doi.org/10.3306/AJHS.2025.40.05.6

Acad J Health Sci 2025; 40(5): 44-52
https://doi.org/10.3306/AJHS.2025.40.05.6
www.ajhealthsciences.com

La evaluación subjetiva de los participantes indicó una disminución del estrés, la ansiedad y la depresión. Los resultados pre y post terapia, utilizando la DASS 21, mostraron una disminución significativa del estrés, la ansiedad y la depresión. La depresión y la ansiedad disminuyen entre 4 y 10 puntos y el estrés disminuye entre 5 y 15 puntos después de la terapia.

La risoterapia tiene éxito en la reducción del estrés, la ansiedad y la depresión que experimentan los estudiantes. Puede ser realizada individualmente por los estudiantes y puede ser una habilidad que se les enseña para reducir sus problemas psicológicos sin recurrir a la intervención institucional.

Palabras clave: Ansiedad. Estudio de caso. Estudiante universitario. Depresión. Terapia de la risa. Estrés.

Introduction

The student group is in a period of mental immaturity and is highly vulnerable to shocks. Research has found that in the post-COVID-19 era, the incidence of psychological problems, such as depression and anxiety, among students is still high[1]. Around 31% of students have a mental health disorder. On the other hand, many students have low mental health literacy. They are unaware of the need for treatment and instead believe that these symptoms of depression and anxiety are typical of college students' stress[2].

While college is exciting for students, they often face challenges while undergoing education, both in academic progress and their personal and social lives[3]. University student life is more emotionally and academically demanding than other life periods[4]. They face various difficulties and struggle that make them more vulnerable to mental health disorders[5]. Many factors trigger psychological problems in students: academic pressure, exams and college load, lack of free time, competition, worries about not being able to meet parental expectations, establishing new personal relationships, studying in a foreign place, financial burdens, and biological factors such as age and gender (predominantly female)[6-8].

Mental health problems during college are predictive of lower academic success. Depression is associated with a two-fold increase in the risk of dropping out of college without graduating[9]. Mental illness among college students is a public health crisis. The rates of depression and anxiety have more than doubled over the past 5 years. In one study, 42.2% of U.S. college students reported feeling depressed, and 63.6% of college students experienced overwhelming anxiety. Almost one in four college students has experienced suicidal ideation[10]. The prevalence of anxiety and depression in students is high in low-income and middle-income countries[11]. Another study found 7.04% of students in Asia had anxiety disorders, and one-fifth of students in China experienced stress, depression, and anxiety[12,13].

Colleges have many opportunities to identify risks and offer interventions to students, such as through mental health campus services[9]. The interventions are essential to helping students who are experiencing psychological issues as managing psychological problems can prevent students' conditions from worsening.

In this study, mental health nurses provide laugh therapy as an intervention for college students with psychological problems. Laugh therapy, as a non-pharmacological intervention, is a universal approach to reducing stress and anxiety. Laughter has influenced cognitive behavior to improve and establish healthy physical, psychological, and social relationships from ancient times. Studies have documented the positive role of laughter in enhancing the quality of life. Laugh therapy may be used for both preventive- and therapeutic purposes[14]. The study focused on the effects of laugh therapy on college students with stress, anxiety, and depression. Laugh therapy was chosen as an intervention because it is simple, low-cost, and delivered by a nurse with minimal training. It used a case study design to perform in-depth case analysis.

Materials and methods

Objective

To describe the effect of laugh therapy as a nursing intervention on college students' psychological problems. The theoretical framework used in nursing care draws on Stuart's stress adaptation model.

Ethical aspects

The study was conducted on three participants. Participants received an explanation and filled out an approval form related to research and publication of case data. The institution's research ethics committee approved the research activities numbered 050/USTB/Ethics/Results/V/2024. Participants read and understood the case report's contents and signed an agreement to publish the data submitted to the researcher.

Type of study

Descriptive research involving three cases. Research is developed according to CARE guidelines (Case Report), which aims to create, disseminate, and

implement adequately according to the standards that case studies do and transparently inform results and guide clinical practice[15,16].

Methodological procedures

This case study describes nursing care provided from June 04-08, 2024, to three participants who experienced psychological problems. Participants were selected using purposive sampling. Determining the sample size of a qualitative case study depends on the researcher's definition of the case and its boundaries. It also depends on the research question and epistemological assumptions. One theory recommends using a minimum of four participants. The researcher initially recruited four participants, but one did not attend all therapy sessions, so the number of participants became three. Nursing care is carried out based on the nursing process. The assessment was conducted by nursing students and psychiatric nursing specialist nurses who are experienced in their fields. Determination of diagnoses, interventions and outcomes refers to NANDA International Nursing Diagnoses: definitions and classification[17], Nursing Intervention Classification (NIC)[18], and Nursing Outcomes Classification (NOC)[19].

Study site

The study site was a university in West Bandung District, Indonesia.

Data collection and organization

The depression anxiety stress scale (DASS) was used to measure anxiety before and after nursing intervention. DASS 21 is an instrument that measures depression, anxiety and stress level consisting of 21 questions. Participants answered according to each symptom felt by choosing 0 (never), 1 (sometimes), 2 (often), and 3 (always). The scale interpretation:

- Depression: 0-9 (normal), 10-13 (mild depression), 14-20 (moderate depression), 21-27 (severe depression) and ≥ 28 (very severe depression).
- Anxiety: 0-7 (normal), 8-9 (mild anxiety), 10-14 (moderate anxiety), 15-19 (severe anxiety) and ≥ 20 (very severe anxiety).
- Stress: 0-14 (normal), 15-18 (mild stress), 19-25 (moderate stress), 26-33 (severe stress) and ≥ 34 (very severe stress)[20,16].

Data analysis

Quantitative data (**Table 4**) were obtained from DASS instruments, measured and analyzed using descriptive statistics to assess the outcome of laugh therapy. Nursing care activities are made in a systematic report guided by the stage of the nursing process. Stuart's stress adaptation model is used as a theoretical foundation for predicting and assessing behavior as an adaptation process.

Results

Case overview

Three students from one of the West Java universities participated in this study, all of whom are female, 19-20 years old, and expressed worry caused by coursework that had to be completed. The worry manifested psychosomatically in the form of dizziness and difficulty sleeping. Participants also expressed difficulty concentrating and always thinking about worries (**Table 1**).

Table 1. Results of nursing assessment.

Participants	Age (years)	Gender	Results
P1	19	female	Restless, dizzy, afraid, not enthusiastic about studying, unable to relax, always thinking about college assignments, and sometimes lazy about learning. The respondent's reasons were a busy schedule, college assignments, and practical exams.
P2	20	female	Restless, dizzy, decreased appetite, and a feeling of fear. Sometimes sleep patterns are disturbed, or difficulty sleeping, confusion, inability to relax, and always thinking about what she is worried about, which makes her feel haunted. The results of the identification of the causes of respondent's said problems with lectures, feeling pressured to study, and issues outside of lectures such as with friends and family.
P3	19	female	Respondent feels restless, dizzy, and a little panicked, always thinking about what she is worried about. She also has problems with college assignments, practices, and a busy lecture schedule.

Assessments related to nursing history were carried out with Stuart's stress adaptation model (**Table 2**).

Nursing diagnosis and intervention

Three participants experienced several behavioral and emotional characteristics: restlessness, expressing fear/worry, expressing distress, and inability to sleep. The physiological characteristics found are decreased appetite and dizziness. Found cognitive characteristics: difficulty concentrating and always thinking about problems. According to NANDA 2021, fear-related stressors and behavioral, physiological, and cognitive characteristics refer to nursing diagnoses: anxiety[21]. Nursing intervention refers to NIC[22] with implementation detailed in **Table 3** and a focus on laugh therapy. The stages of laugh therapy are included in the **supplementary material**.

The nursing intervention "laugh therapy" was carried out for seven days for 25-30 minutes each time. The seven-day intervention, based on short-term therapy, can be provided with at least six sessions. So, the intervention is carried out in six sessions for six days, and the seventh day is evaluation and post-test. Researchers have followed up

Table 2. Stuart's stress adaptation model.

Participants	Predisposing factor	Precipitating stressors	Appraisal of stressor	Coping resources	Coping mechanism
P1	Teenager, female, college student	Busy schedule, college assignments, and practical exams.	Restless, dizzy, afraid, not enthusiastic about studying, unable to relax, always thinking about college assignments, and sometimes lazy about learning.	Social support	Avoidance coping
P2	Teenager, female, college student	Problems with lectures, study, friends and family.	Restless, dizzy, decreased appetite, and a feeling of fear. Sometimes, sleep patterns are disturbed, or difficulty sleeping, confusion, inability to relax, and always thinking about what are worried about, which makes feel haunted.	Social support	Ignoring the problem
P3	Teenager, female, college student	College assignments, practices, and a busy lecture schedule.	Restless, dizzy, and a little panicked, always thinking about what are worried	Social support	Negative thoughts

Table 3. Nursing interventions.

Nursing Intervention (NIC)	Nursing activities
Reduction anxiety	Help clients identify situations that trigger anxiety. Use an instrument to measure anxiety levels. Teach breath exercises to promote relaxation. Teach therapy for the reduction of anxiety
Counseling	Educate about anxiety and train clients to replace thoughts that can increase anxiety with positive thoughts.
Distraction	Encourage clients to choose distraction techniques such as listening to music, deep breathing exercises, and positive affirmations.

Table 4. Results of participants' anxiety levels based on the DASS 21 before and after nursing interventions.

Participants	Before Intervention		After intervention	
	Score	Interpretation	Score	Interpretation
I	D 12	Mild depression	D 8	normal
	A 11	Moderate anxiety	A 7	normal
	S 15	Mild stress	S 8	normal
II	D 17	Moderate depression	D 12	Mild depression
	A 19	Severe anxiety	A 9	Moderate anxiety
	S 20	Moderate stress	S 15	Mild stress
III	D 10	Mild depression	D 0	normal
	A 9	Mild anxiety	A 3	normal
	S 15	Mild stress	S 0	normal

with participants and found that seven days is able to reduce the psychological symptoms experienced. The intervention showed a decrease in stress, anxiety, and depression score before and after the intervention (**Table 4**).

Depression and anxiety decreased by 4-10 points, and stress decreased by 5-15 points after therapy (**Table 4**). The results of the subjective evaluation of the participants were: "I feel calmer, sleep better, and can study well" (P1). "I feel more energetic, sleep better, and have less anxiety." "I feel calm, my headache is gone, and I am enthusiastic about carrying out my duties as a student" (P3).

Discussion

The results of previous studies stated that stress, anxiety, and depression among college students correlate with sleep quality[23]. Over 75% of students aged 18 to 33 have increased stress levels, which are higher than those of other groups[24]. College is considered stressful for students due to the academic load, poor planning and time management, pressure from lecturers, high parental expectations, and lack of sleep. In addition, the competition in college causes students to experience various stress factors, such as fear of failure, low test scores, and pressure to perform well in exams[25]. Anxiety is more experienced by female students who have a higher educational background[26]. The pressures faced by students lead to higher levels of anxiety and depression. The study found that 60.8% of students reported feeling anxious, 38.2% reported feeling depressed, and 10.4% had considered suicide[24]. The anxiety experienced by students can affect individual functioning. Anxiety is a mental health problem that students often experience, so prevention programs are needed to reduce the prevalence of anxiety. The results showed that cognitive behavior therapy and mindfulness can be done well among students[27]. The current results, before the intervention, anxiety was in the mild-severe range, stress and depression were in the mild-moderate range, and after laugh therapy they changed to mild-moderate.

Laughter can reduce stress, anxiety, and depression. This is related to the theory that laughter can suppress the bioactivity effects of epinephrine, cortisol, and 3,4-dihydrophenylacetic acid (the main dopamine catabolite) and increase dopamine and serotonin activity, reducing stress, anxiety, and depression. Emotional expressions such as laughter affect the levels of norepinephrine, dopamine, and serotonin[28,29,14].

Laughter therapy offers an affordable and easily accessible solution for students on campus. By organising group laughter therapy sessions, the campus mental health team can create a supportive environment that not only helps prevent mental health issues, but also effectively addresses challenges such as stress, anxiety, and depression. Engaging in laughter therapy can foster resilience and promote overall well-being among students, making it a powerful resource for enhancing mental health on campus.

Mental health nurses can positively provide nursing care to students to overcome mental health problems (stress, anxiety, and depression) with a non-pharmacological intervention: laugh therapy. Stuart's stress adaptation model contributed to the nursing care provided. Individuals in the context of students will be able to improve their health by maintaining

adaptive behavior and being able to change stressors. Students must be able to adapt and maintain psychological well-being.

The results of a study of laugh therapy on nursing students in Korea in 2015 showed that providing laugh therapy for four sessions (1 session/week) reduced stress and depression levels[30]. The results of a study on nursing students in India in 2021 for 10 days reduced the mean anxiety score on the post-test[31]. The current study had no control group, so it could not be compared. In addition, observations were only made based on subjective data results and post-test measurements. The difference between previous studies and this one is that shorter therapy times can also reduce levels of depression, anxiety, and stress in participants.

Limitations of the study

A limitation of this study is that it is difficult to thoroughly evaluate and explore the components of Stuart's stress adaptation model in the selected case study. The other limitations are the small sample size and the lack of control group and limited generalizability.

Contribution to the field of nursing, health or public policy

The case study conducted contributes to managing stress, anxiety, and depression experienced by students in the educational environment. Laugh therapy can be a standard nursing intervention given to mental health problems experienced by college students.

Conclusion

Laugh therapy can be given as a mental health nursing intervention to overcome mental health problems experienced by students. Students can do laugh therapy as a form of group therapy to overcome mental health problems. Further research is needed to see the effectiveness of laughter therapy with a larger sample and involving a control group.

Funding

This article has not received any specific grant from funding agencies in the public, commercial, or for-profit sectors.

Conflict of interest

The authors declare no conflicts of interest.

References

1. Liu Y, Shen Y, Cai Z. A deep learning-based prediction model of college students' psychological problem categories for post-epidemic era—taking college students in Jiangsu Province, China as an example. Front Psychol 2022;13: 1-10.
2. Lattie EG, Adkins EC, Winquist N, Stiles-Shields C, Wafford QE, Graham AK. Digital mental health interventions for depression, anxiety, and enhancement of psychological well-being among college students: systematic review. J Med Internet Res 2019;21(7):e12869.
3. Carr E, Davis K, Bergin-Cartwright G, Lavelle G, Leightley D, Oetzmann C, et al. Mental health among UK university staff and postgraduate students in the early stages of the COVID-19 pandemic. Occup Environ Med 2022; 79(4):259–267.
4. Pierceall EA, Keim MC. Stress and coping strategies among community college students. Community Coll J Res Pract 2007;31(9):703–712.
5. Wang X, Liu Q. Prevalence of anxiety symptoms among Chinese university students amid the COVID-19 pandemic: a systematic review and meta-analysis. Heliyon 2022;8(8):e10117.
6. Ramón-Arbués E, Gea-Caballero V, Granada-López JM, Juárez-Vela R, Pellicer-García B, Antón-Solanas I. The prevalence of depression, anxiety and stress and their associated factors in college students. Int J Environ Res Public Health 2020;17(19):1–15.
7. Beiter R, Nash R, McCrady M, Rhoades D, Linscomb M, Clarahan M, et al. The prevalence and correlates of depression, anxiety, and stress in a sample of college students. J Affect Disord 2015;173:90–96.
8. Bangasser DA, Curtis A, Reyes BAS, Bethea TT, Parastatidis I, Ischiropoulos H, et al. Sex differences in corticotropin-releasing factor receptor signaling and trafficking: potential role in female vulnerability to stress-related psychopathology. Mol Psychiatry 2010;15(9): 896–904.
9. Lipson SK, Zhou S, Abelson S, Heinze J, Jirsa M, Morigney J, et al. Trends in college student mental health and help-seeking by race/ethnicity: findings from the national healthy minds study, 2013–2021. J Affect Disord 2022;306:138–147.
10. Kodish T, Lau AS, Gong-Guy E, Congdon E, Arnaudova I, Schmidt M, et al. Enhancing racial/ethnic equity in college student mental health through innovative screening and treatment. Administration and Policy in Mental Health and Mental Health Services Research. 2022;49(2):267–282.
11. January J, Madhombiro M, Chipamaunga S, Ray S, Chingono A, Abas M. Prevalence of depression and anxiety among undergraduate university students in low- and middle-income countries: a systematic review protocol. Syst Rev 2018;7(1):57.
12. Cuttilan AN, Sayampanathan AA, Ho RCM. Mental health issues amongst medical students in Asia: a systematic review [2000-2015]. Ann Transl Med 2016;4(4):72.
13. Liu X, Ping S, Gao W. Changes in undergraduate students' psychological well-being as they experience university life. Int J Environ Res Public Health 2019;16(16):2864.
14. Akimbekov NS, Razzaque MS. Laughter therapy: a humor-induced hormonal intervention to reduce stress and anxiety. Curr Res Physiol 2021;4:135–138.
15. Gagnier JJ, Kienle G, Altman DG, Moher D, Sox H, Riley D. The CARE guidelines: consensus-based clinical case reporting guideline development. Glob Adv Health Med 2013;2(5):38–43.

16. Mendonça AB, Pereira ER, Magnago C, Silva RMCRA, Martins A de O. Nursing process for a patient with needle phobia: a case study. Rev Bras Enferm 2020;73(4):1–8.
17. Herdman TH, Kamitsuru S, Takao Lopes C. Nursing diagnoses: definitions and classification 2021-2023. Twelfth. New York: Thieme; 2021. 587 p.
18. Bulecheck GM, Butcher HK, Dochterman JM, Wagner CM. Nursing intervention classification (NIC) Indonesian edition. 6th ed. Elsevier; 2013.
19. Moorhead S, Johnson M, Maas ML, Swanson E. Nursing outcomes classification (NOC) Indonesian edition. 5 th. Elsevier; 2013.
20. Lemay V, Hoolahan J, Buchanan A. Impact of a yoga and meditation intervention on students' stress and anxiety levels. Am J Pharm Educ 2019;83(5).
21. Herdman TH, Kamitsuru S, Takao Lopes C. Nursing diagnoses: definitions and classification 2021-2023. Twelfth. New York: Thieme; 2021. 587 p.
22. Bulecheck GM, Butcher HK, Dochterman JM, Wagner CM. Nursing intervention classification (NIC) Indonesian edition. 6th ed. Elsevier; 2013.
23. Alwhaibi M, Al Aloola NA. Associations between stress, anxiety, depression and sleep quality among healthcare students. J Clin Med 2023;12(13):4340.
24. Huberty J, Green J, Glissmann C, Larkey L, Puzia M, Lee C. Efficacy of the mindfulness meditation mobile app "Calm" to reduce stress among college students: randomized controlled trial. JMIR Mhealth Uhealth 2019;7(6):e14273.
25. Rajanayagam B. Prevalence of anxiety depression and stress among first year medical students in Tamilnadu. Bioinformation 2023;19(5):649–654.
26. Wang X, Zhang N, Pu C, Li Y, Chen H. Anxiety , depression , and PTSD among college students in the post-COVID-19 era: a cross-sectional study. Brain Sci 2022;12(11):1–12.
27. Unwin BK, Goodie J, Reamy B V, Quinlan JD. Care of the college student. Am Fam Physician 2021;104(2): 141–151.
28. Yim J. Therapeutic benefits of laughter in mental health: a theoretical review. Tohoku J Exp Med 2016;239(3): 243–249.
29. Wang F, Yang J, Pan F, Ho RC, Huang JH. Editorial: Neurotransmitters and Emotions. Front Psychol. 2020;11.
30. Yim SY, Park MH. Effects of laughter therapy program on perceived stress and depression in nursing college students. The Journal of the Korea Contents Association 2015;15(11):289–97.
31. Effectiveness of laughter therapy on reduction of stress among nursing students. Indian Journal of Forensic Medicine & Toxicology. 2021;15(1):126-132.

Supplementary material

Stages of laugh therapy.

Stage	
1	Warm up by clapping your hands while saying, 'Ho ho ho… Ha ha ha…".
2	Inhale through your nose, hold for three counts, and then exhale slowly through your mouth.
3	Rotate the shoulders from the front to the back, nod the head down until the chin touches the chest, push the head up and back, and look left and right.
4	Encourage participants to laugh together
5	Polite laughter. Giving instructions for participants to laugh while greeting other participants. The position of participants is looking at each other; participants greet each other while laughing softly.
6	Laughter of appreciation. Participants make a small circle by connecting the tips of their index fingers with their thumbs. Their hands are directed forward and backwards. They look at the other participants, laugh at the target, say ho ho ho…ha ha ha... and clap their hands. After doing this, the participants take a slow and deep breath.
7	A meter of laughter. The left hand is directed to the side straight with the body; the right hand is pulled back like pulling an arrow. Do it in three movements while saying "ae….ae….aeee…", then laugh out loud while stretching both arms, and the head is slightly tilted up, and the laughter comes from the stomach.
8	Milk shakes laughter. Participants imagine holding a glass of milk in their left and right hands. When the tutor gives instructions, the milk is poured from one glass to another while saying, "aeeeee…". Do it alternately. After finishing, the participants laugh as if drinking milk. Do it four times. After that, clap your hands while saying, "Ho ho ho…haha". After that, participants are advised to take a slow and deep breath. Silent laughter. This laughter is done slowly and should not use excessive force. Participants are advised to open their mouths as wide as possible, as if laughing out loud but without sound, look at each other, and make various movements by clapping and moving their heads with funny expressions. Then, participants are advised to take a slow breath.
9	Silent laughter. This laughter is done slowly and should not use excessive force. Participants are advised to open their mouths as wide as possible, as if laughing out loud but without sound, look at each other, and make various movements by clapping and moving their heads with funny expressions. Then, participants are advised to take a slow breath.
10	Humming laughter with closed lips. Participants are encouraged to hum "hmmmmmm…" with their mouths closed so that it feels like it echoes in their heads, the position of participants face each other and make funny facial expressions so that other participants laugh; after finishing, the participants take deep and slow breaths.
11	Swing laughter. Participants form a circle, then take two steps back from the circle while laughing and two steps forward to make the circle smaller while saying "ae ae ae". All participants raise their hands and laugh out loud together, then take two steps back while waving their hands. Participants take two steps forward, saying "aaa… o..o..o.. e..e..e…. u..u..u…." while laughing aloud. Do it four times. After that, retake a deep and slow breath.
12	Lion's laughter. Participants are advised to eliminate feelings of fear and worry. They open their mouths wide by sticking their tongues out as much as possible and open their eyes as wide as possible as if glaring. At this point, participants laugh using pressure from the stomach. After finishing, participants take a slow and deep breath.
13	Cell phone laughter. Participants will be in a different group and face each other as if holding a cell phone while laughing, looking at each other, and returning to the starting position. After finishing, participants are advised to take a deep and slow breath.
14	Laughter rebuttal. Participants are divided into two competing groups and separated by distance. In one group, they look at each other while laughing and pointing their index fingers at the group in front of them. After finishing, they take a deep and slow breath.

15	Laughter of forgiveness. Participants hold each other's ears while crossing their arms and kneeling while laughing. The purpose of this laughter is to forgive each other if there is a dispute. After finishing, take a deep and slow breath.
16	Gradual laughter. The tutor directs the participants to approach him with a broad smile, which gradually turns into a light laugh, continues into a moderate laugh, and ends with a full, enthusiastic laugh. This laugh lasts one minute. After finishing, take a deep and slow breath to be fresh and calm again.
17	Heart-to-heart laughter. This laughter is the last session of the therapy step. All participants held each other's hands while approaching the tutor and laughed together, looking at each other with relief. Participants will also shake hands to establish a sense of familiarity.

ACADEMIC JOURNAL OF HEALTH SCIENCES
MEDICINA BALEAR

Original article

Comparative evolution of metabolic health status in obese individuals using novel and conventional anthropometric indexes: a decade-long analysis in Spanish workers

Evolución comparativa del estado de salud metabólica en individuos con obesidad mediante índices antropométricos convencionales y novedosos: un análisis de una década en trabajadores españoles

Miguel García-Samuelsson[1,2], Pedro Juan Tárraga-López[3], Ángel Arturo López-González[1,2,4,5]*, Carla Busquets-Cortés[1,2], Alberto Ramírez-Gallegos[5], Joan Obrador de Hevia[1,2], José Ignacio Ramírez-Manent[1,4,5,6]

[1]University Institute of Health Sciences (IUNICS), Palma de Mallorca, Spain
[2]Faculty of Dentistry, ADEMA University School, Palma de Mallorca, Spain
[3]Faculty of Medicine, University of Castilla La Mancha, Albacete, Spain
[4]Balearic Islands Health Research Institute Foundation, Palma de Mallorca, Spain
[5]Balearic Islands Health Service, Palma de Mallorca, Spain
[6]Faculty of Medicine, University of the Balearic Islands, Palma de Mallorca, Spain

Received: 15-05-2025
Accepted: 16-06-2025

***Corresponding author:** Ángel Arturo López González. a.lopez@eua.edu.es

Abstract

Introduction: the concept of metabolically healthy obesity (MHO) challenges traditional assumptions about the uniform health risks associated with obesity. However, the prevalence and longitudinal evolution of MHO remain underexplored, particularly when different anthropometric indexes are applied.

Objective: to analyze and compare the prevalence and 10-year evolution of MHO versus metabolically non-healthy obesity (MNHO) using various obesity-related indexes, including body mass index (BMI), waist-to-height ratio (WtHR), relative fat mass (RFM), and METS-VF, in a large working population.

Materials and method: we conducted a retrospective cross-sectional analysis of 68,884 Spanish workers (45,498 men and 23,386 women) from 2010 to 2020. Participants were classified as MHO or MNHO using three diagnostic criteria and evaluated across different obesity indexes. Temporal changes in prevalence were assessed for each category.

Results: men exhibited higher rates of metabolic unhealthiness across all indexes and time points. Regardless of the criteria used, MHO individuals presented significantly lower BMI, WtHR, RFM, and METS-VF values compared to MNHO counterparts ($p<0.001$). Over the decade, all obesity indexes showed an increasing trend in the proportion of metabolically non-healthy individuals. For example, among men with obesity grade I, the percentage of MNHO increased from 56.7% to 79.2% (criterion 2), and among women, from 68.1% to 88.5%.

Cite as: García-Samuelsson M, Tárraga-López PJ, López-González ÁA, Busquets-Cortés C, Ramírez-Gallegos A, Obrador de Hevia J, et al. Comparative evolution of metabolic health status in obese individuals using novel and conventional anthropometric indexes: a decade-long analysis in Spanish workers. Acad J Health Sci 2025; 40(5): 53-66. Available from: https://doi.org/10.3306/AJHS.2025.40.05.7

Acad J Health Sci 2025; 40(5): 53-66
https://doi.org/10.3306/AJHS.2025.40.05.7
www.ajhealthsciences.com

Conclusions: MHO prevalence is substantially influenced by the index and definition applied. Despite stable obesity rates, the metabolic health of obese individuals declined over time. These findings support the need for improved screening strategies integrating multiple indexes beyond BMI to better identify high-risk individuals.

Keywords: Metabolically healthy obesity. Obesity phenotypes. Population-based study. Relative fat mass. Body mass index. Metabolic score for visceral fat. (METS-VF)

Resumen

Introducción: el concepto de obesidad metabólicamente sana (OMS) cuestiona las suposiciones tradicionales sobre los riesgos para la salud asociados de forma uniforme con la obesidad. No obstante, la prevalencia y evolución longitudinal de la OMS siguen siendo poco exploradas, especialmente cuando se aplican diferentes índices antropométricos.

Objetivo: analizar y comparar la prevalencia y la evolución a 10 años de la obesidad metabólicamente sana (OMS) frente a la obesidad metabólicamente no sana (OMNS), utilizando diversos índices relacionados con la obesidad, incluidos el índice de masa corporal (IMC), la razón cintura-estatura (cintura/altura), la masa grasa relativa (RFM) y el puntaje metabólico de grasa visceral (METS-VF), en una amplia población trabajadora.

Materiales y método: se realizó un análisis retrospectivo de corte transversal en 68.884 trabajadores españoles (45.498 hombres y 23.386 mujeres) entre los años 2010 y 2020. Los participantes fueron clasificados como OMS u OMNS según tres criterios diagnósticos y evaluados mediante distintos índices de obesidad. Se analizaron los cambios temporales en la prevalencia de cada categoría.

Resultados: los hombres mostraron mayores tasas de alteración metabólica en todos los índices y puntos temporales. Independientemente del criterio empleado, los individuos clasificados como OMS presentaron valores significativamente inferiores de IMC, cintura/altura, RFM y METS-VF en comparación con sus pares OMNS (p<0,001). A lo largo de la década, todos los índices de obesidad evidenciaron una tendencia creciente en la proporción de personas metabólicamente no sanas. Por ejemplo, entre los hombres con obesidad de grado I, el porcentaje de OMNS aumentó del 56,7% al 79,2% (criterio 2), y entre las mujeres, del 68,1% al 88,5%.

Conclusiones: La prevalencia de OMS está considerablemente influenciada por el índice y la definición utilizados. A pesar de que las tasas de obesidad se mantuvieron estables, la salud metabólica de las personas con obesidad se deterioró con el tiempo. Estos hallazgos respaldan la necesidad de mejorar las estrategias de cribado mediante la integración de múltiples índices más allá del IMC, con el fin de identificar con mayor precisión a los individuos con alto riesgo.

Palabras clave: Obesidad metabólicamente sana. Fenotipos de obesidad. Estudio poblacional. Masa grasa relativa. Índice de masa corporal. Puntaje metabólico de grasa visceral. (METS-VF)

Introduction

Obesity continues to represent one of the most pressing global health concerns, with over one billion individuals affected and its burden steadily increasing across all age groups and socioeconomic strata. The World Health Organization (WHO) estimates that more than 650 million adults were obese in 2022, contributing to more than 4 million deaths annually through associated conditions such as cardiovascular disease (CVD), type 2 diabetes *mellitus* (T2DM), and several types of cancer[1]. Traditionally, obesity has been defined and classified by body mass index (BMI), a simple anthropometric indicator of excess body weight relative to height. However, BMI does not distinguish between fat and lean mass or account for fat distribution, a critical determinant of metabolic health[2].

This limitation has driven increasing attention toward more nuanced classifications of obesity, most notably the concept of metabolically healthy obesity (MHO). Individuals with MHO exhibit an elevated BMI but maintain a favorable cardiometabolic profile, characterized by normal insulin sensitivity, blood pressure, lipid levels, and inflammatory markers[3]. Estimates suggest that between 10% and 30% of obese individuals may be classified as MHO, depending on the criteria used and the population studied[4]. The clinical relevance of MHO remains highly debated, with some authors viewing it as a transient or unstable state rather than a truly protective phenotype[5].

Indeed, longitudinal studies have shown that a significant proportion of MHO individuals progress to metabolically unhealthy obesity (MNHO) over time, particularly with advancing age, weight gain, or the development of central adiposity[6]. In a prospective study by Mongraw-Chaffin et al., approximately 50% of MHO adults transitioned to a metabolically unhealthy phenotype over a 10-year follow-up[7]. Moreover, large meta-analyses have demonstrated that MHO individuals remain at higher risk of cardiovascular events and all-cause mortality than their metabolically healthy normal-weight (MHNW) counterparts[8,9]. These findings suggest that while MHO

may represent a state of relative rather than absolute protection, it still confers elevated long-term health risks.

The instability and prognostic ambiguity of MHO are further complicated by the lack of a standardized definition. Different studies employ varying criteria to define MHO, including the absence of metabolic syndrome components, favorable insulin resistance markers, or specific cutoffs for lipid and glucose values[10]. This inconsistency leads to substantial heterogeneity in prevalence estimates and makes comparisons between studies difficult. Consequently, there is growing interest in refining the identification of MHO and MNHO individuals using more sensitive and physiologically relevant metrics of adiposity and fat distribution.

Alternative anthropometric indices, such as the waist-to-height ratio (WtHR), relative fat mass (RFM), and the metabolic score for visceral fat (METS-VF), have shown promising utility in capturing central adiposity and visceral fat dysfunction, which are key drivers of metabolic impairment[11-13]. WtHR has emerged as a reliable predictor of cardiometabolic risk across various populations and has been recommended as superior to BMI in clinical guidelines for cardiovascular prevention[14]. A WtHR ≥0.5 has been proposed as a universal cutoff for increased cardiometabolic risk, regardless of sex or, ethnicity[15].

Relative fat mass, an equation derived from height and waist circumference, has been shown to outperform BMI in estimating whole-body fat percentage, especially among women and older adults[16]. Unlike BMI, RFM captures the influence of central fat accumulation, which is more closely linked to insulin resistance, lipid abnormalities, and inflammation[17]. Furthermore, the METS-VF index—incorporating WtHR, age, sex, fasting glucose, triglycerides, and HDL-cholesterol—has demonstrated strong associations with visceral fat, hepatic steatosis, and metabolic risk across diverse cohorts[18,19]. Its application in occupational and epidemiological studies offers a promising avenue for improved risk stratification in clinical practice.

Despite the emergence of these novel indices, few studies have systematically compared the prevalence and evolution of MHO versus MNHO using multiple adiposity-based tools. Most investigations rely on BMI and metabolic syndrome definitions alone, neglecting more precise measures of visceral adiposity and metabolic dysfunction. Moreover, limited data are available on the temporal dynamics of metabolic health among obese individuals, particularly in large-scale, real-world cohorts. Occupational health databases, which regularly collect biometric and laboratory data over time, offer a valuable resource for addressing these gaps.

In the Spanish context, recent evidence indicates a steady increase in obesity and overweight prevalence among the working-age population, raising concerns about future burdens of cardiometabolic diseases[20]. A national occupational cohort study conducted between 2010 and 2020 identified a growing proportion of workers shifting from MHO to MNHO, with notable sex-based disparities in obesity patterns[21]. However, most prior analyses were based on BMI alone, without considering alternative indexes such as WtHR, RFM, or METS-VF. Given the evolving nature of obesity phenotypes and the heterogeneity in metabolic risk within obese individuals, a more comprehensive assessment incorporating various indexes is warranted.

The present study aims to address these knowledge gaps by analyzing the prevalence and evolution of MHO versus MNHO in a large cohort of 68,884 Spanish workers over a ten-year period. Using three different diagnostic criteria and four anthropometric/metabolic indexes (BMI, WtHR, RFM, METS-VF), we:

1. Quantify the proportion of MHO individuals across sex and index.
2. Examine temporal changes in MHO/MNHO status from 2010 to 2020.
3. Compare the discriminatory capacity of each index in capturing metabolic deterioration among obese individuals.

By leveraging a rich longitudinal dataset and adopting a multidimensional approach to obesity phenotyping, this study contributes to the understanding of how different measures of adiposity affect MHO classification and its temporal progression. The findings have important implications for clinical screening, early prevention, and personalized management of obesity-related risk in working populations.

Materials and method

Study design and population

This research comprised two complementary components:

1. A cross-sectional analysis to examine the distribution of metabolically healthy obesity (MHO) and metabolically non-healthy obesity (MNHO) phenotypes according to various anthropometric and metabolic indexes.
2. A retrospective longitudinal analysis to assess the 10-year evolution (2010–2020) of MHO/MNHO prevalence among Spanish workers.

Data were obtained from routine annual occupational health examinations performed between January 2010 and December 2020. The full cohort included 68,884 adult workers (45,498 men and 23,386 women), aged 18 to 69 years, from diverse industrial and service sectors throughout Spain. For the longitudinal component, we included only those individuals who had at least one health examination recorded in both the initial period (2010–2012) and the final period (2018–2020).

All examinations were conducted by licensed occupational physicians and nurses using standardized protocols. Written informed consent was obtained from all participants. The study complied with the principles of the Declaration of Helsinki and was approved by the relevant institutional ethics committee.

Inclusion criteria

Participants were eligible for the study if they met all the following conditions:

- A diagnosis of obesity, defined as a body mass index (BMI) ≥ 30 kg/m^2
- Age between 18 and 69 years at the time of evaluation
- Employment in one of the companies participating in the study
- Provision of informed consent to participate in the research

The participant selection and flow through the study are illustrated in **Figure 1.**

Anthropometric and clinical assessments

Anthropometric data included height, weight, and waist circumference. BMI was calculated as weight (kg) divided by height squared (m^2). Waist-to-height ratio (WtHR) was computed by dividing waist circumference (cm) by height (cm). Relative fat mass (RFM) was estimated using the sex-specific equation validated for adult populations:

- For men: RFM = 64 − (20 × height/waist circumference)
- For women: RFM = 76 − (20 × height/waist circumference)[22]

Systolic and diastolic blood pressure were measured in the seated position after a 5-minute rest using calibrated automatic sphygmomanometers. Blood samples were collected after overnight fasting and analyzed for glucose, triglycerides, HDL-cholesterol, LDL-cholesterol, and total cholesterol using standardized enzymatic techniques.

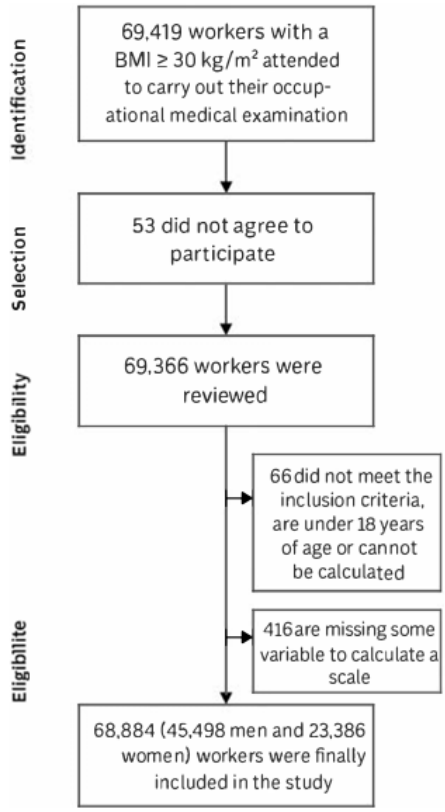

Figure 1. Flow diagram of participant.

The Metabolic Score for Visceral Fat (METS-VF) was calculated using the validated composite formula incorporating age, sex, waist-to-height ratio, glucose, triglycerides, HDL-cholesterol, and BMI, according to the following expression:

METS-VF = 4.466 + 0.011 × (METS-IR)^3 + 3.239 × (waist/height)^3 + 0.319 × sex + 0.594 × ln(age)

Where METS-IR = ln[(2 × glucose) + triglycerides] × BMI / ln(HDL-c), and sex = 1 for men and 0 for women[23]. This index has shown strong correlations with MRI-quantified visceral fat and hepatic steatosis[24].

Definition of metabolically healthy obesity (MHO)

Participants with BMI ≥30 kg/m^2 were categorized as obese. Metabolically healthy obesity (MHO) was identified using three operational definitions adapted from previous studies[25]:

- Criterion 1: Absence of metabolic syndrome (MetS) components (excluding central obesity), based on NCEP ATP III criteria.
- Criterion 2: Presence of no more than one abnormal cardiometabolic parameter (blood pressure, HDL-c, triglycerides, fasting glucose).
- Criterion 3: All cardiometabolic values within the normal range: fasting glucose <100 mg/dL, triglycerides <150 mg/dL, HDL ≥40 mg/dL (men)

or ≥50 mg/dL (women), and blood pressure <130/85 mmHg.

Individuals with ≥2 abnormal parameters were considered to have metabolically non-healthy obesity (MNHO).

Assessment of physical activity and Mediterranean diet adherence

Physical activity was assessed using the short version of the International Physical Activity Questionnaire (IPAQ-SF), which has been validated in European working populations[26]. The questionnaire records the frequency and duration of walking, moderate, and vigorous activity during the preceding seven days. Participants were categorized as physically active if they achieved at least 600 MET-min/week, corresponding to moderate or high activity levels[27].

Adherence to the Mediterranean diet was evaluated using the 14-item Prevention with Mediterranean Diet (PREDIMED) questionnaire**,** which has been validated as a reliable dietary screening tool among Spanish adults[28]. The questionnaire assigns 1 point per item meeting a predefined criterion (e.g., olive oil as main fat, ≥3 servings of legumes/week, ≥3 pieces of fruit/day), with total scores ranging from 0 to 14. A score ≥9 was considered indicative of good adherence[29].

Sociodemographic and lifestyle variables

Participants reported their age, sex, educational level, occupational social class, and smoking status via structured interview.

Educational level was classified as primary, secondary, or university.

Socioeconomic status was determined using the classification system proposed by the Spanish Society of Epidemiology, based on the 2011 National Classification of Occupations (CNO-11). Participants were categorized into three occupational social classes as follows[30]:

- Class I: Executives, university-educated professionals, elite athletes, and artists.
- Class II: Intermediate-level professionals and skilled self-employed workers.
- Class III: Manual laborers and low-skilled workers.

Smoking status was classified as current smoker or non-smoker.

Statistical analysis

Descriptive statistics were presented as means and standard deviations (SD) for continuous variables, and frequencies with percentages for categorical variables. Sex-stratified comparisons were made using T-tests for continuous variables and chi-square tests for categorical variables.

For the cross-sectional analysis, we compared obesity indices (BMI, WtHR, RFM, METS-VF) between MHO and MNHO groups across the three MHO criteria. For the longitudinal analysis, we calculated the percentage change in MHO and MNHO prevalence from 2010–2012 to 2018–2020 within each obesity index category. Paired comparisons were performed for individuals with repeated measures, and statistical significance was assessed using McNemar's test or Wilcoxon signed-rank test as appropriate.

All statistical analyses were conducted using IBM SPSS Statistics version 29.0 (IBM Corp., Armonk, NY, USA). A two-tailed p-value <0.05 was considered statistically significant.

Results

Table 1 provides a comprehensive characterization of the cohort, (n=68,884), highlighting significant sex-based differences across anthropometric, clinical, and behavioral variables. Men exhibited higher mean values for body weight, waist circumference, blood pressure, and serum triglycerides, while women had higher HDL-cholesterol levels and a healthier lifestyle profile, including greater adherence to the Mediterranean diet and lower smoking prevalence. Notably, despite a similar educational distribution, women were more frequently classified in higher social classes. These differences underscore the importance of sex-stratified analysis when evaluating metabolic health and obesity-related risk factors.

Table 2 compares the performance of four obesity indexes (BMI, WtHR, RFM, METS-VF) across various definitions of MHO and MNHO in both sexes. Consistently, MNHO individuals presented significantly worse anthropometric and metabolic index values than MHO counterparts, regardless of the criterion applied (all p<0.001). This trend was observed across both sexes, though absolute values differed, with women displaying higher RFM but lower METS-VF values. The data confirm the robustness of these indexes in differentiating metabolic phenotypes and support the potential utility of alternative measures (e.g., RFM, METS-VF) in clinical settings.

Table 1. Sociodemographic, anthropometric, clinical, and lifestyle characteristics of the study population by sex.

	Men n=45,498	Women n=23.386	
	Mean (SD)	Mean (SD)	p-value
Age (years)	42.9 (10.0)	42.0 (10.4)	<0.001
Height (cm)	173.2 (7.1)	160.0 (6.7)	<0.001
Weight (kg)	99.7 (12.4)	87.5 (12.3)	<0.001
Waist (cm)	96.7 (8.9)	83.3 (8.8)	<0.001
Hip (cm)	108.6 (7.9)	109.5 (9.3)	<0.001
Systolic BP (mmHg)	131.8 (16.2)	124.0 (15.9)	<0.001
Systolic BP (mmHg)	81.0 (10.7)	76.9 (11.0)	<0.001
Total cholesterol (mg/dL)	204.1 (38.8)	200.3 (37.4)	<0.001
HDL-cholesterol (mg/dL)	48.3 (7.0)	51.2 (7.1)	<0.001
LDL-cholesterol (mg/dL)	124.5 (37.5)	127.1 (37.0)	<0.001
Triglycerides (mg/dL)	158.6 (108.4)	110.5 (55.8)	<0.001
Glucose (mg/dL)	92.3 (14.0)	89.0 (13.4)	<0.001
	%	%	p-value
< 30 years	10.0	13.5	<0.001
30-39 years	28.3	28.2	
40-49 years	34.5	32.3	
50-59 years	22.6	21.9	
60-69 years	4.6	4.3	
Elementary school	63.7	64.9	<0.001
High school	32.3	30.6	
University	4.0	4.5	
Social class I	4.6	4.2	<0.001
Social class II	15.7	21.4	
Social class III	79.7	74.4	
No physical activity	96.5	95.3	<0.001
Yes physical activity	3.5	4.7	
No Mediterranean diet	91.8	85.1	<0.001
Yes Mediterranean diet	8.2	14.9	
Non-smokers	68.3	74.0	<0.001
Smokers	31.7	26.0	

Notes: BP, blood pressure. HDL, high density lipoprotein. LDL, low density lipoprotein.
SD, standard deviation

Table 2. Mean values of obesity indexes according to different MHO/MNHO definitions in men and women.

Men	MHO n=8764	MNHO n=36734		MHO 1 n=24264	MNNO 1 n=21234		MHO n=34660	MNHO n=10838	
	Mean (SD)	Mean (SD)	p-value	Mean (SD)	Mean (SD)	p-value	Mean (SD)	Mean (SD)	p-value
BMI	32.4 (2.5)	33.4 (3.3)	<0.001	32.7 (2.7)	33.7 (3.5)	<0.001	32.9 (2.9)	34.1 (3.8)	<0.001
WtHR	0.54 (0.03)	0.57 (0.05)	<0.001	0.54 (0.03)	0.59 (0.06)	<0.001	0.55 (0.04)	0.61 (0.05)	<0.001
RFM	26.5 (2.2)	28.3 (3.2)	<0.001	26.7 (2.3)	29.4 (3.2)	<0.001	27.1 (2.6)	30.8 (2.8)	<0.001
METS-VF	6.8 (0.3)	7.1 (0.3)	<0.001	6.8 (0.3)	7.2 (0.3)	<0.001	6.9 (0.3)	7.3 (0.3)	<0.001
Women	**n=6146**	**n=17240**		**n=14448**	**n=8938**		**n=19976**	**n=3410**	
	Mean (SD)	**Mean (SD)**	**p-value**	**Mean (SD)**	**Mean (SD)**	**p-value**	**Mean (SD)**	**Mean (SD)**	**p-value**
BMI	32.9 (2.7)	34.5 (4.1)	<0.001	33.4 (3.1)	35.3 (4.6)	<0.001	33.9 (3.6)	35.7 (4.8)	<0.001
WtHR	0.50 (0.03)	0.53 (0.05)	<0.001	0.51 (0.03)	0.55 (0.06)	<0.001	0.51 (0.04)	0.58 (0.06)	<0.001
RFM	35.9 (2.6)	37.7 (3.7)	<0.001	36.2 (2.8)	38.9 (4.0)	<0.001	36.6 (3.0)	40.9 (4.0)	<0.001
METS-VF	6.1 (0.4)	6.4 (0.4)	<0.001	6.2 (0.4)	6.6 (0.4)	<0.001	6.3 (0.4)	6.8 (0.4)	<0.001

Notes: MHO, metabolically healthy obesity. MNHO, metabolically non-healthy obesity. BMI, body mass index. WtHR, waist to height ratio. RFM, relative fat mass. METS-VF, metabolic score for visceral fat. SD, standard deviation.

Table 3. Prevalence of MHO across obesity classifications by sex and MHO criteria.

	Men				Women			
		MHO 0	MHO 1	MHO 2		MHO 0	MHO 1	MHO 2
	n	%	%	%	n	%	%	%
BMI obesity I	35,724	21.3	56.5	79.2	16,160	30,4	68.1	88.5
BMI obesity II	7,838	12.1	44.2	67.7	5,146	20.8	53.0	81.3
BMI obesity III	1,936	11.2	32.2	55.4	2,080	7.7	34.6	71.5
WtHR normal	4,888	28.2	72.5	95.3	9,152	32.7	73.5	94.4
WtHR high	40,610	18.2	51.0	73.9	14,234	22.1	54.2	79.6
RFM non obesity	1,792	25,4	71.4	95.1	3,216	34.4	75.1	95.0
RFM obesity	43,706	19.0	52.6	75.4	20,170	25.0	59.7	83.9
METS-VF normal	30,828	25.8	68.0	90.0	22,626	27.2	63.6	87.3
METS-VF high	14,670	5.5	22.5	47.2	760	6.2	6.3	28.4

Notes: MHO, metabolically healthy obesity. BMI, body mass index. WtHR, waist to height ratio. RFM, relative fat mass. METS-VF, metabolic score for visceral fat.

billustrates the distribution of MHO according to obesity severity and classification (BMI, WtHR, RFM, METS-VF) under three criteria. The data reveal a clear inverse relationship between obesity severity and the probability of being classified as MHO. For example, MHO prevalence dropped from 56.5% to 32.2% (men) and from 68.1% to 34.6% (women) when moving from grade I to grade III obesity (BMI). Moreover, alternative measures like RFM and METS-VF yielded higher proportions of MHO among those categorized as non-obese. These findings highlight the limitations of BMI alone in capturing metabolic health and the added value of complementary indexes.

Table 4 presents a comprehensive multivariable logistic regression analysis examining the associations between sociodemographic, lifestyle, and anthropometric factors with the likelihood of presenting metabolically non-healthy obesity (MNHO), using three distinct criteria (A, B, and C). Across all definitions, male sex, older age, lower educational attainment, lower occupational class, physical inactivity, poor adherence to the Mediterranean diet, smoking cessation (non-smoker status), and increasing obesity severity were independently associated with higher odds of MNHO.

Consistently, male participants exhibited a significantly elevated risk of MNHO compared to females, with odds ratios (ORs) ranging from 1.13 to 1.24 depending on the criterion. Age demonstrated a clear dose–response relationship, with individuals aged 60–69 years having nearly a fourfold increased risk of MNHO (OR 3.87; 95% CI: 3.40–4.35) under criterion A. This age-related trend supports prior longitudinal evidence indicating that metabolic health tends to deteriorate with aging, even in the absence of substantial weight gain.

Sociodemographic variables revealed strong gradients: individuals with only elementary education had markedly higher odds of MNHO than their university-educated counterparts (e.g., OR 2.76 under criterion A), and those in social class III exhibited similarly elevated risks. These findings suggest that educational attainment and occupational status may act as proxies for health literacy, access to care, or cumulative exposure to environmental and behavioral risk factors.

Lifestyle variables demonstrated some of the most substantial associations. Physical inactivity emerged as a major determinant, with ORs as high as 5.45 under criterion C—highlighting the critical role of regular physical activity in preserving metabolic health among individuals with obesity. Similarly, poor adherence to the Mediterranean diet was significantly associated with MNHO, with ORs between 1.97 and 2.68, reaffirming the protective effects of healthy dietary patterns on cardiometabolic profiles.

Interestingly, being a non-smoker was associated with increased odds of MNHO, particularly under the strictest definition (criterion C: OR 1.73; 95% CI: 1.66–1.81). While this counterintuitive association may reflect reverse causation—where individuals quit smoking due to deteriorating health—it also underscores the complexity of lifestyle interactions in metabolic phenotyping.

Table 4. Multivariable logistic regression analysis of factors associated with metabolically non-healthy obesity (MNHO) according to three diagnostic criteria.

	MNHO (A) OR (95% CI)	MNHO (B) OR (95% CI)	MNHO (C) OR (95% CI)
Female	1	1	1
Male	1.13 (1.08-1.18)	1.24 (1.18-1.30)	1.19 (1.14-1.25)
< 30 years	1	1	1
30-39 years	1.37 (1.30-1.44)	1.10 (1.07-1.14)	1.15 (1.10-1.21)
40-49 years	1.56 (1.45-1.67)	1.21 (1.16-1.27)	1.32 (1.21-1.43)
50-59 years	2.52 (2.21-2.83)	1.48 (1.39-1.58)	1.59 (1.40-1.79)
60-69 years	3.87 (3.40-4.35)	1.99 (1.81-2.18)	2.02 (1.75-2.28)
University	1	1	1
High school	1.25 (1.19-1.32)	1.18 (1.14-1.23)	1.18 (1.14-1.23)
Elementary school	2.76 (2.30-3.22)	1.69 (1.49-1.90)	1.62 (1.48-1.77)
Social class I	1	1	1
Social class II	1.28 (1.21-1.35)	1.25 (1.19-1.31)	1.25 (1.19-1.32)
Social class III	1.67 (1.45-1.89)	1.88 (1.69-2.08)	1.71 (1.54-1.88)
Yes physical activity	1	1	1
No physical activity	3.30 (2.80-3.81)	3.48 (2.98-3.99)	5.45 (4.60-6.31)
Yes Mediterranean diet	1	1	1
No Mediterranean diet	2.22 (1.98-2.46)	1.97 (1.80-2.15)	2.68 (2.30-3.05)
Smokers	1	1	1
Non-smokers	1.13 (1.09-1.17)	1.28 (1.23-1.33)	1.73 (1.66-1.81)
Obesity I (BMI)	1	1	1
Obesity II (BMI)	1.63 (1.45-1.81)	1.44 (1.35-1.54)	1.29 (1.21-1.38)
Obesity III (BMI)	2.52 (2.25-2.79)	1.79 (1.65-1.93)	1.65 (1.44-1.87)
WtHR normal	1	1	1
WtHR high	1.29 (1.22-1.36)	1.61 (1.53-1.69)	3.04 (2.76-2.33)
RFM normal	1	1	1
RFM high	1.58 (1.39-1.78)	1.82 (1.60-2.05)	1.79 (1.55-2.04)
METS-VF normal	1	1	1
METS-VF high	4.07 (3.76-4.37)	5.88 (5.60-6.17)	9.57 (9.07-10.08)

Notes: MNHO, metabolically non-healthy obesity. BMI, body mass index. WtHR, waist to height ratio. RFM, relative fat mass. METS-VF, metabolic score for visceral fat. OR, odds ratio.

Anthropometric indicators were strong predictors across all models. Higher BMI categories conferred progressively increased risk, but notably, indexes of central adiposity (WtHR, RFM, and especially METS-VF) demonstrated stronger associations with MNHO. METS-VF, in particular, showed a striking gradient, with individuals in the high METS-VF category having nearly tenfold increased odds of MNHO under criterion C (OR 9.57; 95% CI: 9.07–10.08). This finding validates the clinical utility of METS-VF as a superior marker of visceral adiposity and metabolic dysfunction, outperforming conventional measures like BMI.

In summary, **Table 4** underscores the multifactorial nature of metabolic unhealthiness in obesity. The findings highlight the value of incorporating behavioral and sociodemographic factors alongside refined anthropometric indexes—particularly METS-VF—into risk stratification strategies. These insights support the development of targeted interventions focusing on lifestyle modification, education, and central adiposity reduction to prevent the transition to metabolically non-healthy obesity.

Table 5 provides a longitudinal perspective, revealing a significant decline in the prevalence of MHO over the 10-year period across all indexes and definitions. This decline was particularly pronounced in individuals with severe obesity and those classified using non-BMI indexes. For instance, among men with grade II obesity (criterion 2), MHO prevalence decreased by 37.2%, while among women with high WtHR, the decrease reached 59.3%. The consistency of these findings across multiple definitions underscores a worrying trend: While the degree of obesity may remain stable, metabolic health appears to be worsening. These results call for renewed public health strategies focusing on metabolic rather than purely anthropometric risk assessment.

Discussion

Our comprehensive analysis-featuring both cross-sectional and retrospective components-revealed key insights into metabolically healthy obesity (MHO) among a large Spanish worker cohort. First, MHO prevalence demonstrated significant variation depending on the anthropometric index (BMI, WtHR, RFM, METS-VF) and definition used. Second, individuals classified as MHO consistently showed more favorable metabolic profiles than their MNHO counterparts across all indices. Third, a marked rise in MNHO prevalence was observed between 2010 and 2020, despite stable overall obesity rates, suggesting a decline in metabolic health status.

Interpretation of findings

The wide variation in MHO prevalence aligns with existing meta-research demonstrating disparity due to inconsistent definitions. One meta-analysis reported prevalence estimates ranging from 2% to 44% depending on diagnostic criteria and population sampled[31]. Our findings reinforce this, particularly highlighting that central adiposity-based indices like WtHR, RFM, and the comprehensive MER-curated METS-VF detect individuals with metabolic disturbances overlooked by BMI alone. This trend is supported by recent studies that underscore central fat as a more accurate predictor of metabolic risk than BMI, alone[32,33].

The longitudinal deterioration of metabolic health observed in our cohort mirrors global trends. For example, Mongraw-Chaffin et al. reported a 50% transition from MHO to unhealthy status over 10 years, with those showing greater central adiposity at baseline more likely to convert[34]. Similarly, Drid et al. found that individuals with higher WtHR had an accelerated progression to metabolic syndrome[35]. Our results thus contribute to a growing consensus that MHO is often a temporary state, heavily influenced by central adiposity accumulation and visceral fat activity.

Strengths

1. Large, well-characterized cohort with mixed design

Our study's inclusion of 68,884 individuals with repeat measurements across two time periods strengthens both external validity and temporal inference. The mixed cross-sectional and retrospective approach aligns with methodological recommendations for robust MHO research[36].

2. Use of multiple complementary adiposity indices

Beyond BMI, we included WtHR, RFM, and METS-VF. Recent evaluation suggests that METS-VF correlates more strongly with MRI-quantified visceral adiposity and metabolic syndrome than BMI or WC alone[37]. This multidimensional approach enhances risk stratification and clinical relevance.

3. Real-world occupational health data

Data collection via mandated workplace health assessments reduces selection bias and ensures standardized procedures. Occupational epidemiology frameworks endorse such well-documented routine settings for longitudinal metabolic research[38].

4. Sex-stratified analyses

By analyzing men and women separately, we highlighted gender differences in obesity-related metabolic risk. Consistent with prior studies, women exhibited lower visceral fat and slower progression to MNHO[39], yet still experienced metabolic declines—supporting calls for gender-tailored interventions[40].

Limitations

1. Lack of direct imaging references

Although METS-VF correlates well with MRI, the absence of imaging data limits direct confirmation of visceral fat estimates. A recent systematic review notes that while surrogate indices are useful, imaging provides superior diagnostic accuracy[41].

Table 5. Temporal trends (2010–2020) in the prevalence of MHO by obesity indexes and criteria in men and women.

Men		MHO 0 pre	MHO 0 post		MHO 1 pre	MHO 1 post		MHO 2 pre	MHO 2 post	
	n	%	%	Difference	%	%	Difference	%	%	Difference
BMI Obesity I	20,317	21.4	16.8	21.3	56.7	40.3	28.9	79.2	54.4	31.3
BMI Obesity II	4,496	12.0	8.3	31.2	43.9	27.6	37.2	67.3	39.6	41.2
BMI Obesity III	1,086	9.8	5.9	39.8	33.3	19.3	41.9	56.9	28.6	49.8
WtHR normal	16,998	28.2	23.9	15.8	72.8	55.8	23.3	95.3	64.0	32.8
WtHR high	8,911	18.3	12.3	32.8	51.2	31.3	38.9	73.8	39.2	46.9
RFM non obesity	996	24.3	20.3	18.6	70.5	55.1	21.8	94.9	70.9	25.3
RFM obesity	24,903	19.2	13.5	29.6	52.8	33.8	35.9	75.4	45.8	39.2
METS-VF normal	17,635	25.9	21.3	17.8	68.1	51.2	24.8	90.0	61.4	31.8
METS-VF high	8,264	5.3	3.6	31.2	22.5	12.9	42.8	46.6	22.2	52.3
Women	**n**	**%**	**%**	**Difference**	**%**	**%**	**Difference**	**%**	**%**	**Difference**
BMI Obesity I	9,156	30.3	24.7	18.6	68.1	52.5	22.9	88.5	64.6	27.8
BMI Obesity II	2,911	20.9	15.6	25.3	53.4	36.7	31.3	81.5	52.2	35.9
BMI Obesity III	1,221	7.7	5.1	33.7	33.8	20.3	39.8	71.7	42.1	41.3
WtHR normal	12,440	32.8	25.3	22.8	73.9	55.6	24.8	94.4	64.4	31.8
WtHR high	848	21.9	13.4	38.9	54.0	30.9	42.7	79.8	32.5	59.3
RFM non obesity	1,823	33.0	29.0	12.2	75.2	60.7	19.3	94.8	71.8	24.3
RFM obesity	11,465	25.1	18.7	25.6	59.6	41.5	30.3	84.0	51.9	38.2
METS-VF normal	12,853	27.0	21.9	18.9	63.6	47.8	24.8	87.3	60.8	30.3
METS-VF high	435	2.5	1.5	41.6	5.7	3.3	42.9	29.2	12.1	58.5

Notes: MHO, metabolically healthy obesity. BMI, body mass index. WtHR, waist to height ratio. RFM, relative fat mass. METS-VF, metabolic score for visceral fat. PRE=year2010, POST=year2020. The formula for calculating the difference is [POST−PRE/PRE] as a percentage.

2. Lifestyle data assessed only once per participant

Physical activity and Mediterranean diet adherence were captured at a single time point via IPAQ-SF and PREDIMED questionnaires. As prior cohort analyses indicate, changes in lifestyle behaviors significantly impact metabolic outcomes, and single measurements may not reflect long-term habits[42].

3. Potential residual confounding

Despite adjustments for basic lifestyle and demographic factors, our analyses could not address genetic predispositions or environmental exposures (e.g. air pollution, workplace stress), which are known modifiers of metabolic health[43].

4. Healthy-worker survivor effect

Including only those with measurements in both periods may skew results toward healthier individuals remaining in the workforce. This bias is well-documented in occupational cohort designs and may underestimate metabolic deterioration[44].

5. Non-assessment of medication usage

We did not account for lipid-lowering, antihypertensive, or glucose-regulating medications, which could impact classification of metabolic health status. Other studies have found adjusting for medication can significantly alter MHO categorization[45].

Clinical and public health implications

Our findings have direct implications for clinical practice and public health strategies:

1. Expand routine obesity assessment beyond BMI**:** Incorporate central adiposity indices like WtHR and METS-VF in workplace screenings or primary care to detect at-risk individuals timely.
2. Early intervention based on central adiposity**:** Tailored lifestyle interventions focused on reducing visceral fat—through structured exercise programs and Mediterranean-style diets—have demonstrated efficacy in reversing metabolic deterioration[46].
3. Gender-sensitive approaches**:** While women initially may appear metabolically healthier, they also experience progressive decline, underscoring the need for sustained prevention strategies across sexes[40].

Future investigations should:

- Include repeated longitudinal measures of lifestyle behaviors to capture behavior-related metabolic transitions.
- Incorporate imaging modalities (MRI, CT, DXA) in clinical cohorts to validate surrogate indices and refine MHO definitions.
- Conduct randomized trials to determine whether targeting central adiposity can delay or prevent the transition from MHO to MNHO.
- Explore interactions with genetic, occupational, and environmental factors to create predictive algorithms for metabolic health deterioration.

Conclusions

This study of over 68,000 Spanish workers reveals that MHO prevalence varies substantially based on the adiposity index and definition used, with central adiposity markers (WtHR, RFM, METS-VF) identifying higher-risk individuals than BMI alone. Our longitudinal analysis demonstrates a significant increase in MNHO prevalence over a decade, signaling a concerning decline in metabolic health even when obesity rates remain stable. These findings highlight the inadequacies of BMI-centric screening and emphasize the need for comprehensive anthropometric and metabolic assessment. Integrating central adiposity measures into routine health evaluations could enable earlier identification of at-risk individuals, guide prevention efforts, and support targeted workplace interventions to mitigate metabolic deterioration.

Data availability statement

Due to ethical and privacy considerations, the dataset is not publicly available. Data are stored in a secure database managed by ADEMA University School. The institution's Data Protection Officer is Ángel Arturo López González.

Funding

This article has not received any specific grant from funding agencies in the public, commercial, or for-profit sectors.

Conflicts of Interest

The authors declare no conflicts of interest.

Ethics approval

This study was conducted in strict accordance with national and international ethical standards governing research involving human participants, including the Declaration of Helsinki. All necessary measures were implemented to ensure participant anonymity and the confidentiality of personal data. Ethical approval was granted by the Ethics and

Research Committee of the Balearic Islands (Comité de Ética de la Investigación de las Islas Baleares), under approval reference IB 4383/20, dated 26th November 2020. Participation was entirely voluntary, and all individuals were thoroughly informed of the study's purpose and procedures prior to providing signed informed consent. To ensure confidentiality, participants were assigned unique identification codes accessible only to the project coordinator. No personally identifiable information will be published or disclosed. Participants were fully informed of their rights under current regulations, including access to their data and the right to request its modification, deletion, or restriction. The study complied fully with Organic Law 3/2018 of 5th December, on the Protection of Personal Data and Guarantee of Digital Rights.

Written informed consent was obtained from all individuals participating in the study.

Author contributions

MGS: Conceptualization, investigation, and original manuscript writing.

PJTL: Validation, statistical analysis.

ÁALG: Methodology, manuscript review.

JOdH: Data collection and curation.

CBC: Methodology, original manuscript writing.

ARG: Validation, data collection, and curation.

JIRM: Conceptualization, manuscript review.

All authors have read and agreed to the published version of the manuscript.

References

1. World Health Organization. Obesity and overweight. WHO. 2022.
2. Neeland IJ, Turer AT, Ayers CR, Powell-Wiley TM, Vega GL, Farzaneh-Far R, et al. Dysfunctional adiposity and the risk of prediabetes and type 2 diabetes in obese adults. JAMA 2019; 322(5):442–53.
3. Bluher M. Metabolically healthy obesity. Nat Rev Endocrinol 2020; 16(1):13–24.
4. Phillips CM. Metabolically healthy obesity across the life course: epidemiology, determinants, and implications. Ann N Y Acad Sci 2017; 1391(1):85–100.
5. Stefan N, Schick F, Häring HU. Causes, characteristics, and consequences of metabolically unhealthy normal weight and metabolically healthy obese individuals. J Intern Med 2017; 280(6):568–86.
6. Slagter SN, Corpeleijn E, Van der Klauw MM, Sijtsma A, Swart-Busscher LG, Perenboom CW, et al. Dietary patterns and shifts in metabolic health status over 10 years in a general population cohort. Eur J Nutr 2020; 59(6):2713–23.
7. Mongraw-Chaffin ML, Peters SAE, Huxley RR, Woodward M. The transitional nature of metabolically healthy obesity: a systematic review and meta-analysis. JAMA 2018; 319(9):942–53.
8. Kramer CK, Zinman B, Retnakaran R. Are metabolically healthy overweight and obesity benign conditions? Ann Intern Med 2013; 159(11):758–69.
9. Zheng R, Zhou D, Zhu Y, Li X, Wang J, Wang C, et al. Metabolically healthy obesity and cardiovascular disease: a systematic review and meta-analysis. Front Cardiovasc Med 2021; 8:678258.
10. Rey-Lopez JP, de Rezende LF, Pastor-Valero M, Tess BH. The prevalence of metabolically healthy obesity: a systematic review and critical evaluation of the definitions used. Obes Rev 2014; 15(10):781–90.
11. Ashwell M, Gibson S. A proposal for a primary screening tool: "Keep your waist to less than half your height". BMC Med 2014; 12:207.
12. Lin WY, Lee LT, Chen CY, Lo H, Hsia HH, Liu IL, et al. Optimal cut-off values for obesity: using simple anthropometric indices to predict cardiovascular risk factors in Taiwan. Int J Obes 2002; 26(9):1232–8.
13. Woolcott OO, Bergman RN. Defining cutoffs to diagnose obesity using the relative fat mass (RFM): a study in the US adult population. Int J Obes 2018; 42(4):679–84.
14. NICE. Obesity: identification, assessment and management. Clinical guideline [CG189]. National Institute for Health and Care Excellence (UK). 2022.
15. Browning LM, Hsieh SD, Ashwell M. A systematic review of waist-to-height ratio as a screening tool for the prediction of cardiovascular disease and diabetes. Nutr Res Rev 2010; 23(2):247–69.
16. Al-Gindan YY, Hankey CR, Govan L, Gallagher D, Heymsfield SB, Lean ME. Derivation and validation of simple equations to predict total body fat percentage in adults using anthropometric variables. Am J Clin Nutr 2014; 100(4):1041–8.
17. Lee Y, Park Y, Kim Y, Park S, Kim YJ, Kim NH, et al. Predictive ability of RFM and BMI for visceral adiposity and cardiometabolic risk. Sci Rep 2021; 11(1):23420.
18. Bello-Chavolla OY, Antonio-Villa NE, Vargas-Vázquez A, Fermin-Martinez CA, Bahena-López JP, Aguilar-Salinas CA, et al. METS-VF: a new index for visceral adiposity estimation in population studies. Nutr Metab Cardiovasc Dis 2020; 30(12):2184–93.
19. Wang Y, Yu C, Cao Q, Wang J, Lu J, Luo L, et al. METS-VF as a marker for hepatic steatosis and metabolic dysfunction in Chinese adults. J Clin Lipidol 2022; 16(3):368–76.
20. Aranceta-Bartrina J, Pérez-Rodrigo C, Alberdi-Aresti G, Ramos-Carrera N, López-Sobaler AM. Prevalence of general obesity and abdominal obesity in the Spanish adult population 2014–2015: the ENPE study. Rev Esp Cardiol 2016; 69(6):579–87.
21. García Samuelsson M, Tárraga López PJ, López González AA, Paublini H, Martínez-Almoyna Rifá E, Ramírez Manent JI. Prevalencia de obesos metabólicamente sanos aplicando tres criterios diferentes en población española: variables asociadas. An Facultad Med 2025; 12(1): e201. Available from: https://doi.org/10.25184/anfamed2025v12n1a2.
22. Lee Y, Park Y, Kim Y, Park S, Kim YJ, Kim NH, et al. Predictive ability of RFM and BMI for visceral adiposity and cardiometabolic risk. Sci Rep 2021; 11(1):23420.

23. Bello-Chavolla OY, Almeda-Valdes P, Gómez-Velasco D, Viveros-Ruiz T, Cruz-Bautista I, Romo-Romo A, et al. METS-VF: a novel index for visceral fat estimation validated against MRI. Clin Nutr 2021; 40(3):1284–91.
24. Wang T, Liu Y, Li Y, Nie X, Yang X, Liu J, et al. METS-VF as a predictor of metabolic dysfunction-associated fatty liver disease in Chinese adults. Front Endocrinol 2023; 14:1086540.
25. Prince RL, Kuk JL, Ambler KA, Dhaliwal J, Ball GD. Predictors of metabolically healthy obesity in children. Diabetes Care 2014; 37(5):1462–8.
26. Cleland CL, Hunter RF, Tully MA, Scott D, Kee F, Donnelly M. Validity of the Global Physical Activity Questionnaire (GPAQ) and the IPAQ in assessing physical activity in a large population. Int J Behav Nutr Phys Act 2014; 11:123.
27. Gába A, Dygrýn J, Mitáš J, Jakubec L, Frömel K. Validity of the IPAQ in Czech adults using ActiGraph accelerometer. Cent Eur J Public Health 2020; 28(1):44–50.
28. García-Conesa MT, Philippou E, Pafilas C, Massaro M, Quarta S, Andrade V, et al. Exploring the validity of the 14-item Mediterranean Diet Adherence Screener (MEDAS): a cross-national study in seven European countries around the Mediterranean region. Nutrients 2020; 12(10):2960.
29. Pérez-Martínez P, García-Ríos A, Delgado-Lista J, Perez-Jimenez F, Lopez-Miranda J. Mediterranean diet rich in olive oil and obesity, metabolic syndrome and diabetes mellitus. Curr Pharm Des 2011; 17(8):769–77.
30. Domingo-Salvany A, Bacigalupe A, Carrasco JM, Espelt A, Ferrando J, Borrell C, et al. Propuestas de clase social neoweberiana y neomarxista a partir de la Clasificación Nacional de Ocupaciones 2011. Gac Sanit 2013; 27(3):263-72. Available from: https://doi.org/10.1016/j.gaceta.2012.12.009.
31. Bell JA, Hamer M, Batty GD, Gong J, Kivimäki M, Sabia S, et al. Persistent metabolically healthy obesity and risk of COVID-19 hospitalization: UK biobank prospective cohort study. Int J Obes 2021; 45(3):633–42.
32. Zheng J, Liu Y, Wang M, Li H, Wu X, Zhou H, et al. Waist-to-height ratio predicts metabolic syndrome in type 2 diabetes patients better than BMI and waist circumference. Acta Diabetol 2020; 57(2):199–207.
33. Tavares do Carmo M, Ferreira G, Silva R, Cunha N, Rodrigues D, Figueiredo A, et al. Relative fat mass vs BMI and waist circumference to predict metabolic syndrome: a cohort study. Clin Nutr 2021; 40(9):5260–8.
34. Mongraw-Chaffin ML, Peters SAE, Huxley RR, Woodward M, Aung K, Freeman J, et al. Transition from metabolically healthy obesity to unhealthy status. Obes Rev 2020; 21(5):e13060.
35. Drid P, Ostojic SM, Sekulic D, Copic N, Drapsin M, Milinkovic D, et al. Waist-to-height ratio predicts metabolic syndrome incidence better than waist circumference. Public Health Nutr 2022; 25(4):1024–32.
36. Mooney SJ, Birkhead GS, Cohen B, Lee DC, Chan J, Long C, et al. Combining cross-sectional and longitudinal data strengthens obesity phenotype research. Int J Obes 2022; 46(9):1625–35.
37. Kim JY, Choi YS, Lee SH, Park S, Ahn J, Han K, et al. METS-VF validation study against MRI in Korean adults. Metabolism 2021; 117:154725.
38. Park HA, Lee S, Kim Y, Chung H, Jang J, Ko Y, et al. Routine workplace health assessments reduce metabolic risk: evidence from an industrial cohort. Occup Med 2021; 71(5):234–41.
39. Winkler G, Kiss S, Karádi I, Jermendy G, Varga B, Tóth K, et al. Sex differences in progression of metabolic syndrome across Europe. BMC Med 2020; 18(1):244.
40. Goossens GH, Blaak EE, Wagenmakers AJ, Verdich C, Sørensen TI, Matsuda M, et al. Female-specific metabolic adaptation and cardiovascular risk during obesity. Nat Rev Endocrinol 2021; 17(6):337–52.
41. Neeland IJ, Poirier P, Després JP, Lavie CJ, Scally M, Bouchard C, et al. Imaging adiposity more accurately identifies insulin resistance than BMI. Diabetes Care 2020; 43(1):121–8.
42. Ruiz JR, Ortega FB, Castro-Piñero J, Martínez-Gómez D, Vicente-Rodríguez G, Rey-López JP, et al. Physical activity variability and incident metabolic syndrome: a prospective study. Diabetologia 2020; 63(8):1548–60.
43. Xu X, Liu C, Huang G, Li Y, Zhao B, Wang J, et al. Air pollution, genetics, and obesity: interaction effects on metabolic dysfunction. Environ Sci Technol 2021; 55(12):8381–9.
44. Li J, Meng X, Luo J, Wang S, Du Y, Zhang H, et al. Healthy worker survivor effect in longitudinal occupational health research. Occup Environ Med 2022; 79(3):187–93.
45. Park JY, Lee SH, Choi HJ, Kim JH, Bae SH, Lee JY, et al. Effect of lipid-lowering medication use on metabolic health classification in obese individuals. J Clin Lipidol 2021; 15(2):259–70.
46. Koutnikova H, Canivenc-Lavier MC, Nazare JA, Andreeva VA, Illy C, Fezeu L, et al. Mediterranean diet, visceral fat, and metabolic syndrome: randomized intervention results. Ann Intern Med 2021; 174(5):667–77.

ACADEMIC JOURNAL OF HEALTH SCIENCES
MEDICINA BALEAR

Case report

Is ileal-ileocecal valve proximity safe for ileoileal anastomosis? A pediatric case report

¿Es segura la proximidad a la válvula ileocecal para una anastomosis ileoileal? Informe de un caso pediátrico

Cumali Berkan-Ünal*, Fatma Sarac

Basaksehir Çam and Sakura City Hospital, Istanbul, Turkey

Received: 14-01-25
Accepted: 23-03-25

***Corresponding author:** Cumali Berkan Ünal. berkanunal42@gmail.com

Abstract

Objective: anastomosis very close to the ileocecal valve after small bowel resection is a concern for the surgeon, since it is a region with relatively weak arterial blood supply. In this case report, it was aimed share a 2-year-old patient who underwent small bowel resection due to volvulus and ileoileal anastomosis at a distance of 1 cm from the ileocecal valve.

Case report: a two-year-old male patient was admitted to the emergency department (ED) with complaints of abdominal pain, vomiting, and inability to defecate for 2 days. The patient's clinical examination was unremarkable except for soft abdominal distension. He was taken to emergency operation with the preliminary diagnosis of intestinal obstruction, as his abdominal distension increased in a short time and there was fecaloid drainage from the nasogastric tube. During the exploration, volvulus and lad bands were observed. From the ileocecal valve, 1 cm ileum was preserved, and 80 cm small bowel resection and ile ileostomy were performed.

Conclusion: although anastomoses made too close to the ileocecal valve after small bowel resections involving the terminal ileum are considered risky, they can be safely applied in selected cases where the abdomen is clean.

Keywords: Ileocecal valve. Anastomosis. Pediatric.

Resumen

Objetivo: las anastomosis realizadas en proximidad a la válvula ileocecal tras una resección del intestino delgado representan un desafío para los cirujanos, ya que esta región se caracteriza por un suministro arterial relativamente deficiente. Este reporte de caso tiene como objetivo presentar a un paciente de dos años que fue sometido a una resección de intestino delgado debido a un vólvulo, seguido de una anastomosis ileoileal ubicada a 1 cm de la válvula ileocecal.

Reporte de caso: un paciente masculino de dos años fue ingresado al departamento de urgencias con un cuadro de dos días de dolor abdominal, vómitos y ausencia de defecación. El examen clínico no reveló hallazgos relevantes, salvo una leve distensión abdominal. Debido a la rápida progresión de la distensión y la presencia de drenaje fecaloideo por la sonda nasogástrica, se decidió realizar una cirugía de urgencia con diagnóstico presuntivo de obstrucción intestinal. Los hallazgos intraoperatorios incluyeron vólvulo y bandas de Ladd. Se preservó un segmento de íleon de 1 cm desde la válvula ileocecal y se resecó un segmento de 80 cm de intestino delgado. Posteriormente, se realizó una anastomosis ileoileal.

Cite as: Berkan-Ünal A, Sarac F. Is ileal-ileocecal valve proximity safe for ileoileal anastomosis? A pediatric case report. Acad J Health Sci 2025; 40(5): 67-71. Available from: https://doi.org/10.3306/AJHS.2025.40.05.8

Acad J Health Sci 2025; 40(5): 67-71
https://doi.org/10.3306/AJHS.2025.40.05.8
www.ajhealthsciences.com

Conclusión: aunque las anastomosis realizadas en proximidad a la válvula ileocecal tras resecciones del íleon terminal se consideran de alto riesgo, pueden llevarse a cabo de manera segura en casos seleccionados donde la cavidad abdominal se encuentre limpia.

Palabras clave: Válvula ileocecal. Anastomosis. Pediatría.

Introducción

The ileocecal valve plays an important role in regulating the passage of contents from the small intestine to the colon. It slows down the transition of small bowel content into the colon, enhances absorption, and prevents reflux from the cecum into the small intestine. In cases where small bowel resection is required, preservation of the ileocecal valve is a crucial part of treatment for some patients. Traditionally, after a small bowel resection of 10-15 cm near the ileocecal valve, a right hemicolectomy is added to the surgical procedure due to the risk of malnutrition and high pressure in the ileal segment near the cecum. The ileocecal valve can withstand pressures of up to 50-60 cm of water. This preference is primarily due to the poor blood supply to the terminal ileum and the fact that its blood supply comes solely from the ileocolic artery. In this case report, we aim to highlight the importance of the ileocecal valve and show that in selected cases, an anastomosis can be safely performed close to the ileocecal valve, as we present a case of an ileo-ileal end-to-end anastomosis performed about 1 cm from the valve.

Case report

The patient presented with a history of absent passage of gas and stool for two days with abdominal pain and vomiting. There was also a history of constipation for three months. The patient had no known additional disease and had not undergone surgery before. The general condition was stable, on physical examination abdominal distension was noted with no rebound tenderness. Rectal examination were unremarkable. Laboratory results showed White Blood Cell (WBC): 21.08 10^9/L, C Reactive Protein (CRP): 0,4 mg/L, Creatine Kinase (CK): 860 U/L.

- **Ultrasound:** mild free fluid accumulation was observed in the perihepatic, perisplenic regions, and between bowel loops. There was notable intestinal content accumulation, particularly in the left lower quadrant.

  After admission, a nasogastric (NG) tube was inserted. Despite NG tube drainage, a hours later there was worsening abdominal distension, and the NG contents became fecaloid. Based on the acute abdomen diagnosis (volvulus, ileus), the patient was taken for surgery.

- **Surgery:** The operation was started with a midline incision, hemorrhagic necrotic fluid was observed in the abdominal cavity. Upon exploring the intestines, Ladd's band were found to be causing mesenteric volvulus, I and the bowel showed severe ischemia. Following excision of the bands, a 10x7 cm necrotic Meckel's diverticulum was also removed. After the bands were released, healthy ileum was seen up to 2 cm from the ileocecal valve, with a Meckel's diverticulum at the 50 cm mark. A total of 80 cm of ischemic bowel was excised, while the ileocecal valve and 2 cm of healthy ileum were preserved. An ileo-ileal double-layer anastomosis was performed and appendectomy was performed afterwards, a suction drain was placed in the abdomen before closing the surgical site.

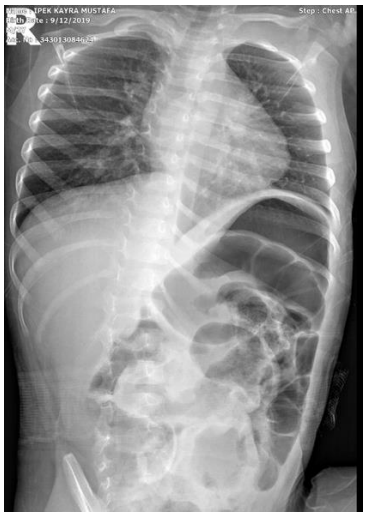

Figure 1. Dilated intestine segment on abdominal x-ray.

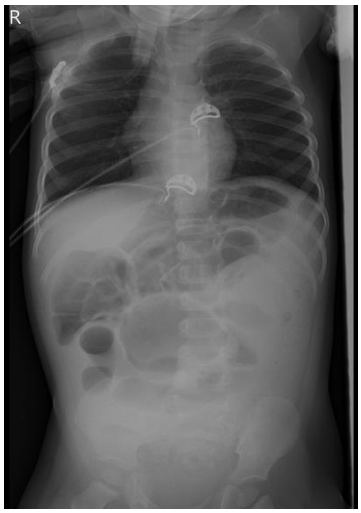

Figure 2. No intestinal gas in the pelvis on abdominal x-ray.

Figure 3. Ileal segment with impaired circulation.

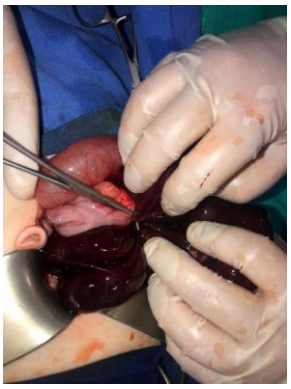

Figure 4. Ladd's band.

Figure 5. Meckel's diverticulum.

Figure 6. After ileoileal anastomosis view.

Postoperatively, the patient was monitored. On the 9th postoperative day, due to low oxygen saturation, hypotension, and apathy, a COVID PCR test and a respiratory viral panel were ordered. No electrolyte imbalances were found. The test result of COVID-19 was positive, along with Influenza A and Human Bocavirus tests. Spontaneous gas and stool discharge were observed on the 4th postoperative day. The drain was removed on the 6th day, and 6th day oral feeding was started. The patient was discharged on the 10th postoperative day and was called for a follow-up one week later. No problems were observed in the patient's 1st postoperative year follow-up.

Rodrigo et al. investigated a study discussing the safety of ileo-ileal anastomosis close to the ICV in neonates for FIP. The paper was a retrospective study evaluating 24 neonates according to complications that occurred at different locations around the anastomosis site. No statistical difference in complications such as dehiscence, stricture, and mortality was appreciated between anastomoses carried out <5 cm versus those ≥5 cm away from the ICV site. Rodrigo et al. demonstrated that performing ileo-ileal anastomosis within 5 cm of the ileocecal junction in neonates with focal intestinal perforation (FIP) is both safe and effective[1].

In a retrospective study conducted by Bhutra et al. with 210 patients, they stated that ileocecal anastomoses including the appendicular stump after resection can be safely performed without requiring major resection in lesions located 15 cm away from the ileocecal valve[2].

In the study by Pohl et al., they stated that enterocolic side-to-side anastomosis without ileocecal valve resection may be an alternative treatment option in patients diagnosed with Crohn's disease[3].

In the case report of Kaya et al., they showed that anastomosis performed 1-2 cm away from the ileocecal valve after resection due to a tumoral lesion seen in the terminal ileum of an 18-year-old female patient could be performed safely[4].

In the case report of Köse et al., they stated that after resection of the 50 cm bowel segment including the necrotic terminal ileum of a 60-year-old female patient who underwent surgery for incarcerated umbilical hernia, ileoileal anastomosis performed at a distance of 4 cm from the ileocecal valve can be performed safely and that preservation of the valve in massive small bowel resections doubles the absorption capacity of the remaining small bowel[5].

Sekmenli et al. In another case report in 2016, they argued that anastomosis close to the terminal ileum would not cause clinical problems, and that anastomosis with preservation of the ileocecal valve would

increase the quality of life, especially in children with a longer life expectancy[6].

In distal ileum pathologies, anastomoses close to the ileocecal valve are not preferred due to high intraluminal pressure and anastomosis leakage. Sever et al. reported no postoperative surgical complications in the prevalvular anastomosis performed in a series of 8 patients, and they showed that prevalvular anastomosis can be performed without right hemicolectomy and ileocecal valve resection in distal ileum pathologies[7].

In a retrospective review by Jiang et al. of 48 patients who underwent ileoileostomy in the area adjacent to the ileocecal valve and 34 patients who underwent ileocecal resections and ileocolostomy, no postoperative surgical complications were observed, and diarrhea and electrolyte imbalance were found to be lower in patients who underwent ileocecal stenosis. The study showed that ileoileostomy in the area adjacent to the ileocecal valve was safe and caused fewer complications[8].

Authors	Year of publication	Study	Number of patients	Death	cm near ICV	Comorbidity
Rodríguez et al.	2021	Retrospective	6	1	<5 cm vs >5 cm	
Bhutra et al.	2017	Retrospective	210	1	<15 cm	
Sever et al.	2006	Retrospective	8		1-3 cm	
Jiang et al.	2012	Retrospective	82		2-5 cm	
Pohl et al.	2013	Case report	1		15-20 cm	Crohn Disease
Kaya et al.	2015	Case report	1		1-2 cm	
Köse et al.	2016	Case report	1		4 cm	COPD, Obesity
Sekmenli et al.	2016	Case Report	1		5 cm	Abdominal Surgery
Our case	2021	Case report	1		2 cm	

Discussion

The ileocecal valve plays a critical role in slowing the transition of small bowel contents into the colon, enhancing the absorption of B12 and bile salts. It also prevents reflux from the cecum into the terminal ileum. Ileocecal valve resections lead to several issues, including the risk of the small bowel mucosa encountering colon content, which can cause inflammation, diarrhea, malnutrition, and hypoalbuminemia. In pediatric populations, the rapid passage of small bowel content into the colon can lead to electrolyte imbalances and growth retardation. Diseases like intussusception, intestinal atresia, and necrotizing enterocolitis are common in children, and resection of the terminal ileum may be necessary in such cases. In adults, conditions like mesenteric ischemia, Crohn's disease, and small bowel tumors may require resections. Jiang et al. compared 48 children who underwent ileoileostomy and 34 children who underwent ileotransversostomy. They found that serum total bilirubin and vitamin B12 levels were lower in the ileotransversostomy group after one week, and while no mortality or anastomotic leaks occurred in either group, postoperative diarrhea and electrolyte imbalances were more common in the ileotransversostomy group. The safety of anastomoses performed 2-5 cm from the ileocecal valve has been noted in previous studies. Serova et al. and Sever et al. have shown that ileo-ileal anastomoses close to the cecum can be performed safely. In one study, they performed primary repairs or prevalvular ileo-ileal anastomoses in 8 pediatric patients. The distance from the anastomosis to the cecum ranged from 1-3 cm, and the safety of prevalvular anastomoses was found to depend more on good preoperative preparation and proper surgical technique than on the primary pathology. In our case, resection due to ischemic ileum caused by volvulus was followed by an ileo-ileal end-to-end anastomosis performed about 1 cm from the ileocecal valve without complications. A literature review revealed a lack of sufficient studies on the safety of such anastomoses in pediatric patients. Larger studies would be beneficial in this regard.

Declaration of generative AI in scientific writing

This article used artificial intelligence software exclusively for English editing.

Conflicts of interest

The authors declare no conflicts of interest.

Funding

This article has not received any specific grant from funding agencies in the public, commercial, or for-profit sectors.

References

1. Martos Rodríguez M, Guillén G, López-Fernández S, Martin Gimenez M, Ruiz CW, Ribes C, et al. Anastomosis near to the ileocecal valve in neonates with focal intestinal perforation, is it safe. J Matern Fetal Neonatal Med 2022;35(25):7011–4.
2. Bhutra S, Singh A, Devpura T. Emergency ileo-cecal anastomosis with inclusion of appendicular stump in terminal ileal pathology: a newer approach. Niger J Surg 2018;24(2):116–20.
3. Pohl J. Side-to-side ileocolic anastomosis. Video J Encycl GI Endosc. 2013;1(2):405.
4. Kaya B, Bat O, Celik HK, Tunca A, Tekirdağ AI, Şener A. The safety of ileo-ileal anastomosis near ileocecal valve. A case report and review of the literature. Compr Med 2017;7(1):41–3.
5. Köse E. İleoçekal valvüle çok yakın yapılan ileo-ileal anastomoz. Cukurova Med J 2016;41(Suppl 1):124–5.
6. Sekmenli T, Gündüz M, Çiftci I. How safe is anastomosis near the ileocecal valve in distal ileal pathologies? [Distal ileum patolojilerinde ileoçekal valve yakın anastomoz ne kadar güvenli?]. 2016.
7. Sever N, Cevizci MN, Karadağ ÇA, Dokucu Aİ. Distal ileum patolojilerinde prevalvuler anastomoz güvenli midir. Çocuk Cerrahisi Derg 2008;22(2):62–5.
8. Jiang WW, Xu XQ, Geng QM, Zhang J, Chen H, Lv XF, et al. Enteroenteroanastomosis near adjacent ileocecal valve in infants. World J Gastroenterol 2012;18(48):7314.

ACADEMIC JOURNAL OF HEALTH SCIENCES
MEDICINA BALEAR

Case report

Metformin modulates keratinocyte autophagy and the NLRP3 inflammasome pathway

La metformina modula la autofagia de los queratinocitos y la vía del inflamasoma NLRP3

Ke Tian[1], Jing Lv[2], Xiaojuan Shang[2], Yu Shi[2], Hui Yang[2], Zihan Zhen[2], Guoying Miao[1], Chunxia Yao[1]*

[1]Department of Dermatology, Affiliated hospital of Hebei University of Engineering, Handan, China
[2]School of Medicine, Hebei University of Engineering, Handan, China

Received: 22-02-25
Accepted: 15-05-25

***Corresponding author**: Chunxia Yao. yaoyao20050208@163.com

Abstract

Introduction: Atopic Dermatitis (AD) is a chronic inflammatory skin condition with impaired skin barrier function and immune imbalance. Metformin, known for its anti-inflammatory and autophagy-regulating properties, shows potential in treating inflammatory diseases. This study investigates its effects on AD via the autophagy/NLRP3 inflammasome axis and calcium signaling.

Materials and methods: BALB/c mice were induced with AD-like lesions using DNCB. Metformin was administered to assess its impact on skin lesions, inflammation, and autophagy. HaCaT cells were treated with DNCB and Metformin to evaluate effects on cell proliferation, apoptosis, and autophagy. Western blot and immunohistochemistry were used to analyze autophagy markers and inflammasome components. Calcium signaling was assessed using the Fluo-4 Calcium Assay Kit.

Results: Metformin reduced skin lesion severity, decreased epidermal thickness, and improved skin barrier function. It attenuated DNCB-induced upregulation of IL-1β, IL-18, and NLRP3 inflammasome components. In HaCaT cells, Metformin reversed DNCB-induced autophagy inhibition and promoted cell proliferation while inhibiting apoptosis. Calcium signaling, enhanced by DNCB, was mitigated by Metformin and the CaSR inhibitor NPS-2143.

Conclusions: Metformin alleviates AD symptoms by modulating autophagy, the NLRP3 inflammasome, and calcium signaling, suggesting its potential as a therapeutic agent. Future work should validate these findings in more complex models and explore personalized treatment strategies.

Keywords: Metformin. Autophagy. NLRP3 inflammasome. Keratinocyte. Atopic dermatitis. Calcium-sensing receptor.

Resumen

Introducción: la dermatitis atópica (DA) es una enfermedad cutánea inflamatoria crónica caracterizada por una disfunción de la barrera cutánea y un desequilibrio del sistema inmunológico. La metformina, conocida por sus propiedades antiinflamatorias y reguladoras de la autofagia, muestra potencial como tratamiento en enfermedades inflamatorias. Este estudio investiga sus efectos sobre la DA a través del eje autofagia/inflamasoma NLRP3 y la señalización del calcio.

Materiales y método: se indujeron lesiones similares a DA en ratones BALB/c mediante la aplicación de DNCB. Se administró metformina para evaluar su impacto en las lesiones cutáneas, la inflamación y la autofagia. Asimismo, se trataron células HaCaT con DNCB

Cite as: Tian K, Lv J, Shang X, Shi Y, Yang H, Zhen Z, et al. Metformin modulates keratinocyte autophagy and the NLRP3 inflammasome pathway. Acad J Health Sci 2025; 40(5): 72-81. Available from: https://doi.org/10.3306/AJHS.2025.40.05.9

Acad J Health Sci 2025; 40(5): 72-81
https://doi.org/10.3306/AJHS.2025.40.05.9
www.ajhealthsciences.com

y metformina para analizar los efectos sobre la proliferación celular, la apoptosis y la autofagia. Se utilizaron técnicas de Western blot e inmunohistoquímica para analizar marcadores de autofagia y componentes del inflamasoma. La señalización del calcio se evaluó utilizando el kit Fluo-4 Calcium Assay.

Resultados: la metformina redujo la gravedad de las lesiones cutáneas, disminuyó el grosor epidérmico y mejoró la función de la barrera cutánea. Atenuó la sobreexpresión inducida por DNCB de IL-1β, IL-18 y de los componentes del inflamasoma NLRP3. En las células HaCaT, la metformina revirtió la inhibición de la autofagia inducida por DNCB, promovió la proliferación celular e inhibió la apoptosis. La señalización del calcio, que se incrementó con DNCB, fue atenuada por la metformina y por el inhibidor del receptor sensor de calcio (CaSR), NPS-2143.

Conclusiones: la metformina alivia los síntomas de la DA mediante la modulación de la autofagia, el inflamasoma NLRP3 y la señalización del calcio, lo que sugiere su potencial como agente terapéutico. Futuros estudios deberán validar estos hallazgos en modelos más complejos y explorar estrategias de tratamiento personalizadas.

Palabras clave: Metformina. Autofagia. Inflamasoma NLRP3. Queratinocitos. Dermatitis atópica. Receptor sensor de calcio.

Introduction

Atopic dermatitis (AD) is a prevalent chronic inflammatory skin condition marked by impaired skin barrier function and immune system imbalance[1]. The incidence of AD is escalating globally, particularly among children, with prevalence rates surpassing 20%[2]. Patients with AD often experience severe symptoms such as intense itching, erythema, exudation, and lichenification, which significantly diminish their quality of life[3]. Although various treatments are available, including glucocorticoids, calcineurin inhibitors, and biologics (e.g., dupilumab), long-term use can lead to adverse effects like skin atrophy and immune suppression[4-6]. Consequently, a deeper investigation into the pathogenesis of AD and the development of more effective therapeutic approaches are crucial in the field of dermatology.

Autophagy, a cellular degradation mechanism, has garnered increasing attention for its role in skin diseases[7]. It is essential for maintaining cellular homeostasis, regulating immune responses, and managing stress[8]. Research indicates that autophagy dysfunction in macrophage may be closely linked to the pathogenesis of AD[9]. When autophagy is disrupted, it can result in the accumulation of intracellular damage, which in turn activates inflammatory pathways and intensifies skin inflammation[10]. Furthermore, there is a complex interplay between autophagy and the NLRP3 inflammasome: the activation of autophagy can inhibit the assembly of the NLRP3 inflammasome, thereby reducing the secretion of inflammatory factors. Conversely, the activation of the NLRP3 inflammasome can suppress autophagy, leading to increased cellular damage[11]. Therefore, modulating the balance between autophagy and the NLRP3 inflammasome could potentially serve as a novel therapeutic strategy for AD. Even NLRP3 can act as a key transcription factor of IL-33 in epithelial cells, independent of the inflammasome, mediating the pathological process of AD[12].

Metformin, a well-known antidiabetic medication, has increasingly been recognized for its potential applications beyond diabetes in recent years. Studies have shown that metformin has multiple therapeutic effects, including anti-inflammatory, antioxidant, and autophagy-regulating properties[13]. Metformin can inhibit the activation of the NLRP3 inflammasome and reduce the secretion of inflammatory factors by activating the AMPK signaling pathway[14]. Additionally, it can promote autophagy activation by modulating the mTOR signaling pathway[15]. These findings suggest that metformin may have therapeutic potential in treating inflammatory diseases by modulating the NLRP3 inflammasome and autophagy. However, it remains unclear whether metformin can improve AD by regulating the autophagy/NLRP3 inflammasome pathway in keratinocytes.

This study aims to investigate the potential mechanisms by which metformin improves AD through the regulation of the autophagy/NLRP3 inflammasome pathway in keratinocytes and to explore its potential therapeutic value in AD treatment. This research will not only enhance our understanding of the pathogenesis of AD but also provide a theoretical foundation for developing new therapeutic strategies based on the NLRP3 inflammasome and autophagy, thereby expanding the application prospects of metformin in dermatology.

Materials and methods

Animal model and treatment protocol

Eight-week-old BALB/c mice were acclimated for one week prior to the experiment. Under isoflurane anesthesia, a 5 cm² area on the lower back of each mouse was shaved. The mice were then randomly assigned into three groups, with eight animals per group. The control group had vaseline applied to their backs. The DNCB group underwent sensitization with 200 µL of a 1% DNCB solution on days 1, 4, and 7. Subsequently,

from day 14 to day 30, this group was challenged with 50 μL of a 0.5% DNCB solution three times weekly. The DNCB + Metformin group, in addition to the DNCB treatment, received applications of metformin cream on their back skin three times weekly for 30 days. Sample collection occurred on day 31 (**Figure 1A**).

Mice back lesion severity scoring

The severity of back lesions in mice was assessed based on four key symptoms: erythema, infiltration/papule, exfoliation, and exudation/scab. Each symptom was scored on a scale of 0 to 3, where 0 indicates no presence of the symptom, 1 indicates mild, 2 indicates moderate, and 3 indicates severe. The final score for each mouse was calculated by summing the individual scores of the four symptoms, resulting in a total possible score ranging from 0 to 12 points. This cumulative score was used to quantify the overall degree of skin inflammation[16].

Skin barrier function test

Skin barrier function was assessed using a multifunctional skin tester (model 9). For transepidermal water loss (TEWL) measurement, the Tewameter probe was positioned on the dorsal skin overlying the transverse process of the first lumbar vertebra on the right side of the mice for 30 seconds. Stratum corneum hydration (SCH) was evaluated using the Cornemeter probe[17].

Histopathological examination

Following euthanasia under anesthesia, dorsal skin samples were excised from the mice, fixed in 4% formaldehyde solution, and processed routinely for paraffin embedding. Sections were sliced and stained with hematoxylin-eosin. Epidermal thickness was measured microscopically after sealing. For each section, three random fields were selected, and within each field, two distinct points were chosen to measure the vertical distance from the stratum corneum to the basal layer of the epidermis. Additionally, some sections were subjected to immunohistochemical staining for NLRP3 and LC3-II, followed by DAB color development and sealing. The expression of these proteins in the epidermis was then observed microscopically.

Cell culture

HaCaT cells, obtained from the Cell Bank of the Chinese Academy of Sciences, were cultured in DMEM medium enriched with 10% fetal bovine serum and 1% penicillin–streptomycin solution. The culture was incubated at 37°C within a humidified incubator containing 5% CO_2. After a 24-hour incubation period post-seeding into 6-well plates, 96-well plates, or 10 cm dishes, cells were subjected to differential treatments. Control cells were maintained in basic culture medium devoid of any additives. For the DNCB treatment group, cells were exposed to a medium containing 100 μM DNCB. In the DNCB + Metformin group, cells received a combined treatment of 100 μM DNCB and 10 mM Metformin. Lastly, cells in the DNCB + NPS-2143 group were treated with 100 μM DNCB alongside 10 μM NPS-2143. All subsequent experimental procedures were initiated 48 hours post-treatment.

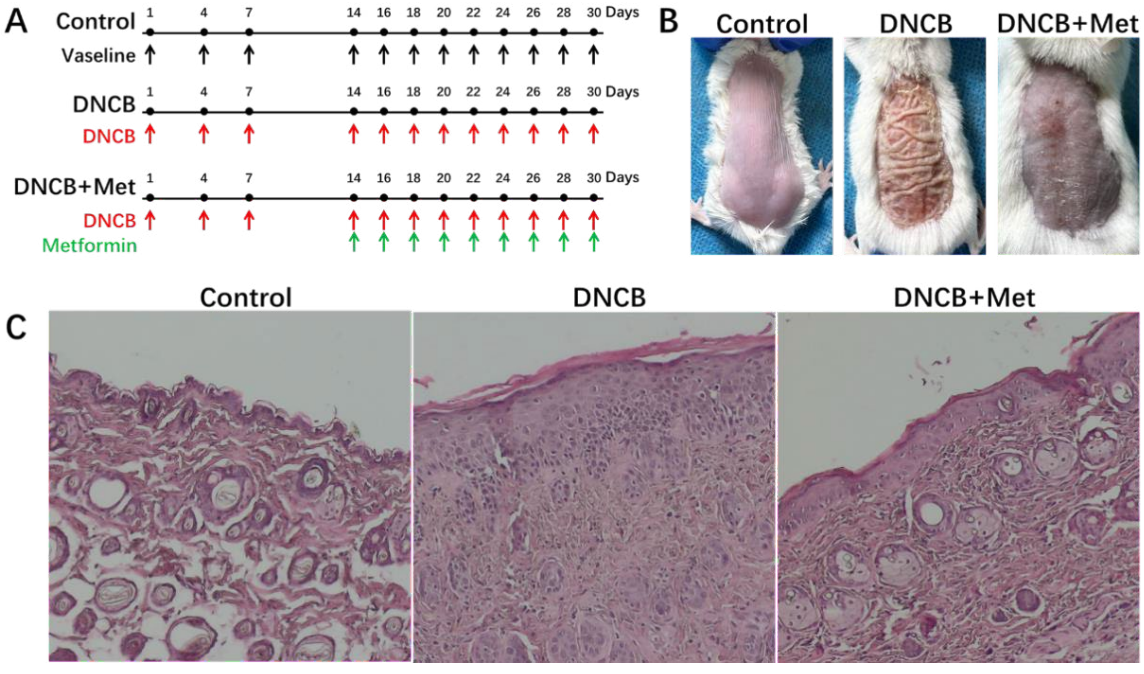

Figure 1. Effect of Metformin on Atopic Dermatitis in Mice Induced by DNCB. A. Schematic diagram of the animal experiment. B. Representative features of skin lesions at day 30. C. Histological analysis using H&E staining (200×magnification).

Cell proliferation and apoptosis assays

Cell proliferation was assessed using the Cell Counting Kit-8 (CCK-8) (C0037, Beyotime), while apoptosis was evaluated via Annexin V-FITC/PI double staining kit (C1062L, Beyotime), both conducted in accordance with the manufacturers' protocols.

Western blot

Total protein was extracted from cells or tissues using RIPA lysis buffer, and protein concentration was determined by the BCA method. Equal amounts of protein (30 μg) were subjected to SDS-PAGE and transferred onto PVDF membranes. Membranes were blocked with 5% nonfat milk at room temperature for 1 hour, followed by incubation with primary antibodies at 4°C overnight. After washing three times with TBST (10 minutes each), membranes were incubated with secondary antibodies conjugated to Alex Fluor for 1 hour at room temperature. Protein bands were visualized using the Licor Odyssey System (LI-COR Biosciences, USA), and band intensities were quantified using ImageJ software. The primary antibodies used were as follows: NLRP3 (sc-134306, Santa Cruz), Caspase-1 (sc-56036, Santa Cruz), IL-1β (sc-12742, Santa Cruz), IL-18 (GTX32675, GeneTex), ATG5 (sc-133158, Santa Cruz), LC3 (sc-398822, Santa Cruz), CaSR (sc-47741, Santa Cruz), and β-actin (sc-81178, Santa Cruz).

ELISA assays

The levels of IL-1β and IL-18 in mouse serum and cell culture supernatants were measured using ELISA kits (PI301 and PI553, Beyotime) according to the manufacturer's instructions.

Calcium ion and GFP-LC3II fluorescence Signal Detection

Calcium ion levels were assessed using the Fluo-4 Calcium Assay Kit (S1061S, Beyotime), while GFP-LC3II fluorescence signals were detected using the GFP-LC3II Fusion Protein Adenovirus Kit (C3006-1ml, Beyotime). All procedures were conducted in accordance with the respective kit protocols.

Statistical analysis

Statistical analyses were performed using SPSS version 26.0. Data are presented as the mean ± standard deviation (SD). Comparisons among multiple groups were conducted using one-way analysis of variance (ANOVA), followed by the LSD-t test for pairwise comparisons. A p-value of less than 0.05 was considered to indicate statistical significance.

Results

Effect of metformin on atopic dermatitis in mice induced by DNCB

To elucidate the impact of Metformin on atopic dermatitis (AD), BALB/c mice were induced with AD-like lesions using DNCB. Over a period of one month, mice underwent sensitization with 1% DNCB followed by challenges with 0.5% DNCB, culminating in the development of AD-like lesions. Compared to the control group, mice in the DNCB group exhibited varying degrees of acanthosis, erythema, papules, and other dermatological changes. Metformin treatment significantly mitigated these symptoms, as observed both macroscopically and microscopically (**Figure 1**).

Metformin notably reduced the severity score of dorsal lesions (8.38 ± 0.99 in the DNCB group vs. 4.50 ± 0.35 in the Metformin-treated group) and decreased epidermal thickness (40.39 ± 2.74 μm in the DNCB group vs. 21.95 ± 2.03 μm in the Metformin-treated group). Additionally, Metformin ameliorated DNCB-induced skin barrier dysfunction, as evidenced by improvements in transepidermal water loss (TEWL) and stratum corneum hydration (SCH) [18]. Specifically, TEWL decreased from 10.1 ± 1.37 g/m²/h in the DNCB group to 5.64 ± 0.68 g/m²/h in the Metformin-treated group, while SCH increased from 19.35 ± 1.77% to 26.86 ± 1.75% (**Table 1**).

Table 1. Comparative analysis of severity score, epidermal thickness, and barrier function in DNCB-induced atopic dermatitis-like mice.

	Dermatitis score	Epidermis thickness (μm)	TEWL (g/cm²/h)	SCH (uS)
Control	0.88+0.60	9.96+0.76	3.55+0.39	47.96+1.34
DNCB	8.38+0.99*	40.39+2.74*	10.1+1.37*	19.35+1.77*
DNCB+Met	4.50+0.35**	21.95+2.03**	5.64+0.68**	26.86+1.75**
F value	126.047	403.456	94.144	576.044
P value	< 0.001	< 0.001	< 0.001	< 0.001

Notes: *compared with control group; ** compared with DNC WD, P < 0.05.

These results indicate that metformin can improve the skin injury caused by DNCB and restore the epidermal barrier function.

Modulation of NLRP3 inflammasome by metformin in AD-like mice

The activation of the NLRP3 inflammasome is known to trigger the production of IL-1β and IL-18, which are key regulators and responders in inflammatory processes. To explore the impact of Metformin on the NLRP3 inflammasome, we initially assessed the levels of IL-1β and IL-18 in mouse serum. Our results revealed a significant elevation in these cytokines in the DNCB-treated group. Metformin treatment effectively attenuated the DNCB-induced increases in IL-1β and IL-18 levels (**Figure 2A**).

Further investigation into the expression of NLRP3, Caspase-1, IL-1β, and IL-18 proteins was conducted using Western blot analysis. As depicted in **figures 2B** and **2C**, DNCB treatment led to a substantial upregulation of these proteins, whereas Metformin administration significantly curbed their expression. Consistent with these findings, immunohistochemical analysis demonstrated that NLRP3 expression was markedly higher in the DNCB group compared to the control group, and Metformin treatment effectively inhibited this increase (**Figure 2D**).

These results suggest that metformin can improve DNCB induced epidermis inflammation.

Effect of metformin on autophagy in mice induced by DNCB

Emerging evidence underscores the integral role of autophagy in the pathogenesis of atopic dermatitis (AD). ATG5 and LC3, pivotal autophagy markers in mammalian cells, are commonly utilized to assess autophagic activity. Upon autophagy activation, LC3-I undergoes conversion to LC3-II.

To delineate the autophagic status in AD, we scrutinized the expression profiles of ATG5 and LC3 in DNCB-induced mice. Western blot analyses unveiled that DNCB significantly downregulated the expression of ATG5 and LC3-II, whereas Metformin treatment effectively reversed this decline (**Figure 3A**). Consistent with these findings, immunohistochemical analyses revealed a marked reduction in LC3-II expression in the DNCB group, which was notably restored by Metformin treatment (**Figure 3C**).

These results imply that under physiological conditions, the epidermis maintains a basal level of autophagy, which is crucial for the normal proliferation and differentiation of keratinocytes. DNCB treatment, by inhibiting epidermal autophagy, precipitates the

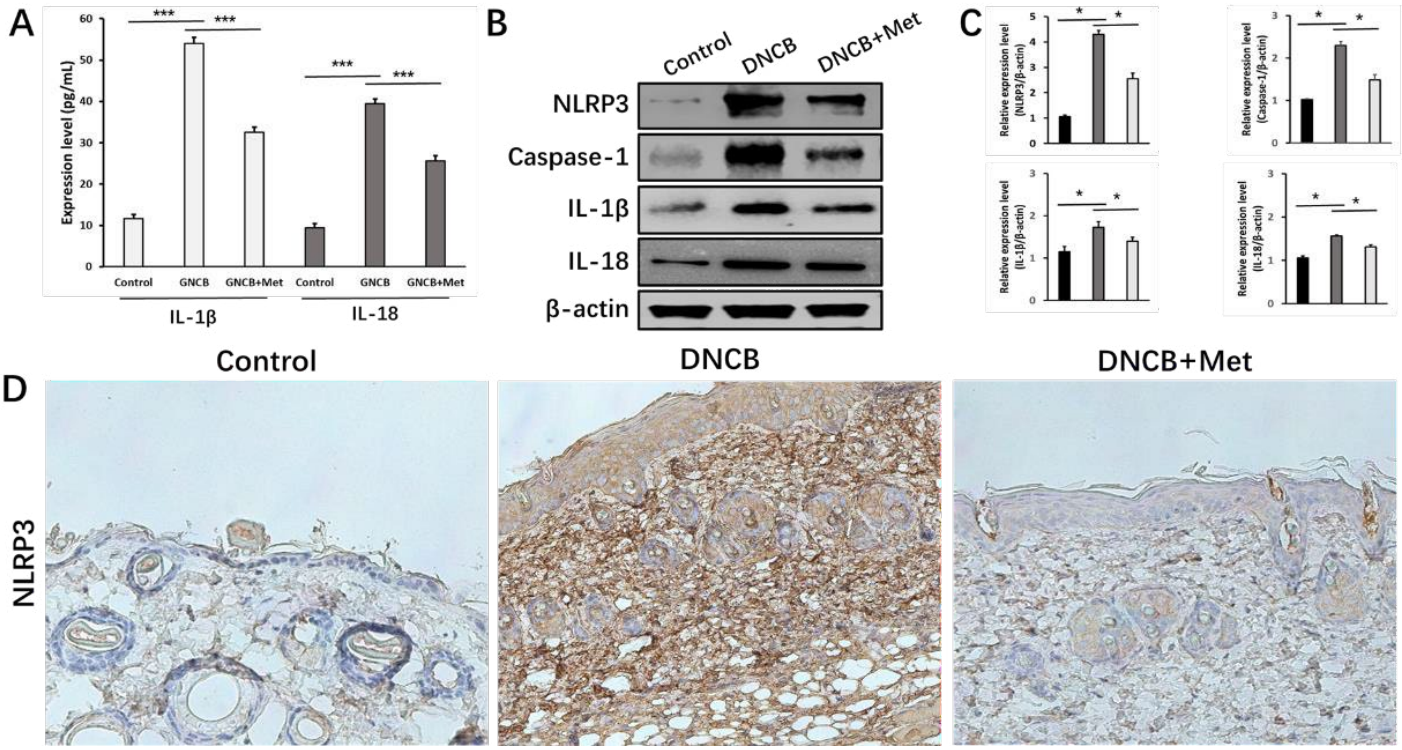

Figure 2. Modulation of NLRP3 Inflammasome by Metformin in AD-Like Mice. A. The levels of serum IL-1β and IL-18 of in each group. B. and C. Western blot to show protein NLRP3, Caspase-1, IL-1β, IL-18 and β-actin in each group. D. Changes in expression of protein NLRP3 in the dorsal skin were observed through immunohistochemistry.

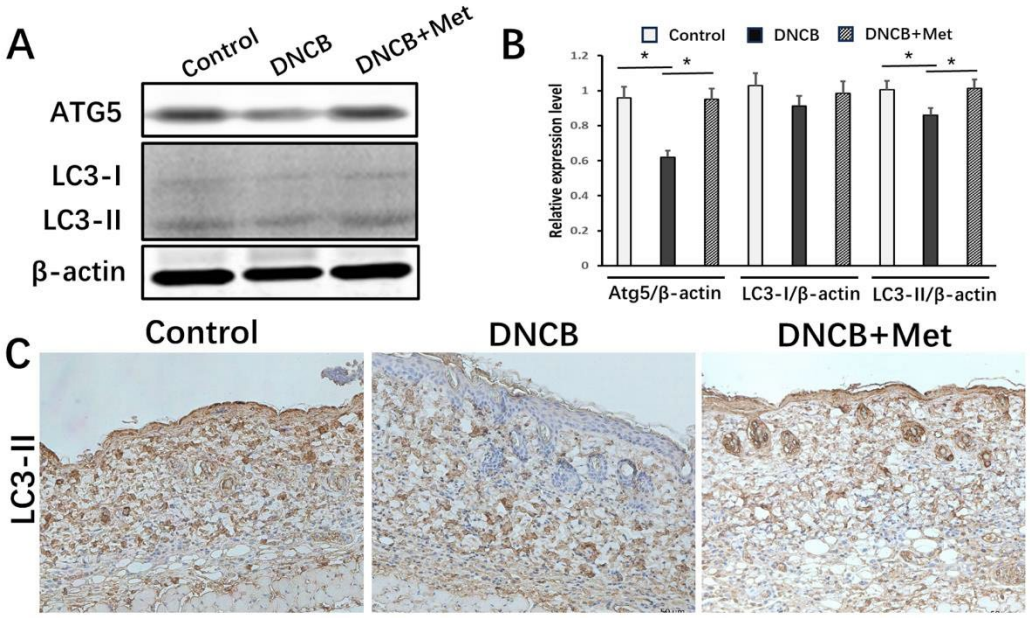

Figure 3. Effect of Metformin on Autophagy in Mice Induced by DNCB. A. and B. Western blot to show protein ATG5, LC3-I, LC3-II and β-actin in each group. C. Changes in expression of protein LC3-II in the dorsal skin were observed through immunohistochemistry.

development of AD. Metformin, by counteracting the inhibitory effects of DNCB on epidermal autophagy, restores autophagic function, thereby exerting a therapeutic effect on AD.

Effects of DNCB and metformin on the proliferation and apoptosis of HaCaT cells

Inflammation and autophagy are pivotal in regulating the normal function of the epidermis, with keratinocytes being the primary cells responsible for maintaining this function[19]. Given our findings that DNCB induces inflammation and inhibits autophagy, while Metformin mitigates DNCB-induced inflammation and promotes autophagy, we investigated the effects of these agents on the proliferation and apoptosis of human keratinocytes (HaCaT cells) *in vitro*.

DNCB significantly inhibited cell proliferation and promoted apoptosis, whereas Metformin exerted opposing effects by inhibiting apoptosis and enhancing cell proliferation (**Figure 4A** and **4D**). Additionally, we measured the levels of IL-1β and IL-18 in the cell culture supernatant. The expression of these cytokines was upregulated in the DNCB-treated group, an effect that Metformin partially reversed (**Figure 4B** and **4C**). Flow cytometry further confirmed that DNCB promoted apoptosis, an effect that Metformin treatment effectively mitigated.

To assess autophagy, HaCaT cells were infected with a GFP-LC3 fusion protein adenovirus[20]. Control cells exhibited dense punctate fluorescence, indicative of autophagosomes. In contrast, DNCB-treated cells displayed uniformly scattered cytoplasmic fluorescence, suggesting impaired autophagy. Cells treated with both DNCB and Metformin showed intermediate fluorescence signals, indicating partial restoration of autophagy (**Figure 4E**). These results collectively demonstrate that normal HaCaT cells exhibit basal autophagy, which is inhibited by DNCB but can be partially rescued by metformin.

Mechanisms of DNCB and metformin in regulating inflammation and autophagy via calcium signaling

Calcium is a critical regulatory molecule in the proliferation and differentiation of keratinocytes both in vivo and in vitro. Given its pivotal role, we hypothesized that the calcium-sensing receptor (CaSR) might be implicated in the intracellular signaling pathways activated by DNCB and modulated by Metformin. To test this hypothesis, we examined the expression of CaSR in HaCaT cells. Our findings revealed that DNCB treatment significantly upregulated CaSR expression, an effect that was attenuated by metformin (**Figure 5A**).

Utilizing the Fluo-4 Calcium Assay Kit to label calcium ions[21], we observed minimal fluorescence in normal control cells under fluorescence microscopy. In contrast, DNCB treatment markedly enhanced calcium ion fluorescence. Both Metformin and the CaSR inhibitor NPS-2143 effectively suppressed this DNCB-induced calcium ion fluorescence (**Figure 5B**). Moreover, NPS-2143, akin to Metformin, inhibited DNCB-induced

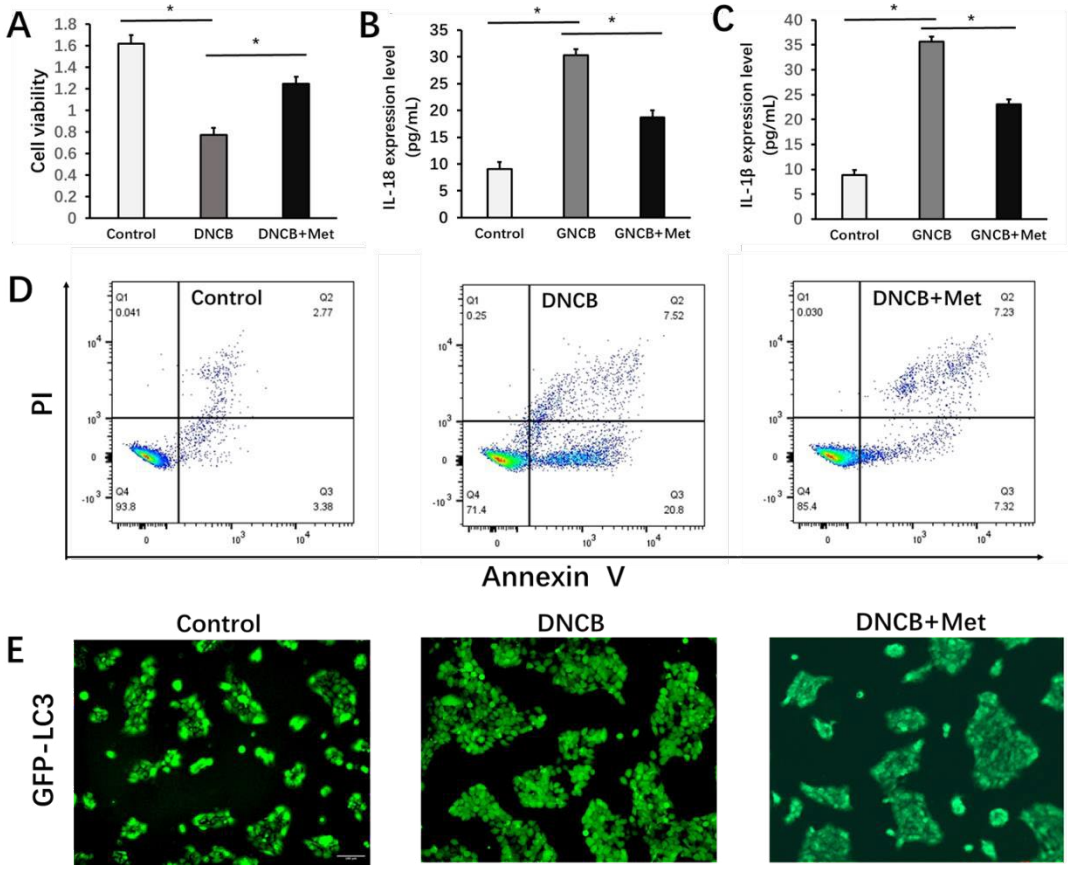

Figure 4. Effects of DNCB and Metformin on the Proliferation and Apoptosis of HaCaT Cells. A. CCK-8 assay shows cell viability in each group. B. and C. The levels of IL-1β and IL-18 in each group cell culture supernatants was measured by ELISA kit. D. GFP-LC3 images of the each group under the fluorescence microscope.

upregulation of IL-1β and IL-18 (**Figure 5C**) and mitigated DNCB's effects on cell proliferation and apoptosis (**Figures 5D** and **5E**).

These results collectively suggest that CaSR-mediated calcium signaling is instrumental in regulating the proliferation and apoptosis of keratinocytes, thereby influencing inflammation and autophagy.

Discussion

This study elucidated the molecular mechanisms by which metformin ameliorates atopic dermatitis (AD) by modulating the keratinocyte autophagy/NLRP3 inflammasome axis via the calcium signaling pathway, thereby providing a robust theoretical foundation for repurposing this established drug for novel therapeutic applications.

In our study, we successfully recapitulated the clinical hallmarks of AD in a DNCB-induced mouse model and demonstrated that metformin significantly mitigated the severity of skin lesions while restoring skin barrier function. This observation aligns with the findings of Leng Xue et al., who reported that phenformin, a metformin derivative, alleviated psoriasis-like inflammatory responses in an imiquimod-induced psoriasis model by downregulating c-Myc expression in keratinocytes, thus highlighting its potential as a topical therapeutic agent for psoriasis[22]. Additionally, other research has indicated that metformin can attenuate dermatitis in animal models by inhibiting NFκB activity[23]. However, it is important to note that, unlike psoriasis, which is primarily driven by Th17 polarization, the pathophysiological core of AD lies in Th2 polarization. This distinction suggests that metformin may possess a broader spectrum of immunomodulatory capabilities.

Our data revealed that DNCB markedly amplified the inflammatory response in keratinocytes and concurrently suppressed autophagy levels within these cells, thereby disrupting the delicate balance between inflammation and autophagy. This imbalance was effectively reversed by metformin treatment. These findings resonate with the existing literature underscoring the pivotal roles of inflammation and autophagy in the pathogenesis of AD[24,25]. In a similar vein, Sameh Saber et al. reported that metformin can suppress inflammation and induce autophagy, exerting a protective effect in colitis[26]. However, most of prior studies have predominantly focused on the modulation of inflammation and autophagy in immune cells.

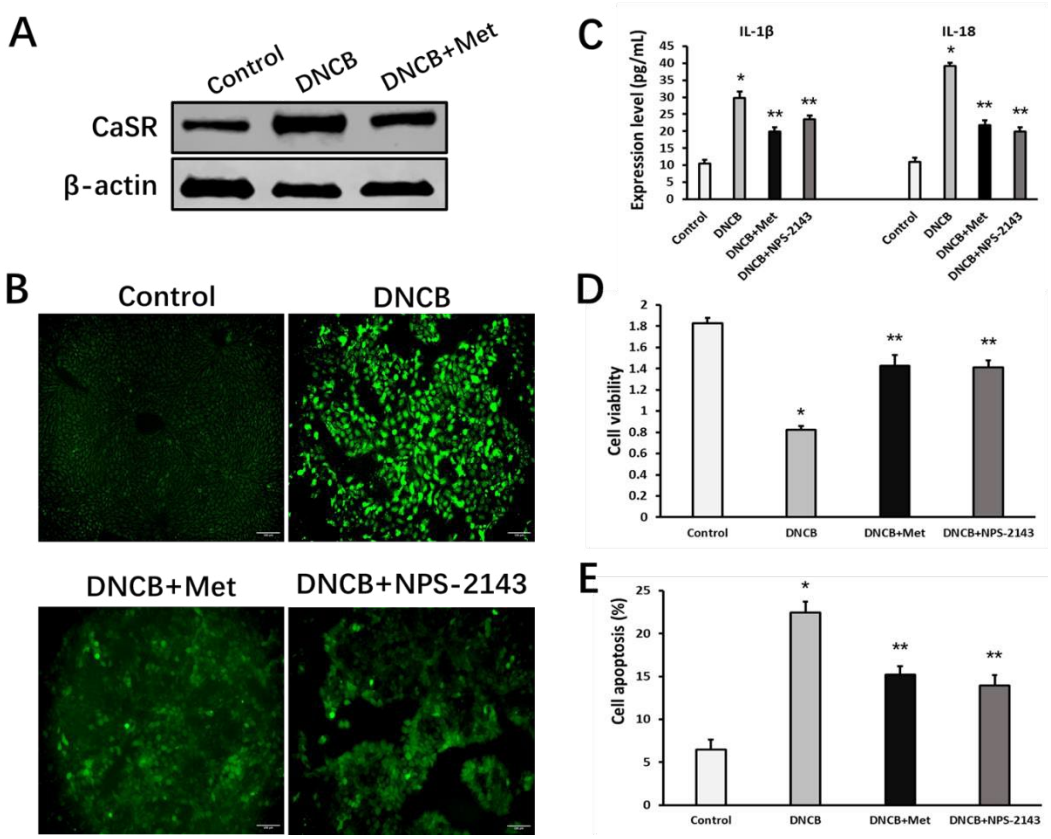

Figure 5. Calcium signaling involves in the effect of DNCB and Metformin on inflammation, cell proliferation and apoptosis. A. Western blot to show protein CaSR in each group. B. Calcium ion fluorescence images of each group. C. The levels of IL-1β and IL-18 in each group cell culture supernatants. * Compared with control group. ** Compared with DNCB group.

Our study innovatively uncovers the crucial role of keratinocyte inflammation and autophagy in AD, thereby expanding the understanding of the disease's pathogenesis.

This study demonstrated that metformin significantly alleviated DNCB-induced AD-like lesions by modulating the autophagy and NLRP3 inflammasome pathways. These findings provide a theoretical underpinning for the potential therapeutic application of metformin in AD treatment. Given its low cost and widespread use, metformin holds significant economic advantages for AD therapy. However, long-term systemic administration may induce gastrointestinal and other adverse effects, underscoring the necessity for the development of topical formulations, such as metformin cream[27]. Additionally, combination therapies targeting the autophagy-inflammatory axis, like metformin paired with the autophagy inducer rapamycin, warrant further investigation.

For the first time, this study explored the role of the calcium-sensing receptor (CaSR) in DNCB-induced AD models. The results indicated that DNCB markedly upregulated CaSR expression, an effect that metformin effectively counteracted. Moreover, the CaSR inhibitor NPS-2143 exhibited anti-inflammatory and autophagy-promoting effects akin to metformin. These observations suggest that CaSR-mediated calcium signaling may be a crucial factor in AD pathogenesis, thereby broadening the understanding of AD's etiology and offering a novel avenue for future research. Traditionally, calcium homeostasis imbalances have been primarily associated with skin barrier defects[28,29]. Our data, however, imply that this signaling pathway directly regulates inflammation and autophagy homeostasis. Notably, the similarity in effects between NPS-2143 (a CaSR inhibitor) and metformin in mitigating inflammation and enhancing autophagy suggests that metformin's therapeutic efficacy may be mediated through calcium signaling. This insight paves the way for the development of novel calcium channel regulators and further exploration of CaSR inhibitors' potential in AD treatment.

Although DNCB models effectively simulate the Th2-skewed inflammation characteristic of AD, they fall short in fully replicating the chronic relapsing nature of human AD. Future research should validate these findings in more complex disease models, such as those induced by MC903 and IL-33 overexpressing transgenic mice[30,31]. Additionally, this study did not account for age, a factor that may influence drug

response given the distinct autophagy capabilities of keratinocytes in elderly patients compared to children and young adults[32]. Single cell sequencing data have revealed multiple keratinocyte subpopulations within AD lesions, each potentially responding differently to treatment, highlighting another area for future exploration.

Conclusions

Utilizing a DNCB-induced AD mouse model and in vitro cell experiments, this study systematically elucidated the molecular mechanisms by which metformin ameliorates AD through the calcium signaling pathway, modulating keratinocyte autophagy and the NLRP3 inflammasome. These findings not only provide new therapeutic targets for AD but also offer theoretical support for repurposing metformin. Future work should aim to validate these results in more complex disease models and explore personalized treatment strategies based on patient molecular subtyping.

Conflicts of interest

The authors declare no conflicts of interest.

Funding

This study was sponsored by the S&T Program of Hebei (Grant No. 20377795D) and Hebei Natural Science Foundation (Grant No. H2020402004).

Author contributions

Guoying Miao: design.

Chunxia Yao: authorization of research, collection of data, manuscript.

Ke Tian and Xiaojuan Shang: animal experiments.

Jing Lv and Yu Shi: charts and statistics.

Hui Yang and Zihan Zhen: in vitro experiments.

All authors read and approved the final manuscript.

Ethics declarations

The study was approved by the Ethics Committee of Hebei University of Engineering (No. BER-YXY-2021023).

References

1. Langan SM, Irvine AD, Weidinger S. Atopic dermatitis. Lancet 2020;396(10247):345–360. Available from: 10.1016/S0140-6736(20)31286-1.
2. Touborg T, Frølunde S, Seeberg F, Deleuran M, Vestergaard Ch. Setting patient-centered treatment goals in atopic dermatitis: shared decision and A treat-to-target strategy. Curr Treat Options Allergy 2025; 12(5). Available from: https://doi.org/10.1007/s40521-025-00382-3.
3. Liming W, Ali K. Efficacy of dupilumab with concomitant topical calcineurin inhibitors treatment for preschool children with atopic dermatitis: a retrospective cohort study. Ann Med 2025;57(1):2449589. Available from: 10.1080/07853890.2025.2449589.
4. Garate D, Thang CJ, Chang CT, Owji S, Murphy TL, Golovko G, et al. Risk of malignancy associated with use of dupilumab versus other treatments in atopic dermatitis patients: a national database analysis. J Allergy Clin Immunol Pract 2025 Mar;13(3):698-701.e1. Available from: 10.1016/j.jaip.2024.11.015.
5. Drucker AM, Morra DE, Prieto-Merino D, Ellis AG, Yiu ZZN, Rochwerg B, et al. Systemic immunomodulatory treatments for atopic dermatitis: update of a living systematic review and network meta-analysis. JAMA Dermatol 2022;158(5):523-532. Available from: 10.1001/jamadermatol.2022.0455.
6. Müller S, Witte F, Ständer S. Pruritus in atopic dermatitis-comparative evaluation of novel treatment approaches. Dermatologie 2022;73(7):538–549. Available from: 10.1007/s00105-022-05011-7.
7. Xue S, Lin Y, Chen H, Yang Z, Zha J, Jiang X, et al. Mechanisms of autophagy and their implications in dermatological disorders. Front Immunol 2024;15:1486627. Available from: 10.3389/fimmu.2024.1486627.
8. Chen Y, Wu Y, Tian X, Shao G, Lin Q, Sun A. Golgiphagy: a novel selective autophagy to the fore. Cell Biosci 2024;14(1):130. Available from: 10.1186/s13578-024-01311-8.
9. Zhu Y, Liu Y, Ma Y, Chen L, Huang H, Huang S, et al. Macrophage autophagy deficiency-induced CEBPB accumulation alleviates atopic dermatitis via impairing M2 polarization. Cell Rep 2023;42(11):113430. Disponible en: 10.1016/j.celrep.2023.113430.
10. Lin Y, Wu X, Yang Y, Wu Y, Xiang L, Zhang C. The multifaceted role of autophagy in skin autoimmune disorders: a guardian or culprit? Front Immunol 2024;15:1343987. Available from: 10.3389/fimmu.2024.1343987.
11. Chen L, Mao LS, Xue JY, Jian YH, Deng ZW, Mazhar M, et al. Myocardial ischemia-reperfusion injury: the balance mechanism between mitophagy and NLRP3 inflammasome. Life Sci 2024;355:122998. Available from: 10.1016/j.lfs.2024.122998.
12. Zheng J, Yao L, Zhou Y, Gu X, Wang C, Bao K, et al. A novel function of NLRP3 independent of inflammasome as a key transcription factor of IL-33 in epithelial cells of atopic dermatitis. Cell Death Dis 2021;12(10):871. Available from: 10.1038/s41419-021-04159-9.
13. Yao L, Wang L, Zhang R, Soukas AA, Wu L. The direct targets of metformin in diabetes and beyond. Trends Endocrinol Metab 2024. Available from: 10.1016/j.tem.2024.07.017.
14. Petrasca A, Hambly R, Kearney N, Smith CM, Pender EK, Mac Mahon J, et al. Metformin has anti-inflammatory effects and induces immunometabolic reprogramming via multiple mechanisms in hidradenitis suppurativa. Br J Dermatol 2023 Nov 16;189(6):730-740. Available from: 10.1093/bjd/ljad305.
15. Zhang T, Zhou L, Makarczyk MJ, Feng P, Zhang J. The anti-aging mechanism of metformin: from molecular insights to clinical applications. Molecules 2025;30(4):816. Available from: 10.3390/molecules30040816.
16. Leung DY, Hirsch RL, Schneider L, Moody C, Takaoka R, Li SH, et al. Thymopentin therapy reduces the clinical severity of atopic dermatitis. J Allergy Clin Immunol 1990;85(5):927-33. Available from: 10.1016/0091-6749(90)90079-j.

17. Wang L, Xian YF, Loo SKF, Ip SP, Yang W, Chan WY, et al. Baicalin ameliorates 2,4-dinitrochlorobenzene-induced atopic dermatitis-like skin lesions in mice through modulating skin barrier function, gut microbiota and JAK/STAT pathway. Bioorg Chem 2022;119:105538. Available from: 10.1016/j.bioorg.2021.105538.
18. Sander N, Stölzl D, Fonfara M, Hartmann J, Harder I, Suhrkamp I, et al. Blockade of interleukin-13 signalling improves skin barrier function and biology in patients with moderate-to-severe atopic dermatitis. Br J Dermatol 2024;191(3):344-350. Available from: 10.1093/bjd/ljae138.
19. Girolomoni G, Pastore S. The role of keratinocytes in the pathogenesis of atopic dermatitis. J Am Acad Dermatol 2001;45(1):S25–8. Available from: 10.1067/mjd.2001.117021.
20. Zhang P, Zhang W, Hong Z, Jiang J, Wu N, Lin J, et al. Elucidating the role of CYFIP2 in conferring cisplatin resistance in esophageal squamous cell carcinoma. Sci Rep 2024;14(1):27130. Available from: 10.1038/s41598-024-77420-8.
21. Xie Z, Li T, Su W, Lou Y, Zhang Y, Zhou X, et al. Extension domain of amyloid processor protein inhibits amyloidogenic cleavage and balances neural activity in a traumatic brain injury mouse model. CNS Neurosci Ther 2024;30(2):e14402. Available from: 10.1111/cns.14402.
22. Leng X, Wang S, Zhuang D, Feng T, Jiang X, Xu S, et al. Topical application of phenformin ameliorates the psoriasis-like inflammatory response via the inhibition of c-Myc expression in keratinocytes. Biochem Biophys Res Commun 2024;736:150503. Available from: 10.1016/j.bbrc.2024.150503.
23. Choi SY, Lee C, Heo MJ, Choi YM, An IS, Bae S, et al. Metformin ameliorates animal models of dermatitis. Inflammopharmacology 2020;28(5):1293-1300. Available from: 10.1007/s10787-020-00704-8.
24. Sun Y, Zhou Y, Peng T, Huang Y, Lu H, Ying X, et al. Preventing NLRP3 inflammasome activation: therapeutic strategy and challenges in atopic dermatitis. Int Immunopharmacol 2025;144:113696. Available from: 10.1016/j.intimp.2024.113696.
25. Borzutzky A, Larco JI, Luna PC, McElwee E, Cezar Pires M, Rico Restrepo M, et al. Atopic dermatitis in Latin America: a Roadmap to Address Data Collection, Knowledge Gaps, and Challenges. Dermatitis 2022; 33(6S):S83-S91.
26. Saber S, El-Kader EMA. Novel complementary coloprotective effects of metformin and MCC950 by modulating HSP90/NLRP3 interaction and inducing autophagy in rats. Inflammopharmacology 2021;29(1):237-251. Available from: 10.1007/s10787-020-00730-6.
27. Granja BV, De Matos PR, Rosa GP, Pinheiro J, Azevedo F, Pedrosa AF. Treatment of central centrifugal cicatricial alopecia with topical metformin 10% cream: case report and literature review. Int J Dermatol 2025;64(1):213-215. Available from: 10.1111/ijd.17345.
28. Zheng H, Gu L, Zhao F, Zhang C, Wang Z, Zhou H, et al. SerpinB7 deficiency contributes to development of psoriasis via calcium-mediated keratinocyte differentiation dysfunction. Cell Death Dis 2022;13(7):635. Available from: 10.1038/s41419-022-05045-8.
29. Tu CL, Crumrine DA, Man MQ, Chang W, Elalieh H, You M, et al. Ablation of the calcium-sensing receptor in keratinocytes impairs epidermal differentiation and barrier function. J Invest Dermatol 2012;132(10):2350-2359. Available from: 10.1038/jid.2012.159.
30. Huang D, Liu X, Gao X, Choi CK, Giglio G, Farah L, et al. Meteorin-like protein/METRNL/Interleukin-41 ameliorates atopic dermatitis-like inflammation. Allergy 2025;80(2):474-488. Available from: 10.1111/all.16150.
31. Imai Y, Yasuda K, Nagai M, Kusakabe M, Kubo M, Nakanishi K, et al. IL-33-induced atopic dermatitis-like inflammation in mice is mediated by group 2 innate lymphoid cells in concert with basophils. J Invest Dermatol 2019;139(10):2185-2194.e3. Available from: 10.1016/j.jid.2019.04.016.
32. Kim HS, Park SY, Moon SH, Lee JD, Kim S. Autophagy in human skin fibroblasts: impact of age. Int J Mol Sci 2018;19(8):2254. Available from: 10.3390/ijms19082254.

ACADEMIC JOURNAL OF HEALTH SCIENCES
MEDICINA BALEAR

Case report

Sinonasal glomangiopericytoma: diagnosis and surgical management

Glomangiopericitoma nasosinusal: diagnóstico y manejo quirúrgico

Aleksandrina Topalova-Shishmanova*, Karen Dzhambazov, María Koleva-Ivanova, Georgi Pavlov

Medical University of Plovdiv, Plovdiv, Bulgaria

Received: 18-01-25
Accepted: 20-03-25

***Corresponding author:** Aleksandrina Topalova Shishmanova. a.r.topalova@gmail.com

Abstract

Introduction: Glomangiopericytoma (GPC) is a rare sino-nasal soft tissue tumor which occurs mostly in the late adult life (60s or 70s) with a slight predominance in women. GPC exhibits benign behavior with low malignant potential and an excellent overall survival rate. Total surgical resection is considered the primary treatment of GPC in the nasal cavity and paranasal sinuses.

Case report: We report the case of a 46-year-old male admitted to hospital due to uncontrolled nasal bleeding from the left nostril and nasal obstruction on the same side. After removing the nasal packing, an endoscopic examination was performed and a tumor mass in the left nasal middle meatus was revealed. On the CT scan the mass was enhanced and demonstrated well-defined borders and sphenopalatine's blood supply. The tumor was surgically removed via endoscopic endonasal excision and the diagnosis of glomangiopericytoma was confirmed further on by a histopathological examination.

Conclusion: It is of vital importance to distinguish GPS from the other diagnosed masses of the nasal cavities or paranasal sinuses. Proper clinical identification and in time complete surgical resection are associated with a lower risk of intraoperative complications and recurrences.

Keywords: Glomangiopericytoma. Sinonasal tumor. Haemangiopericytoma. Endoscopic endonasal resection.

Resumen

Introducción: el glomangiopericitoma (GPC) es un tumor raro de partes blandas de localización nasosinusal, que se presenta predominantemente en la edad adulta tardía (década de los 60 o 70 años), con una ligera mayor prevalencia en mujeres. La GPC presenta un comportamiento benigno, con bajo potencial maligno y una excelente tasa de supervivencia global. La resección quirúrgica total se considera el tratamiento de elección para los casos de GPC en la cavidad nasal y los senos paranasales.

Reporte de caso: se presenta el caso de un varón de 46 años ingresado en el hospital debido a una epistaxis incontrolada por la fosa nasal izquierda, acompañada de obstrucción nasal ipsilateral. Tras la retirada del taponamiento nasal, se realizó una endoscopia que evidenció una masa tumoral en el meato medio nasal izquierdo. En la tomografía computarizada (TC), la masa mostró realce tras la administración de contraste, bordes bien definidos y vascularización dependiente de la arteria esfenopalatina. El tumor fue extirpado quirúrgicamente mediante una resección endoscópica endonasal, y el diagnóstico de glomangiopericitoma fue confirmado posteriormente mediante examen histopatológico.

Cite as: Topalova-Shishmanova A, Dzhambazov K, Koleva-Ivanova M, Pavlov G. Sinonasal glomangiopericytoma: diagnosis and surgical management. Acad J Health Sci 2025; 40(5): 82-87. Available from: https://doi.org/10.3306/AJHS.2025.40.05.10

Acad J Health Sci 2025; 40(5): 82-87
https://doi.org/10.3306/AJHS.2025.40.05.10
www.ajhealthsciences.com

Conclusiones: es de vital importancia diferenciar la GPC de otras masas diagnosticadas en las cavidades nasales o senos paranasales. Una identificación clínica adecuada, así como una resección quirúrgica completa y oportuna, se asocian con un menor riesgo de complicaciones intraoperatorias y recurrencias.

Palabras clave: Glomangiopericitoma. Tumor nasosinusal. Hemangiopericitoma. Resección endoscópica endonasal.

Introduction

Stout and Murray reported the first incidence of GPC in 1942. Hemangiopericytoma was the original classification for it[1,2]. The term 'hemangiopericytoma' was proposed because the lesion was thought to exhibit features of both a capillary hemangioma and a glomus tumor. The definition of the disease has been hotly contested since it was first described[3]. Of all sinonasal tumors, 0.5% to 1.0% are sinonasal glomangiopericytomas, making them an extremely rare vascular neoplasm of the nasal cavity or paranasal sinuses[4].

It is a borderline soft tissue tumor with low malignant potential, also known as sinonasal-type hemangiopericytoma, which arises from the pericyte cells surrounding the capillaries. According to the World Health Organization (WHO), GPC is classified as a distinct entity among sinonasal tumors with a perivascular myoid phenotype[5].

The etiology of GPC is idiopathic. Predisposing factors include pregnancy, corticosteroid use, history of trauma, and hypertension. Although there is no evidence to support the use of adjuvant medications, complete surgical resection remains the preferred course of treatment. The prognosis is generally favorable, although GPC has shown a tendency for delayed recurrence.

Case report

A 46-year-old man with no comorbidities was admitted to the emergency department with complaints of left nasal congestion and severe nasal bleeding over the past few days. The patient reported minimal, periodic nosebleeds over the last three months. On the day of admission, an initial assessment was performed, followed by treatment with nasal packing and systemic hemostatic drugs. The nasal packing was removed after two days, and an endoscopic examination of the nasal cavity revealed a reddish mass between the middle turbinate and septum (**Figure 1**).

An enhanced computed tomography (CT) scan was performed immediately after the endoscopy. It revealed a heterogeneous soft tissue mass that invaded the nasal septum, posterior ethmoidal cells, and the entire left nasal cavity. It also extended into a significant portion of the nasopharynx. There was no clear evidence of destruction in the region of the ethmoidal roof (**Figure 2**).

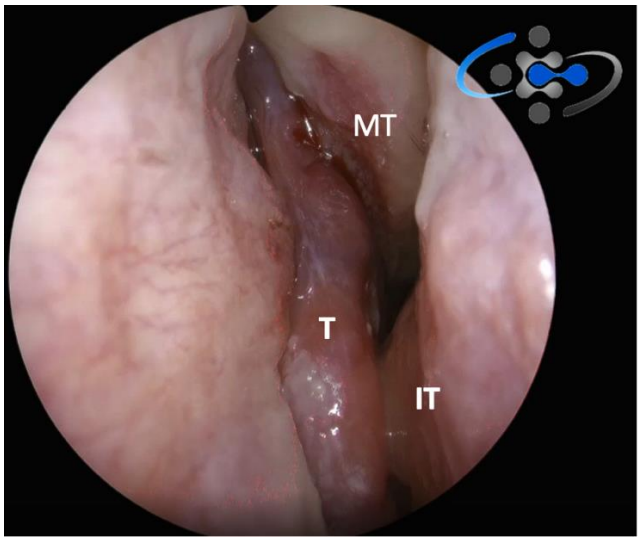

Figure 1. Endoscopic view of the tumor in the middle meatus on the left side of the nose. (T- tumor, IT- inferior turbinate; MT- middle turbinate).

In terms of differential diagnosis, the following tumors were considered: hemangiopericytoma, angiofibroma, a polyp and inverted papilloma, carcinoma.

Two weeks later, the patient underwent endoscopic endonasal excision of the tumor. During the procedure, we visualized its borders of spread. To minimize the risk of hemorrhage, we decided to perform sphenopalatine artery ligation on the same side. Additionally, some erosions of the anterior cells of the ethmoidal labyrinth were noted, partially destroyed by tumor growth. There was infiltration in the area of the nasal septum that reached the olfactory area. After resection of the nasal septum mucosa, the olfactory fibers were exposed. No CSF leak was observed. The maxillary and sphenoid sinuses appeared to be intact.

The frozen section diagnoses showed a glomangiopericytoma.

The pathology report confirmed the final diagnosis of sinonasal glomangiopericytoma with negative resection margins.

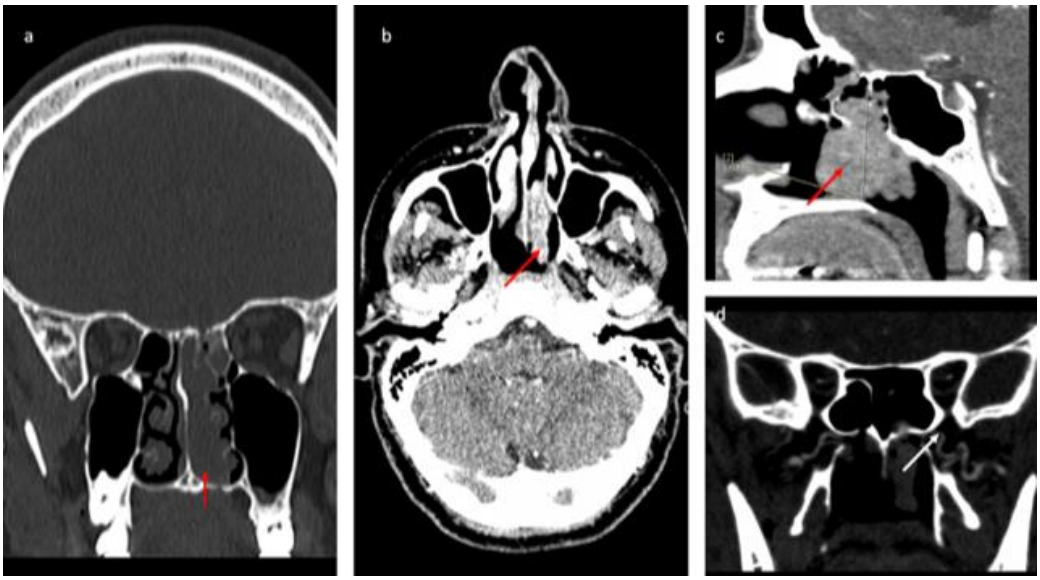

Figure 2A. Coronal CT illustrates the tumor in the entire nasal cavity (red arrow).
Figure 2B and 2C. Axial and sagittal CT showing tumor spreading to the nasal septum and nasopharynx (red arrow).
Figure 2D. CT angiography demonstrates the prevalence of sphenopalatine artery's blood supply to the tumor (white arrow).

A well-circumscribed, diffuse, subepithelial proliferation of spindled cells, developing in sheets and short fascicles, with effacement of submucosal structures, was observed histologically in the tumor mass. With an underlying 'Grenz' zone, the sinonasal epithelium remained intact, covering it. The cytological characteristics of the cells included spindled nuclei with smooth nuclear outlines, homogeneous chromatin, eosinophilic to vacuolated cytoplasm, and bland, uniformly spaced cells with ambiguous cell boundaries. Stromal edema-producing, comparatively hypocellular zones were present in certain areas. The cells were closely associated with a well-developed vascular network, composed of many capillary-sized vessels and staghorn-shaped, asymmetrical vessels. There was inflammatory infiltration, including plasma cells, lymphocytes, and mast cells. Cyclin D1, β-catenin, and smooth muscle actin (SMA) showed diffuse and robust staining by immunohistochemical methods **(Figure 3**).

Histologically, the tumor mass showed a well-circumscribed, diffuse, subepithelial proliferation of spindled cells growing in sheets and short fascicles with effacement of submucosal structures. The overlying sinonasal epithelium was intact with an underlying "Grenz" zone. The cells were cytologically bland and evenly spaced with indistinct cell borders, with eosinophilic to vacuolated cytoplasm, and spindled nuclei with smooth nuclear contours and uniform chromatin. Some areas had stromal edema yielding relatively hypocellular zones. The cells were intimately associated with a prominent vascular network composed of irregularly shaped, staghorn-type vessels with numerous capillary-sized vessels. An inflammatory infiltrate including mast cells, lymphocytes, and plasma cells was present. Immunohistochemical stains demonstrated diffuse and strong staining for smooth muscle actin (SMA), Cyclin D1 and b-catenin. These morphologic and immunophenotypic features corresponded with perivascular myoid differentiation and were diagnostic of sinonasal glomangiopericytoma.

The patient has been under regular endoscopic follow-up of the nasal cavity and has remained disease-free for a year now.

Discussion

Sinonasal glomangiopericytoma (GPC) is a benign tumor distinct from other hemangiopericytomas. In general, these lesions appear as 'beef' red or 'aubergine' purple polypoid hemorrhagic masses. Glomangiopericytoma is often difficult to distinguish from other benign vascular tumors, such as leiomyoma, angiofibroma, and solitary fibrous tumors[6].

The comparison table below summarizes the distinguishing features of GPC in comparison to its mimics (**Table 1**).

Glomangiopericytoma commonly occurs in the nasal cavity and paranasal sinuses, but it can also be found in a large variety of regions such as the orbit, the lungs, the liver, and even in soft tissues. It typically affects adults between the ages of 60 and 70

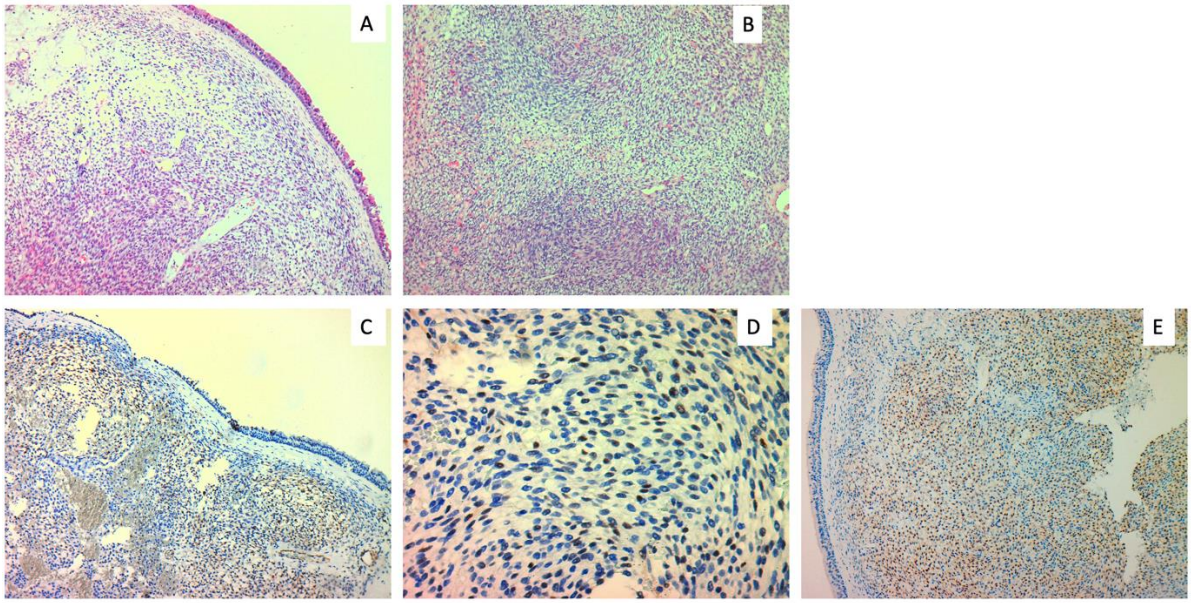

Figure 3A. Fragment of polypoid lesion showing intact surface sinonasal epithelium with subepithelial Grenz zone and diffuse proliferation of spindle cells and prominent vascular stroma, hematoxylin-eosin, x 200.
Figure 3B. Cytologically bland spindle cell proliferation has a fascicular growth arrangement and mast cells are presented in the background, hematoxylin-eosin, x200.
Figure 3C. Smooth muscle actin expression in glomangiopericytoma. Immunohistochemistry anti-smooth muscle actin, x400.
Figure 3D. Cyclin D1 expression in glomangiopericytoma. Immunohistochemistry anti-cyclin D1, x200.
Figure 3E. B-catenin expression in glomangiopericytoma. Immunohistochemistry anti-b-catenin, x200.

Table 1. Differential diagnosis of glomangioperycitoma[7-10].

Tumor type	Age groups	Localization	Clinical signs	CT Imaging
Glomangiopericytoma (GPC)	Between 40-60 years	Nasal cavity, sinuses	Unilateral nasal obstruction, unilateral nose bleeding, headache.	Heterogenous vascular mass.
Hemangiopericytoma	Similar to GPC	Similar to GPC	Nasal obstruction and unilateral nose bleeding.	Vascularized mass with bony remodeling.
Inverted papilloma	Occurs at the 40-year-old group	Similar to GPC	Nasal obstruction, epiphora, chronic rinosinusitis, nerve palsies.	Bony changes and sinus involvement.
Juvenile angiofibroma	Young men (10 – 20 years)	Nasal cavity, pterygopalatine fosa	Nasal obstruction, unilateral epistaxis, proptosis, cranial nerve palsies.	Vascular mass with soft tissue invasion. Sinus involvement.
Nasal polyp	>10 years	Nasal cavity, sinuses	Nasal congestion, rhinorrhea, anosmia, facial pressure.	Smooth, rounded masses with sinus opacification.
Squamous cell carcinoma	>60 years	Nasal cavity, sinuses, nasopharynx.	Nasal obstruction, unilateral epistaxis, pain, cranial nerve palsies, epiphora.	Irregular mass with bony destruction, neck lymphadenopathy.

with a slight female predominance. The ethmoid and sphenoid sinus are the most commonly affected.

Clinical presentation of GPC varies and largely depends on the tumor location. Patients with sinonasal GPC usually present with nasal obstruction, epistaxis, and rhinorrhea.

The endoscopy of the nasal cavity and the CT scan examination are crucial for the diagnosis. The diagnosis of GPS relies on a combination of clinical, radiological, and histopathological findings. Determining the size of the tumour and its relationship to surrounding structures can be accomplished with the assistance of imaging techniques like computed tomography (CT) and magnetic resonance imaging (MRI). On imaging GPCs appear as well-defined, round or lobulated hypointense soft tissue masses. They frequently show erosive bone remodeling, especially in the sinonasal cavity. Biopsy and histological examination, including immunochemistry, are necessary for the definitive diagnosis.

GPCs may be confused with a variety of benign or borderline spindle cell and vascular neoplasms occurring in the sinonasal tract[11]. Pathologists may face a significant diagnostic challenge if there is considerable overlap between the morphological features and immunohistochemical expression of different markers among these entities, particularly when specimens are insufficient. Although no single marker can eliminate immunohistochemical overlap between sinonasal GPC and its histological counterparts, an expanded immunohistochemical panel helps support the diagnosis in challenging cases, without the need for molecular investigations. While no single marker resolves the immunohistochemical overlap between sinonasal GPC and its histological mimics, an extended immunohistochemical panel aids in diagnosis in diagnostically challenging cases, without requiring molecular studies[12,13]. Our case demonstrates that strong and diffuse expression of SMA, β-catenin, and cyclin D1, associated with the characteristic histological findings, is most likely related to sinonasal GPC.

Surgical resection is the first choice treatment for GPC. The main goal is to achieve complete tumor excision with negative margins[13,14]. However, due to its tendency to infiltrate surrounding structures, achieving complete tumor resection can be challenging. Radiation therapy may be used as an adjuvant treatment option to reduce the risk of local recurrence. The role of chemotherapy in the management of GPC remains uncertain[15]. By cutting off the tumor's blood supply, preoperative embolisation of afferent vessels may facilitate surgical excision easier. Ophthalmic artery embolisation was reported by Weber et al. before a large sinonasal haemangiopericytoma was surgically removed[16].

In case of large highly vascularised tumors with the pterygopalatinal fossa or orbital involvement, embolization prior surgery could ensure better conditions for successful tumor removal while minimizing severe blood loss. During endonasal endoscopic tumor resection proper hemostasis is crucial in order to avoid excessive bleeding necessitating a conversion to an external approach. Due to the small number of reported cases and the lack of enough experience, definite criteria for preoperative GPC embolization have not been proposed yet[16,17].

The prognosis for GPC depends on several factors, such as tumor size, location, histological grade, and the extent of surgical excision. A large number of reported studies (e.g., Thomson et al.) show that recurrences are related to inadequate tumor resection, often reappearing within the first year[18-21]. This can lead to revision surgery and an increased risk of hemorrhage.

Conclusion

Glomangiopericytoma is a rare tumor of pericytes that primarily affects the nasal cavity and paranasal sinuses. It poses significant diagnostic challenges due to its diverse clinical and histological manifestations. The mainstay of treatment includes complete surgical excision with negative resection margins. Due to its potential for local recurrence regular postoperative lifelong follow-up is strongly recommended.

Conflicts of interest

The authors declare no conflicts of interest.

Funding

This article has not received any specific grant from funding agencies in the public, commercial, or for-profit sectors.

References

1. Dandekar M, McHugh JB. Sinonasal glomangiopericytoma: case report with emphasis on the differential diagnosis. Arch Pathol Lab Med 2010;134(10):1444-9. Available from: 10.5858/2010-0233-CR.1.
2. Park ES, Kim J, Jun S-Y. Characteristics and prognosis of glomangiopericytomas: a systematic review. Head Neck 2017;39(9):1897-909. Available from: 10.1002/hed.24818.
3. Ghaloo SK, Dhanani R, Pasha HA, Wasif M, Fatima S, Ikram M. Glomangiopericytoma: A rare tumour of sinonasal cavity. J Pak Med Assoc 2020;70(12(B)):2469-71. Available from: 10.47391/JPMA.948.

4. Moussaoui ZNE, Najjar ZA, Diab N, Saker Z, Choukr H, Aoude AK, et al. Clinical and histopathological findings of a rare sinonasal glomangiopericytoma. Autops Case Rep 2023;13:e2023424. Available from: 10.4322/acr.2023.424.
5. Stelow EB, Bishop JA. Update from the 4th edition of the World Health Organization classification of head and neck tumours: tumors of the nasal cavity, paranasal sinuses and skull Base. Head Neck Pathol 2017;11(1):3-15. Available from: 10.1007/s12105-017-0791-4.
6. Abou Al-Shaar H, Macdonald KI, Labib MA. Glomangiopericytoma simulating an intracavernous meningioma. Surg Neurol Int 2016;7(5):S142-7. Available from: 10.4103/2152-7806.177888.
7. Thompson LDR, Bishop JA. Update from the 5th Edition of the World Health Organization Classification of Head and Neck Tumors: Nasal Cavity, Paranasal Sinuses and Skull Base. Head Neck Pathol. 2022;16(1):1-18. Available from: 10.1007/s12105-021-01406-5.
8. Ikubor JE, Okolugbo NE, Okhakhu AL. Radiological features of juvenile nasopharyngeal angiofibroma. J West Afr Coll Surg. 2013;3(4):84-91.
9. Franchi A. Sinonasal tumor pathology: what's new? Pathologica. 2017;109(1):9-13.
10. Al-Jobory YM, Pan Z, Manes RP, Omay SB, Ikuta I. Sinonasal Glomangiopericytoma: Review of Imaging Appearance and Clinical Management Update for Rare Sinonasal Neoplasm. Yale J Biol Med. 2021;94(4):593-597.
11. Chaouki A, Najib Z, Mkhatri A, Rouadi S, Mahtar M. Glomangiopericytoma of the inferior nasal turbinate: a case report. Int J Surg Case Rep 2021;79:409-12. Available from: 10.1016/j.ijscr.2021.01.051.
12. Dandekar M, McHugh JB. Sinonasal glomangiopericytoma: case report with emphasis on the differential diagnosis. Arch Pathol Lab Med 2010;134(10):1444-9. Available from: 10.5858/2010-0233-CR.1.
13. Obeidin F, Jennings LJ, Alexiev BA. Sinonasal glomangiopericytoma: a clinicopathologic study. Pathol Res Pract 2019;215(5):983-7. Available from: 10.1016/j.prp.2019.02.004.
14. Sharma N, Mandlik D, Patel P, Patel P, Joshipura A, Patel M, et al. A rare case of sinonasal glomangiopericytoma post operative accidental diagnosis and managment: a case report. Int J Surg Case Rep 2019;62:54-7. Available from: 10.1016/j.ijscr.2019.06.066.
15. Billings KR, Fu YS, Calcaterra TC, Sercarz JA. Hemangiopericytoma of the head and neck. Am J Otolaryngol 2000;21(4):238-43. Available from: 10.1053/ajot.2000.8378.
16. Weber W, Henkes H, Metz KA, Berg-Dammer E, Kühne D. Haemangiopericytoma of the nasal cavity. Neuroradiology 2001;43(2):183-6. Available from: 10.1007/pl00006046.
17. Ledderose GJ, Gellrich D, Holtmannspötter M, Leunig A. Endoscopic resection of sinonasal hemangiopericytoma following preoperative embolisation: a case report and literature review. Case Rep Otolaryngol 2013;2013:796713. Available from: 10.1155/2013/796713.
18. Psoma E, Karkos PD, Dova S, Gavriilidis M, Markou K, Kouskouras C, et al. Sinonasal glomangiopericytoma treated with preoperative embolisation and endoscopic sinus surgery. Ecancermedicalscience 2016;10:692. Available from: 10.3332/ecancer.2016.692.
19. Roy NP, Desai DP, Jain SA. Glomangiopericytoma of nasal cavity. Indian J Pathol Microbiol 2015;58(4):554-6. Available from: 10.4103/0377-4929.168864.
20. Asimakopoulos P, Syed MI, Andrews T, Syed S, Williams A. Sinonasal glomangiopericytoma: is anything new? Ear Nose Throat J 2016;95(2):E1-5. Available from: 10.1177/014556131609500202.
21. Thompson LD, Miettinen M, Wenig BM. Sinonasal-type hemangiopericytoma: a clinicopathologic and immunophenotypic analysis of 104 cases showing perivascular myoid differentiation. Am J Surg Pathol 2003;27(6):737-49. Available from: 10.1097/00000478-200306000-00004.

ACADEMIC JOURNAL OF HEALTH SCIENCES
MEDICINA BALEAR

Case report

Optimization of renal irrigation using a high-flow catheter in percutaneous nephrolithotomy: preliminary results

Optimización de la irrigación renal mediante un catéter de alto flujo en la nefrolitotomía percutánea: resultados preliminares

Antonio Servera-Ruiz de Velasco[1]*, Begoña Ballesta-Martínez[2]

[1]Department of Urology, Hospital de Manacor, Mallorca, Spain
[2]Department of Urology, University Hospital del Vinalopo, Alicante, Spain

Received: 23-02-25
Accepted: 08-04-25

***Corresponding author:** Antonio Servera-Ruiz de Velasco. anservera@gmail.com

Abstract

Since the introduction of the supine position in percutaneous nephrolithotomy (PCNL), one persistent challenge has been the upward migration of stone fragments toward the upper renal pole, exacerbated by lumbar spine anatomy. This article presents a technical innovation utilizing a high-flow catheter, originally intended for ureteral stent placement, repurposed as a targeted irrigation channel to the upper pole. This innovation generates a strong, continuous flow that prevents fragment migration, and enhances fragment evacuation and surgical visibility. In a preliminary series of five cases, the technique proved to be safe and reproducible, and achieved those objectives. These initial findings underscore the clinical potential of this method and justify further evaluation through larger prospective studies to validate its efficacy and impact on reducing secondary interventions.

Keywords: Percutaneous nephrolithotomy. Directed renal irrigation. High-flow catheter. Residual fragments. Technical innovation. Lithotripsy.

Resumen

Desde la introducción de la posición supina en la nefrolitotomía percutánea (PNL), uno de los desafíos persistentes ha sido la migración de fragmentos hacia el polo renal superior, dificultada por la anatomía lumbar. Este artículo presenta una innovación técnica que consiste en utilizar un catéter de alto flujo, originalmente diseñado para la colocación de catéteres ureterales, como canal de irrigación dirigido específicamente al polo superior renal. Esta innovación genera un flujo continuo y potente que previene la migración de fragmentos y mejora su evacuación y la visibilidad quirúrgica. En una serie preliminar de cinco casos, la técnica demostró ser segura y reproducible, y logró dichos objetivos. Estos hallazgos iniciales subrayan el potencial clínico de este método y justifican una mayor evaluación mediante estudios prospectivos más amplios para validar su eficacia y su posible impacto en la reducción de intervenciones secundarias.

Palabras clave: Nefrolitotomía percutánea. Riesgo renal dirigido. Catéter de alto flujo. Fragmentos residuales. Innovación técnica. Litotricia.

Cite as: Servera-Ruiz de Velasco A, Ballesta-Martínez B. Optimization of renal irrigation using a high-flow catheter in percutaneous nephrolithotomy: preliminary results. Acad J Health Sci 2025; 40(5): 88-90. Available from: https://doi.org/10.3306/AJHS.2025.40.05.11

Acad J Health Sci 2025; 40(5): 88-90
https://doi.org/10.3306/AJHS.2025.40.05.11
www.ajhealthsciences.com

Introduction

Since its introduction by Professor Valdivia in 1987, the supine position for percutaneous nephrolithotomy (PNL) has become widely adopted. A significant challenge associated with this position is the downward orientation of the upper renal pole due to the lumbar spine curvature and psoas muscle prominence, which facilitates the migration of residual stone fragments. The direction and magnitude of irrigation flow may play a critical role in mitigating this problem. The primary objective of this report is to document the conceptual development and initial implementation of a novel technical approach involving directed irrigation of the upper renal pole through a large-caliber ureteral catheter, aiming to prevent fragment migration and facilitate surgical efficiency. Detailed clinical and experimental data will be explored extensively in subsequent publications.

Case report

We present a technical innovation utilizing a catheter originally designed for JJ ureteral stent placement, specifically from the Resonance® Metallic Stent Set (Cook Medical, Bloomington, Indiana, United States). This catheter, initially serving as a positioning element, has been repurposed as an irrigation channel directed to the upper renal pole during PNL. As this catheter is not commercially available as a standalone product, modifications were made to optimize its functionality specifically for this new indication, and this adaptation has been registered at the Spanish Patent and Trademark Office (OEPM). The modified irrigation channel has an internal diameter ranging from 6 to 8 Fr, larger than the channel of a standard 12 Fr nephroscope, and an external diameter of 8 to 10 Fr, typical for ureteral catheters in PNL procedures.

With the patient in the supine position and after standard preparation, cystoscopy is performed, followed by the insertion of a guidewire into the renal cavities. The composite ureteral catheter is advanced over the wire until its tip is positioned 0.5–1 cm below the superior renal papilla, confirmed through fluoroscopy with diluted contrast (50%). Subsequently, the internal stylet is removed, leaving the external end connected to a conventional irrigation system.

Percutaneous puncture and tract dilation follow, placing the Amplatz sheath. Once direct visualization of the renal pelvis is achieved through nephroscopy, the irrigation system is activated, directing a robust and continuous flow from the superior calyceal group towards the renal access sheath. This directional flow, combined with the catheter's physical presence, significantly reduces fragment migration caused by gravity during lithotripsy, enhancing fragment evacuation and visualization.

Discussion

The described technique represents a simple and safe solution, offering substantial improvements without increasing procedural complexity. The repurposed catheter demonstrates remarkable versatility, providing effective irrigation specifically targeted at the upper renal pole. Its use significantly enhances the evacuation of stone fragments and debris generated during lithotripsy, effectively addressing a common drawback of supine-position PNL.

The catheter delivers consistent, high-volume irrigation flow directed toward the superior calyceal group, actively counteracting gravitational forces that facilitate fragment migration. Furthermore, the catheter occupies physical space within the renal calyx, reducing available room for fragment ascent and thus potentially lowering the incidence of residual postoperative fragments. This could directly translate into fewer secondary interventions and reduced healthcare costs.

Preliminary experience, although limited to five cases, indicates promising clinical outcomes, including reduced surgical times and an absence of associated complications. These initial findings provide a robust basis for future, more comprehensive investigations, including prospective randomized studies to definitively validate this technique against traditional irrigation methods in PNL. Additionally, further exploration of intrarenal pressure dynamics resulting from this irrigation strategy would be beneficial.

Practically, the ease of implementation and reproducibility of the proposed system represent notable advantages. Using a well-known urological catheter reduces the learning curve and facilitates rapid adoption.

In conclusion, the described technical innovation has clear clinical potential for improving surgical outcomes in PNL through optimized renal irrigation. Given its simplicity, safety, and initial effectiveness, this technique warrants extensive evaluation, opening new avenues for future research and clinical improvement.

Conflict of interest

The author declares that he has registered the patent application with the Spanish Patent and Trademark Office (OEPM).

Funding

This article has not received any specific grant from funding agencies in the public, commercial, or for-profit sectors.

References

1. Valdivia Uria JG, Valle Gerhold JA, López López JA, Villarroya Rodríguez S, Ambroj Navarro M, Ramirez Fabián M, et al. Technique and complications of percutaneous nephroscopy: experience with 557 patients in the supine position. J Urol 1998;160:1975-8.

www.ramib.org

Junta Directiva de la Reial Acadèmia de Medicina de les Illes Balears

President: Excm. Sr. Joan Besalduch Vidal
Vicepresident: Lluís Masmiquel Comas
Secretari General: Javier Cortés Bordoy
Vicesecretari: Josep Mª Vicens Gómez
Tresorer: Joan Benejam Gual
Bibliotecària: Antonia Barceló Bennasar

Acadèmics d'honor

2007 – Excm. Sr. Ciril Rozman, Premi Jaime I
2021 – Excm. Sr. Oriol Bonnín Gubianas, Doctor Honoris Causa per la UIB

Acadèmics numeraris

M. I. Sra. Juana M. Román Piñana
M. I. Sr. Bartomeu Anguera Sansó
M. I. Sr. Alfonso Ballesteros Fernández
M. I. Sr. Ferran Tolosa i Cabaní
M. I. Sr. Macià Tomàs Salvà
M. I. Sra. Joana M. Sureda Trujillo
M. I. Sr. Joan Buades Reinés
M. I. Sr. José L. Olea Vallejo
M. I. Sr. Pere Riutord Sbert
Excm. Sr. Joan Besalduch Vidal
M. I. Sr. Fèlix Grases Freixedas
M. I. Sr. Antoni Cañellas Trobat
M. I. Sr. Josep Francesc Forteza Albertí
M. I. Sr. Jordi Ibáñez Juvé
M. I. Sr. Joan March Noguera
M. I. Sr. Ángel Arturo López González
M. I. Sra. Pilar Roca Salom
M. I. Sr. Lluís Masmiquel Comas
M. I. Sr. Sebastià Crespí Rotger
M. I. Sra. Antònia Barceló Bennassar
M. I. Sr. Javier Garau Alemany
M. I. Sr. Jordi Reina Prieto
M. I. Sr. Joan M. Benejam Gual
M. I. Sr. Claudio Rubén Mirasso Santos
M. I. Sr. Josep Mª Vicens Gómez
M. I. Sr. Rafael Morales Soriano

Acadèmics supernumeraris

M. I. Sr. Àlvar Agustí García-Navarro
M. I. Sra. Marta Emma Couce Matovelle

Acadèmics emèrits

M. I. Sr. Arnau Casellas Bernat
M. I. Sr. Javier Cortés Bordoy

www.ramib.org

Protectors de la Reial Acadèmia

Banca March
Conselleria de Presidència
ASISA
Conselleria de Salut
Col·legi Oficial de Metges de les Illes Balears
Fundació Patronat Científic del Col·legi de Metges de les Illes Balears

Benefactors de la Reial Acadèmia

Salut i Força

Patrocinadors de la Reial Acadèmia

Clínica Rotger
Metges Rosselló
Grup Hospitalari Quirónsalud
Col·legi Oficial d'Infermeria de les Illes Balears
Associació Espanyola contra el Càncer a les Illes Balears
Col·legi Oficial de Farmacèutics de Balears
Escola Universitària ADEMA

ACADEMIC JOURNAL
OF HEALTH SCIENCES
MEDICINA BALEAR

www.ajhealthsciences.com